NTNU – Trondheim
Norwegian University of
Science and Technology

Potential of Stirling Engine and Organic Rankine Cycle for Energy Recovery in Ship Machinery Systems

Potensial for energigjenvinning ved hjelp av
Stirling motor eller Organisk Rankine-syklus
i skipsmaskinerisystemer

Ine Oma

Master of Science in Mechanical Engineering
Submission date: April 2015
Supervisor: Eilif Pedersen, EPT
Co-supervisor: Christos Chryssakis, DNV GL

Norwegian University of Science and Technology
Department of Energy and Process Engineering

NTNU

Norwegian University
of Science and Technology

Department of Energy
and Process Engineering

EPT- M-2014-83

MASTER THESIS

FOR

STUD. TECH. INE OMA

FALL 2014

POTENTIAL OF STIRLING ENGINE AND ORGANIC RANKINE CYCLE FOR ENERGY RECOVERY IN SHIP MACHINERY SYSTEMS

Potensial for energigjenvinning ved hjelp av Stirling motor eller Organisk Rankine-syklus i skipsmaskinerisystemer

Background and objective

Marine diesel engines discharge about 50% of the input energy to the atmosphere through the exhaust gas, jacket water and lubrication oil. How this waste heat could be recovered by the use of advanced technologies is of high interest from both an economical perspective in terms of lowering operational costs, and an environmental perspective in order to reduce pollution and meet emission regulations. Considering this, it is important to analyse and compare potential technologies that can increase the overall efficiency of a ship's machinery system.

The aim of the work is to perform a comparative study of the potential for recovering energy from a marine diesel engine by using Stirling engine or Organic Rankine cycle systems. This will include thermodynamic analyses of both systems based on methods found in available literature. The technical feasibility of these systems in addition to implementation into the current machinery system shall be discussed. Additionally, a final discussion of cost and space requirements of both systems will be done. The work is part of the ongoing HRS project (Harvesting, Recovery and Storage of Energy) at the DNV GL Research & Innovation department. Measurements will be available from the ship BW GDF Suez Paris to identify energy losses in the engine and operational profile of the ship.

The following tasks are to be considered:

1. Carry out a literature survey on existing designs and studies of Waste Heat Recovery potential by using Stirling engines or ORC systems
2. Identify potential for energy recovery in the ship under consideration. Perform an exergy analysis of the waste heat sources of the marine engine based on measurement data and fluid properties from REFPROP, EES or other available program.
3. Perform a thermodynamic analysis of both Stirling engine and Organic Rankine cycle systems. Ideal performance should be calculated in addition to identify main losses and give estimations of real performance based on available methods.
4. Discuss technical feasibility with consideration to operational profile and propose implementation into existing machinery system.
5. Discussion of cost and space requirements for both systems.
6. Write a proposal for further work

Within 14 days of receiving the written text on the master thesis, the candidate shall submit a research plan for his project to the department.

When the thesis is evaluated, emphasis is put on processing of the results, and that they are presented in tabular and/or graphic form in a clear manner, and that they are analyzed carefully.

The thesis should be formulated as a research report with summary both in English and Norwegian, conclusion, literature references, table of contents etc. During the preparation of the text, the candidate should make an effort to produce a well-structured and easily readable report. In order to ease the evaluation of the thesis, it is important that the cross-references are correct. In the making of the report, strong emphasis should be placed on both a thorough discussion of the results and an orderly presentation.

The candidate is requested to initiate and keep close contact with his/her academic supervisor(s) throughout the working period. The candidate must follow the rules and regulations of NTNU as well as passive directions given by the Department of Energy and Process Engineering.

Risk assessment of the candidate's work shall be carried out according to the department's procedures. The risk assessment must be documented and included as part of the final report. Events related to the candidate's work adversely affecting the health, safety or security, must be documented and included as part of the final report. If the documentation on risk assessment represents a large number of pages, the full version is to be submitted electronically to the supervisor and an excerpt is included in the report.

Pursuant to “Regulations concerning the supplementary provisions to the technology study program/Master of Science” at NTNU §20, the Department reserves the permission to utilize all the results and data for teaching and research purposes as well as in future publications.

The final report is to be submitted digitally in DAIM. An executive summary of the thesis including title, student’s name, supervisor's name, year, department name, and NTNU's logo and name, shall be submitted to the department as a separate pdf file. Based on an agreement with the supervisor, the final report and other material and documents may be given to the supervisor in digital format.

☐ Work to be done in lab (Water power lab, Fluids engineering lab, Thermal engineering lab)
☐ Field work

Department of Energy and Process Engineering, 14. January 2014

Olav Bolland	Associate Professor Eilif Pedersen
Department Head	Academic Supervisor

Research Co-advisor: Phd. Christos Chryssakis – Senior Researcher, DNV GL

Preface

This paper summarizes my master thesis during the spring semester 2015 at the Institute of Energy and Process Engineering, under the faculty of Engineering Science and Technology at the Norwegian University of Science and Technology, NTNU. This master thesis is given to me from DNV GL, Det Norske Veritas Germanischer Lloyd. The work is part of the ongoing HRS project (Harvesting, Recovery and Storage of Energy) at the DNV GL Maritime Transport Research and Innovation department.

This thesis consists of five parts. The first is a literature survey of existing designs and research of the potential for waste heat recovery by utilizing Stirling engines or ORC systems. The second part is an exergy analysis of the main waste heat sources from the dual fuel engine of the case vessel. The third and fourth part is a thermodynamic analysis of ORC systems and Stirling engine respectively. The last part is a feasibility discussion of both technologies where aspects as space requirement, cost, implementation into existing machinery and technical feasibility are evaluated.

I would like to thank; my supervisors, Professor Eilif Pedersen at the Department of Marine Technology and Ph.D. Christos Chryssakis, Senior Researcher at Maritime Transport at DNV GL Norway for always answering questions in a thorough and understandable manner and for very valuable guidance on how to approach problems. Ph.D. Candidate Dig Vijay Singh for great help, good technical explanations and most appreciated continuously feedback throughout my work period. Ph.D. Bahman Raeissi and M.Sc. Hans Anton Tvete, Senior Researchers at Maritime Transport at DNV GL for great help with processing measurement data from the case vessel and for answering questions regarding the operation of the ship. Lastly, I would like to thank my boyfriend, Jørgen Braaten, for great support during the entire work period. Stine B. Haugsdal and Synne Kathinka Bertelsen, my fellow students at the office for great help with simulation programs and general support during enjoyable office hours.

Trondheim, 15.04.2015

Ine Oma

Summary

Increasing fuel prices and stricter environmental regulations on emissions are motivating the maritime industry to be innovative on how to save fuel and reduce emissions. New technologies and more efficient use of existing systems can help solving these problems. In this report, a comparative study of the potential for recovering waste heat from a marine dual fuel engine by using Stirling engine or Organic Rankine cycles has been performed. The case vessel was the liquefied gas carrier BW GDF Suez Paris, with four Main Generator Engines, two rated at 11.4 MW, and two at 5.7 MW. The exergy and thermodynamic analyses in this study were based on measurement data from one of the 11.4 MW engines. All calculations and simulations were conducted using the commercial F-Chart Software Engineering Equation Solver.

An exergy analysis was performed on the two main waste heat sources of the case vessel's engine; the exhaust stream and the high temperature jacket cooling water. The exergy in the exhaust stream was 1300 kW at 40% load and increased to 2000 kW for 100% load, which corresponds to 28.5% and 17.6% of the engine's power output respectively. For the cooling water, the exergy was approximately 700-850 kW, or about 6-7.5% of the engine's power output at 100% load.

Three different Organic Rankine cycles were studied; a conventional subcritical cycle, a subcritical cycle with regeneration and superheat and a trans-critical cycle. A pre-screening of 50 different working fluids was done based on desirable thermophysical, environmental, safety and operational characteristics. A selection of 12 fluids were chosen to be implemented in the thermodynamic analyses. The best thermodynamic performance was found through simulations to be a subcritical cycle with regeneration and benzene as the working fluid, resulting in an efficiency of ≈21%. Considering hydrocarbons' carcinogenic characteristics and flammability, the safest alternative was shown to be a subcritical Organic Rankine cycle with regeneration and R-245fa as the working fluid. This gave an efficiency of 14.5%, corresponding to 2.5% of the Main Generator Engine's power output at 100% load and 4.1% at 40% load.

A Schmidt cycle analysis of an alpha Stirling engine was performed. The efficiency was calculated to be 22-35%. This is equivalent to 3.9% and 6.1% of the case vessel's main generator engine power output at 100% load. The efficiencies calculated for the Stirling engine were sig-

nificantly higher than all the Organic Rankine cycle solutions. The best working fluid for Stirling engines seemed to be nitrogen due to its high availability, low cost and limited leakage and diffusion rate out of the engine.

In the feasibility discussion, it was shown that the size of the Stirling engine might not be such a high concern as is typically stated in available research reports. The total volume of the Stirling engine was calculated to be smaller than the total volume of the Organic Rankine system. For the cost analysis, the shortest time until return on investment was calculated for the Organic Rankine cycle technology. Based on European prices for Liquefied Natural Gas, the Organic Rankine system had 3.9 years until Return on Investment, and the Stirling Engine had 6.6 years.

Based on the literature survey, the thermodynamic analyses and the feasibility discussion, the Organic Rankine system showed to be the best solution for waste heat recovery systems in the near future for ships operating on global shipping routes. However, with sufficient investment in research and development of Stirling engines utilizing working fluids possessing good availability and safety, the Stirling engine might be a better solution considering its superior thermodynamic performance compared to Organic Rankine systems.

Sammendrag

Økende drivstoffpriser og strengere miljøkrav og reguleringer av drivstoffutslipp motiverer den maritime industrien til å tenke nytt på hvordan det er mulig å spare drivstoff og redusere utslipp. Nye teknologier og mer effektiv bruk av eksisterende systemer være med å løse disse problemene. I denne studien har potensialet for gjenvinning av spillvarme fra en kombinert gass/diesel skipsmotor ved bruk av Stirling motor eller organisk Rankinesykluser blitt sammenlignet. Casestudien for oppgaven har vært gasstankskipet BW GDF Suez Paris. Skipet har fire motorer installert, to med 11.4 MW motoreffekt, og to med 5.7 MW. Eksergianalysen og termodynamiske analyser i studien har vært basert på måledata fra en av skipets 11.4 MW hovedmotorer. Alle beregninger og simuleringer har blitt gjennomført ved hjelp av IT-programmet F-Chart Software Engineering Equation Solver.

En eksergianalyse av eksosstrømmen og høytemperatur kjølevannet fra skipets 11,4 MW hovedmotor ble utført. Eksergien i eksosstrømmen var 1300 kW for 40% last og økte til 2000 kW for 100% last. Dette tilsvarer henholdsvis 28.5% og 17.5% av motorens effekt. For kjølevannet ble eksergien 700-850 kW, tilsvarende 6-7.5% av motoreffekten ved 100% last.

Tre forskjellige organiske Rankinesystemer ble studert; en konvensjonell underkritisk syklus, en underkritisk syklus med regenerering og overopphetning, og en transkritisk syklus. 50 ulike arbeidsvæsker ble analysert basert på ønskelige termofysiske, miljø-, sikkerhets- og operative egenskaper. Et utvalg av 12 væsker ble implementert i de termodynamiske analysene. Den beste termodynamiske ytelsen ble funnet gjennom simuleringer til å være en underkritisk syklus med regenerering og benzen som arbeidsvæske, noe som resulterte i en virkningsgrad på ≈21%. Tatt i betraktning hydrokarboners kreftfremkallende egenskaper og høye brannfarlighet, viste det sikreste alternativet å være en underkritisk organisk Rankinesyklus med regenerering og R-245fa som arbeidsvæske. Dette ga en virkningsgrad på 14.5%, tilsvarende 2.5% av hovedmotorens effekt ved 100% last og 4.1% ved 40% last.

En Schmidt-analyse av en alfa Stirling motor ble utført. Effektiviteten ble beregnet til å være 22-35%. Dette svarer til 3.9% og 6.1% av hovedmotorens effekt ved 100% last. Virkningsgradene beregnet for Stirling-motoren var betraktelig høyere enn alle Rankinesyklusene. Det beste arbeidsmediet for Stirling motoren viste seg å være nitrogen basert på nitrogens gode tilgjengelighet,

lave kostnad og begrensede lekasjerate ut av motoren.

Muligheten for å implementere systemene i et marint maskinerisystem ble diskutert. Det viste seg at størrelsen av Stirlingmotorer sannsynligvis ikke er så kritisk og hemmende for videreutvikling og implementering av motoren som det ofte er oppgitt i dagens tilgjengelige forskningsrapporter. Det totale volumet av Stirlingmotoren ble utregnet til å være mindre en totalt volum av Rankinesystemet. I kostnadsanalysen viste Rankinesystemet å ha kortest tid innen avkastning på investeringen ville bli oppnådd. Basert på europeiske priser for flytende naturgass ble det utregnet at Rankinesystemet ville ha 3.9 år inntil avkastning på investering er oppnådd, og Stirlingmotoren 6.6 år.

Basert på litteraturstudiet, termodynamiske analyser og diskusjon av tekniske hindringer for implementering av teknologiene, viste Rankinesystemet seg å være den beste og mest realiserbare løsningen i nær fremtid for å gjenvinne spillvarme fra skipsmotorer som operer globalt. Med tilstrekkelig investering i forskning og utvikling av Stirlingmotorer som benytter arbeidsmedier som innehar god tilgjengelighet og sikkerhet, kan det hende Stirlingmotoren er en bedre løsning tatt i betraktning dens overlegne termodynamisk ytelse sammenlignet med organiske Rankinesystemer.

Abbreviations

BHP Brake horse power

bsfc brake specific fuel consumption

bwr Back work ratio

CFC Chlorofluorocarbon

CW Cooling Water

ECA Emission Control Areas

EES Engineering Equation Solver

EGR Exhaust Gas Recirculation

GWP Global Warming Potential

HCFC Hydrochlorofluorocarbon

HT High temperature

HVAC Heating, Ventilation and Air Conditioning

HX Heat Exchanger

ICE Internal Combustion Engine

LHV Lower Heating Value

LNG Liquefied Natural gas

MAC Mobile Air Conditioning

MGE Main Generator Engine

NBP Normal Boiling Point

ODP Ozone Depletion Potential

ORC Organic Rankine Cycle

SC Striling Cycle

SE Stirling Engine

TC Turbo Charger

TIT Turbine Inlet Temperature

TOE Tons of Oil Equivalent

WHR Waste Heat Recovery

WHRS Waste Heat Recovery Systems

Nomenclature

η_p	%	Isentropic Pump Efficiency
η_t	%	Isentropic Turbine Efficiency
λ	ratio	Air/Fuel Ratio
ρ	kg/m^3	Density
$\dot{\sigma}$	kW/K	Entropy Production
τ	ratio	Temperature Ratio
ϕ	degrees	Crank Angle
C_v	J/K	Heat Capacity
cw		Cooling Water
$\bar{\boldsymbol{e}}_{tot}$	kJ/kmol fuel	Total Specific Exergy Molar Basis
$\bar{\boldsymbol{e}}_f$	kJ/kmol fuel	Total Specific Flow Exergy Molar Basis
$\boldsymbol{e}_{tot}$	kJ/kg fuel	Total Specific Exergy Mass Basis
$\bar{\boldsymbol{e}}^{ch}$	kJ/kmol fuel	Chemical Exergy Contribution
$\bar{\boldsymbol{e}}^{mech}$	kJ/kmol fuel	Thermomechanical Exergy Contribution
f		Fraction, Mass Flow
g	m/s^2	Gravitational Acceleration
$\bar{h}$	kJ/kmol	Enthalpy Molar Basis
h	kJ/kg	Enthalpy Mass Basis
HP		High Pressure
LP		Low Pressure
$\dot{m}$	kg/s	Mass Flow
MW	kg/kmol	Molecular Weight
n_i	kmol/kmol fuel	Kmol of Component i in Exhaust per kmol of Fuel
P	bar	Pressure
P_0	bar	Pressure in Exergy Reference Environment
$\dot{Q}$	kW	Heat Transfer
$\bar{R}$	kJ/kmol·K	Universal Gas Constant
r	ratio	Volume Ratio
$\bar{s}$	kJ/kmol·K	Entropy Molar Basis
s	kJ/kg·K	Entropy Mass Basis
$\bar{s}^\circ$	kJ/kmol·K	Absolute Entropy
SC		Swept Compression Cylinder
SE		Swept Expansion Cylinder
T_0	$^\circ C$	Temperature in Exergy Reference Environment
T	K	Temperature
V	m^3	Volume
v	m^3/kg	Specific Volume
$\dot{V}$	m^3/h	Volumetric Flow
$\dot{W}$	kW	Work
wf		Working Fluid
x	%	Vapor Quality
X	ratio	Dead Volume Ratio
y_i	%mol	Mole Fraction of Component i in Exhaust
y_i^e	%mol	Mole Fraction of Component i in Reference Environment
z	m	Height Difference

List of Figures

List of Tables

Contents

Chapter 1

Introduction

1.1 Background

Increasing fuel prices, stricter environmental regulations on greenhouse gas emissions, oscillating freight rates and a complex and interdependent global economy are altogether pushing and motivating the maritime industry to be innovative on how to save fuel and reduce emissions. Both new technology and more efficient use of existing systems are crucial ingredients in the recipe of finding a solution to the problems.

The Internal Combustion Engine (ICE) has been the primary mover for ships over the past century. During this time, the complexity of marine engines has increased drastically due to economical motivation to reduce fuel consumption and in later times also environmental concerns. Techniques such as enhanced fuel/air mixing, turbocharging, and variable valve timing have been implemented in order to increase thermal efficiency (Sprouse and Depcik, 2013). However, modern marine diesel and dual fuel engines still discharge about 50% of the input fuel energy to the atmosphere through waste heat in the exhaust gas, jacket water and lubrication oil (Woodyard, 2009). This is the main factor which limits the thermal efficiency of a marine engine (Dimopoulos and Kakalis, 2014). Additionally, techniques such as lowering combustion temperature and pressure in diesel engines in order to reduce harmful emission, especially nitrogen oxides (NOx) and particulate matter (PM), lowers the potential efficiency (Sprouse and Depcik, 2013). By harvesting and recycling the waste heat some of the energy can be recovered, and the total fuel utilization efficiency can be significantly improved (Woodyard, 2009). How

this waste heat can be recovered by the use of advanced technologies is of high interest for ship owners both from an economical perspective in terms of lowering operational costs, and from an environmental perspective in order to reduce pollution and meet emission regulations. Bearing this in mind, it is important to analyze and compare potential technologies that can increase the overall efficiency of a ship's machinery system in order to propose feasible solutions to ship owners.

In this work, a comparative study of the potential of harvesting waste heat by the use of Stirling engines (SE) or Organic Rankine cycles (ORC) will be done. Before a thermodynamic performance analysis and a discussion about technical and economical feasibility of both systems, previous studies and current technology of ORC and SE systems will be reviewed.

1.1.1 Organic Rankine Cycle

A Rankine cycle is a closed loop cycle where a working fluid goes through 4 processes (Moran et al., 2010). A heat source causes the working fluid to evaporate to saturated or superheated vapor. This vapor is expanded in a power turbine creating mechanical power or electricity if connected to a generator. The working fluid then condenses in a heat exchanger with a heat sink, and is finally pumped back to the evaporator pressure. If the selected working fluid is organic in nature, the cycle is called an Organic Rankine cycle (Moran et al., 2010). Power generation from waste heat by the use of the steam Rankine cycle and the Organic Rankine cycle have been used for a long time to harvest waste heat from various industrial processes (Chen et al., 2010). There are several advantages with ORC compared to a conventional steam turbine Rankine cycle (Chen et al., 2010) (Shu et al., 2013):

- Lower normal boiling point (NBP) than water; can therefore use lower heat sources for the evaporation process.
- The slope of the saturation vapor curve can be positive for organic fluids, and therefore the process will avoid the two phase zone after expansion. This will avoid corroding on the turbine blades, reduce necessary maintenance and prolong the lifetime of the system.
- No need for overheating the vapor, enabling the possibility to use a smaller and cheaper heat exchanger that will decrease the size of the entire system.

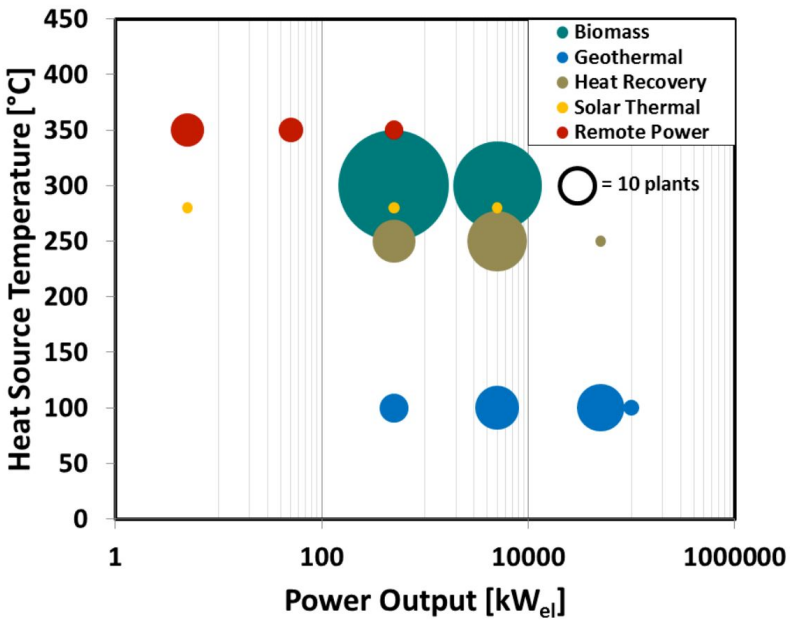

Figure 1.1: Number of ORC systems based on temperature range and power output (Rettig et al., 2011).

Amongst the ORC systems in operation today, geothermal applications have the highest power output, followed by biomass and heat recovery applications, see Figure 1.1 for full overview (Rettig et al., 2011).

Shu et al. (2013) reviewed several waste heat recovery (WHR) solutions for two-stroke IC engines aboard ships. This included technical systems such as power turbine, refrigeration, thermoelectric generation, desalination, combined cycle systems and the Rankine cycle (Shu et al., 2013). The study concludes that the ORC is a good choice for WHR on ships due to its possibility to recover waste heat from medium and low-grade heat sources. However, Shu et al. (2013) also emphasize that a combined cycle system using a combination of two or more different waste heat recovery technologies might be the best solution for further study in order to make full use of the waste heat sources emitted from marine engines.

In 1983 a research of an ORC system connected to a 288 BHP long-haul vehicle diesel engine was sponsored by the U.S. Department of Energy. The ORC system was tested both in the laboratory and on the road. The system showed an average of 12.5% savings in fuel consumption from the highway fuel tests (DiBella et al., 1983). A long haul vehicle engine was chosen over a

small automobile ICE because these engines run at constant speed for longer periods and can provide waste heat at more steady temperatures which is a favorable characteristic for ORC systems (Sprouse and Depcik, 2013). Bearing this in mind, installing ORC systems in cargo ships should give promising results since the engines in these ships run at a constant speed for long periods due to long and often intercontinental voyages.

R. Chammas and D. Clodic did a research on an ORC system connected to an 1.4 liter ICE installed in an electric hybrid vehicle (Chammas and Clodic, 2005). The studied focused on the available thermal energy in both the cooling stream and the exhaust stream. Following working fluids were compared; water, isopentane, R-123, R-245ca, R-245fa, Butane, Isobutane and R-152a, the result can be seen in Figure 1.2. Even though R-123 shows the best performance of the organic fluids, it is stated in the research that R-123 is a Hydrochlorofluorocarbon (HCFC) and will be faced out by the Montreal Protocol due to its high ODP (see Section 4.4 for explanation of ODP) (Chammas and Clodic, 2005). Further on, the study shows that with increased amount of superheat, the efficiency for the dry and isentropic fluids decreases, but for water, which is a wet fluid, the efficiency increases (dry, isentropic and wet fluids are discussed in Section 4.2.3). The higher the operating pressure, the higher will the cycle efficiency become. However, this is a question of trade-off considering increased cost for the equipment that need to handle the higher pressures (Chammas and Clodic, 2005).

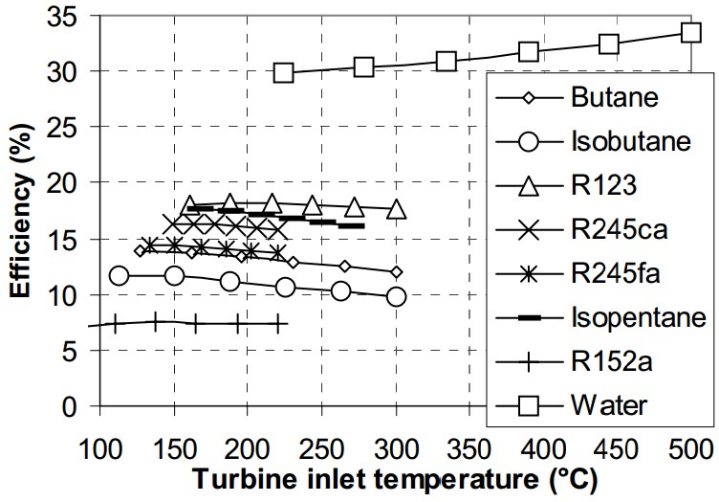

Figure 1.2: Performance of various working fluids vs turbine inlet temp. (Chammas and Clodic, 2005).

A couple of years later, an analysis of a non-regenerative ORC with the working fluids R-12, R-123, R-134a and R-717 was published (Roy et al., 2011). The analysis was a parametric optimization where a computer program was developed to investigate the system based on both the first and second law of thermodynamics. Same as the previous mentioned study of R. Chammas and D. Clodic, R-123 gave the best efficiency with minimum irreversibility. The efficiency varied between 18-19% as can be seen in Figure 1.3. Since R-123 is beeing phased out, it should be noticed that the other working fluids show decent efficiencies and good potential for energy recovery. The choice of correct working fluid for a specific ORC is one of the most important design considerations due to its high influence on the ORC performance (Sprouse and Depcik, 2013).

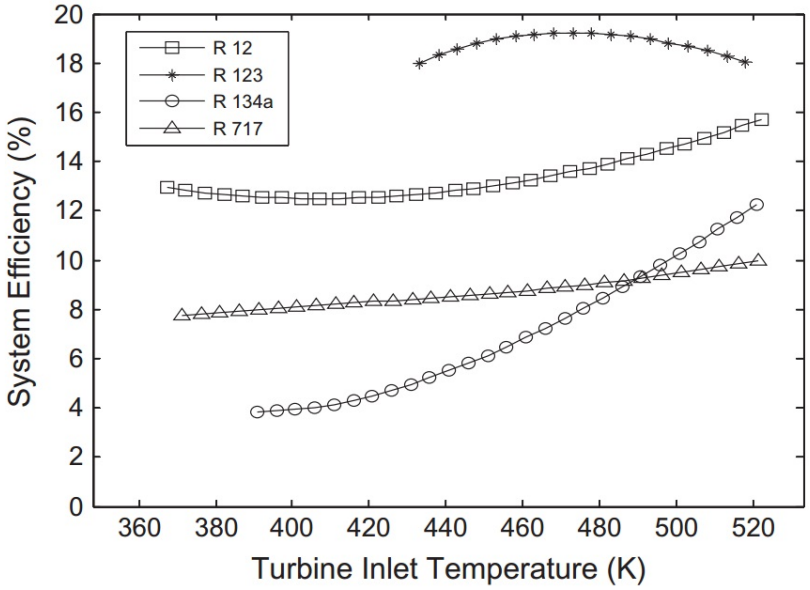

Figure 1.3: Efficiency vs turbine inlet temp. during superheating, P = 2.5 MPa (Roy et al., 2011).

A more recent study published in 2012, performed a theoretical analysis of an ORC system fitted to a heavy diesel truck engine by using a computer simulation model (Katsanos et al., 2012). Pressure drop in the heat exchanger was taken into account additionally to 85% isentropic efficiency for both the pump and the expander. A comparison was done between water and R-245ca. The results showed that the brake specific fuel consumption (bsfc) was significantly improved with 10.2% at 25% engine load and 8.5% at 100% load for R-245ca and 6.1% at 25% engine load to 7.5% at 100% engine load for water (Katsanos et al., 2012).

Bianchi and Pascale (2011) studied sub-critical ORC systems with saturated steam at the evaporator outlet. The cycle was studied with and without a regenerator with efficiency of 80%. The simulations indicated that an ORC with a regenerator would be 1-3% more efficient than a simple ORC without affecting the power output. The highest efficiency of about 20% was gained with benzene (Bianchi and Pascale, 2011). The regenerator was not applied for wet fluids. The regenerator can only be used for dry fluids because these have not entered the two-phase area after expansion. For a dry fluid, the temperature is higher than the condensing temperature at end of expansion, and this temperature can be used to preheat the working fluid before it enters the evaporator so that the thermal energy necessary to evaporate the working fluid will be reduced (Bianchi and Pascale, 2011).

In 2007 it was published a report by SINTEF[1] on the study of how a trans-critical ORC with carbon dioxide (CO_2) as the working medium would work as an electricity producer on fishing boats in the North Sea (Ladam and Skaugen, 2007). The ORC should use the waste heat from the exhaust and cooling water (CW) of the boat's engine. CO_2 has several advantages compared to other organic fluids because it is a natural fluid, environmental friendly, non-toxic, non flammable and has high availability additionally to low price (Chen et al., 2010). In the SINTEF-study it was used computer simulations for the Rankine cycle. The values for the exhaust gas and the cooling water were taken from measured values additionally to some estimates. The performance of the CO_2 power cycle was the same as for known conventional ORC systems for the exhaust gas. Considering the low temperature cooling water heat source, the performance with a CO_2 system was significantly improved. Compared to conventional ORC fluids, the CO_2 system showed 25% improvement. The study showed that 10% of the fuel could be saved by applying an ORC system with CO_2 as the working fluid. Also, the CO_2 system had potential for size reduction compared to conventional ORC systems due to the high density of supercritical CO_2 (Sprouse and Depcik, 2013). A drawback with CO_2 is the fluid's low critical temperature, 31.1°C, that will make it difficult for CO_2 to condense without very good cooling conditions (Chen et al., 2010). This will be an issue for ships operating in warm regions of the world.

[1] SINTEF - Selskapet for Industriell og Teknisk Forskning ved Norges Tekniske Høgskole - the largest independent research organization in Scandinavia (SINTEF, 2015).

Only one example has been found by the author of an ORC built specifically for waste heat recovery in ship machinery systems. Opcon, a swedish company that produces eco-friendly systems for low resource energy utilization, installed in 2012 an Opcon Powerbox ORC on MV Figaro, a Large Car-Truck Carrier (LCTC) (Millikin, 2012) (Opcon Marine, 2015). The Opcon Powerbox ORC utilizes the cooling water from the engine jacket to evaporate the working fluid. To harvest energy from the exhaust stream, Opcon has made the Opcon Powerbox WST, which is a wet steam turbine (WST). Steam is created by exhaust in a boiler. The generated power from the ORC system can be between 40-740 kW, and between 40-825 kW for the WST, both dependent on the available waste heat supply (Opcon, 2012). Due to slow steaming of MV Figaro, Opcon has only had the systems running for 200h one year after installation (Opcon, 2012). The system has been approved by Lloyds Register (Opcon, 2012). Following Opcons own statements, the powerbox shows great potential for energy recovery and one average powerbox can generate 3400 MWh per year (Opcon, 2012).

1.1.2 Stirling Engine

A Stirling engine is a heat engine operating by alternating compression and expansion of a compressible fluid (Walker, 1980). The engine operates on a closed thermodynamic cycle (Thombare and Verma, 2008). The compression is done when the gas is heated from an external heat source. A regenerator composed of a fined mesh pad between the hot and the cold side works as a thermal sponge where it alternates between absorbing and releasing heat (Thombare and Verma, 2008). At the cold side, the gas is expanded by ejecting heat to a heat sink. Air has been a common working fluid for many years, and the engine is often referred to as a air heat engine (Kongtragool and Wongwises, 2005). A fixed quantity of the working fluid is enclosed in the engine permanently. The main advantages with Stirling engine reported in available literature are (Thombare and Verma, 2008) (Kongtragool and Wongwises, 2005):

- It can use any heat source such as solar radiation, geothermal heat, waste heat from industry, biofuel and many more.
- Low fuel consumption.
- High efficiency.

- Low noise levels.
- Clean combustion.
- Capability to run on an extensive range of temperatures.

The Stirling engine was invented almost 200 years ago by Robert Stirling in 1816 (Walker, 1980). This happened 80 years earlier than the invention of the Diesel engine and 60 years earlier than the Otto engine (Walker, 1980). During the course of the two last centuries, major improvements have been done to the performance of the Stirling engine. Numerous attempts have been carried out in order to redesign the engine and to constantly improve the performance. Even though, the commercialization of the sterling engine into the global market has halted as a result of the impressive technological development of the ICE (Thombare and Verma, 2008). Despite the incredible potential of an outstanding thermal efficiency, the Stirling engine is today only used in a few niche industries as propulsion power for submarines, cryogenic heat pumps, electricity generation from solar power plants and a few small scale waste heat power applications (Majeski, 2002).

As of today, Stirling engines do not show as high power outputs as ORC systems. According to Obernberger et al. (2003), Stirling engines have shown promising results for installations with electric power outputs in the range of 10-150 kW.

The Stirling engine is directly proportional to the mean cycle pressure and due to this engines today typically operate within a pressure range of 100-200 bar (Thombare and Verma, 2008). Very high pressures increase the complexity of the engine and can impact reliability and increase the engine's cost and size. High cost is often mentioned by researchers as a limiting factor to the popularization of the Stirling engine (Wu and Wang, 2006) (Kongtragool and Wongwises, 2005) (Thombare and Verma, 2008).

A study of Poullikkas (2005) shows that about 9 MW of electrical power can be recovered from using a Stirling cycle to recover waste heat of a Rolls-Royce RB211 gas turbine generating 27.5 MW of electrical power. This signifies an increase by 33% in total power output.

On the CIMAC[2] World Congress on Combustion Engine Technology in 2010, Ioannis Vlaskos (2010) presented a study where a simulated 16-cylinder low speed Stirling engine was used to harvest waste heat from a hypothetical 5000 kW marine diesel engine. The shaft power of the

[2]CIMAC - Congres International des Moteurs A Combustion Interne (Ioannis Vlaskos, 2010).

engine resulted to be 740 kW at 600 rpm with an overall efficiency of 27%. The Stirling engine improved the specific fuel consumption by 12.9%, from 181 to 157 g/kWh.

The company Cool Energy has developed a Stirling engine that converts low temperature heat energy into electrical power in the range of 3 kW to 20 kW (Cool Energy, 2015). Compared to other Stirling engines, the difference is the use of low temperature heat at around 100°C (Cool Energy, 2015). Most commercial Stirling engines that are available today use temperature sources that are in a much higher range, around 600-1000°C (Cool Energy, 2015). Cool Energy's idea is to harvest waste heat from diesel generators powering telephone towers (Cool Energy, 2015). The Stirling engine can boost the fuel efficiency of a diesel generator with up to 20% (Cool Energy, 2015). The efficiency of the actual Stirling engine varies between 10-25% depending on the inlet temperature (Cool Energy, 2015).

One of the more remarkable project from the last century is The NASA/MTI Automotive Stirling Engine Development project that was established in 1978 (Ernst and Shaltens, 1997). During the 1970s the first oil crisis pushed the U.S. Department of Energy to give NASA the task of fitting an American-made car with a Stirling engine (Ernst and Shaltens, 1997). The maximum efficiency achieved in the project was between 25-30% at a speed between 1500-2000 rpm, causing 30% improvement in fuel efficiency compared to a conventional ICE (Ernst and Shaltens, 1997). Even so, considering the commercialization of the Stirling engine as an automobile engine, two major challenges emerged (Ernst and Shaltens, 1997):

- The engine required some time to warm up before the vehicle would start to move.
- The engine showed difficulties in changing the engine's speed.

For a driver it is crucial to have the possibility to drive the second the key is turned and to control the speed. However, these challenges do not have to be an issue for a Stirling engine that is to be used as a WHR system aboard a ship operating on long routes. The engine will have plenty of time to warm up, and it will not have to change speed since it will not be used for propulsion.

Bianchi and De Pascale reviewed various producers of small scale heat recovery technology. It can be seen from Figure 1.4 that Stirling engines showed the highest efficiencies, however, they are yet not made for power outputs higher than about 100 kW (Bianchi and Pascale, 2011).

TE and MCR is short for Termo-Electric and Micro Organic Rankine.

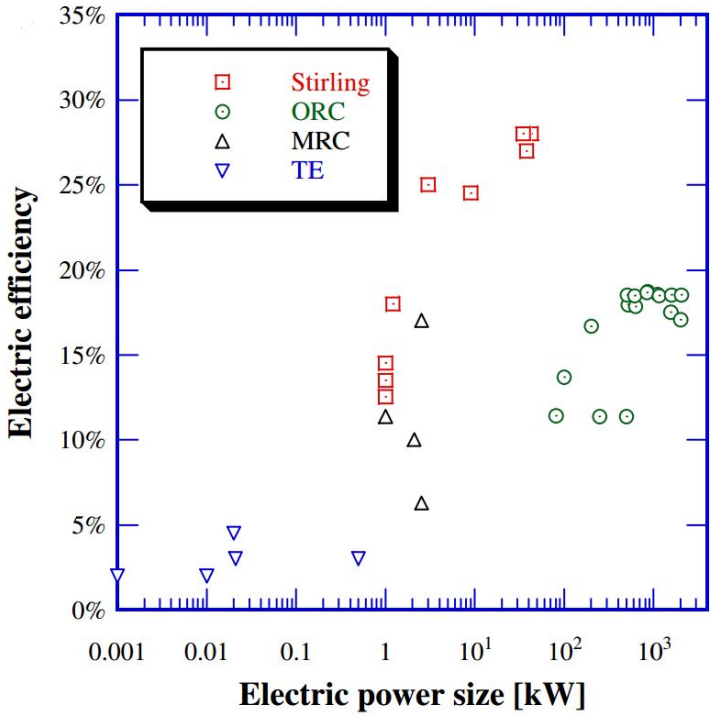

Figure 1.4: Efficiency values of commercial SE and ORC systems (Bianchi and Pascale, 2011).

From the presented research on current ORC and Stirling engine technology it seems as both solutions are promising in order to utilize waste heat from marine engines for power production, even if no prototype of the Stirling engine is yet developed for marine applications.

1.2 Objectives

The objective of this work is to perform a comparative study of the potential for recovering energy from a marine dual fuel engine by using Stirling engines or Organic Rankine cycle systems. The technical feasibility of these systems should be determined in addition to identify solutions on how to implement the systems into the ship's current machinery. Cost and space requirements of both systems will be defined.

This work is part of the ongoing HRS project (Harvesting, Recovery and Storage of Energy) at the DNV GL, Det Norske Veritas Germanischer Lloyd, Maritime Transport Research and Innova-

tion Department.

The following objectives are to be accomplished:

1. Identify potential for energy recovery from the waste heat in both the exhaust stream and the jacket water of the case vessel's engine.
2. Perform a comparative study of a Stirling engine and different ORC systems for recovering waste heat from the case vessel's engine.
3. Determine technical feasibility of Stirling engine and ORC systems with consideration to the ship's operational profile and find possible solutions for implementation into existing machinery system.
4. Identify cost and space requirements for both systems.
5. Write a proposal for further work.

1.3 Approach

The following scientific approaches will be used to solve the problems and meet the objectives stated in the previous section. (Flowcharts for the approches for exergy analysis and thermodynamic analyses of both Stirling engine and ORC systems can be seen in Figure 1.5)

1. The potential for energy recovery from the waste heat in both the exhaust stream and the jacket water of the case vessel's engine will be calculated with an exergy analysis. A model for the exergy analysis will be built in the IT-simulation program; Engineering Equation Solver[3] (EES).
2. Three different models of the ORC systems will be built in EES in order to do a thermodynamic analysis on the potential performance of various ORC systems. One model will be built for a subcritical ORC, one for a subcritical ORC with regeneration and superheat, and the last for a trans-critical cycle. Working fluids that are to be implemented in the thermodynamic analysis will be chosen through a pre-screening based on environmental, safety

[3]EES is a equation-solving program that can numerically solve non-linear algebraic and differential equations. It can do optimization, provide uncertainty analyses, perform linear and non-linear regression. It provides a high accuracy thermodynamic and transport property database provided for hundreds of fluids and gases (Klein and Alvarado, 2002).

and thermophysical properties. The substances that will be included in the pre-screening will be chosen from available literature and research reports on ORC analysis. Optimization in order to find the best pressure and temperature levels will be done with help of built-in optimization procedures in EES.

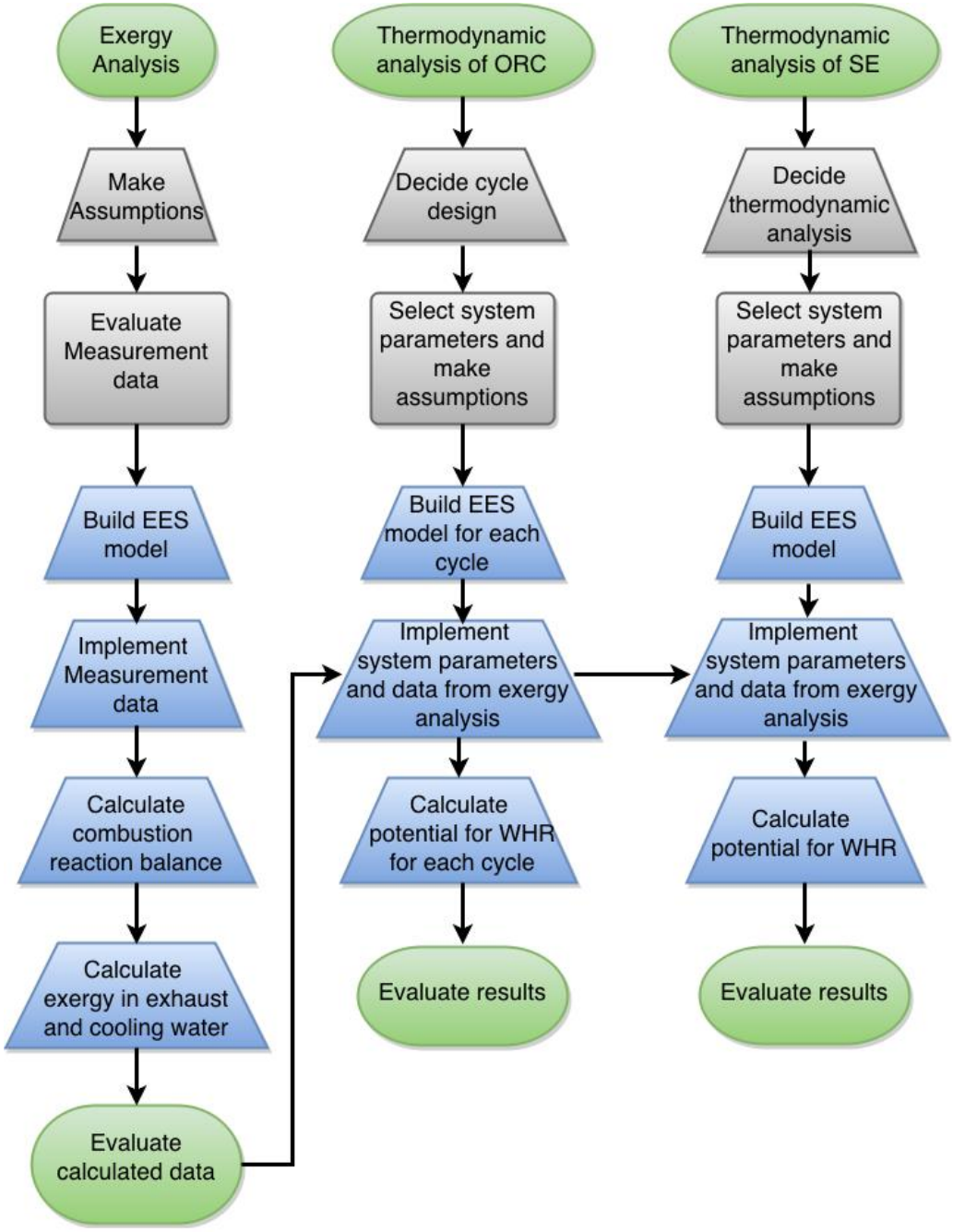

Figure 1.5: Approach for exergy analysis and thermodynamic analysis of ORC and SE (Flowchart developed in Draw.io (2015)).

3. The performance of a Stirling engine will calculated based on both an ideal and a Schmidt cycle analysis.
4. Cost, space requirements and technical feasibility of both systems will be evaluated based on data from available research reports and scientific papers.

1.4 Limitations

1.4.1 Limitations to Exergy Analysis

1. No available measurement data for mass flow of fuel or amount of excess air for combustion reaction calculation have been available. The assumptions taken for these parameters are discussed in Section 3.2.2 and 3.2.3.
2. There was no available data for the temperature after the economizer in order to calculate the potential for waste heat recovery at this point, or to do a proper comparison between the WHRS in this thesis to the already installed economizer.
3. Only data for the largest main generator engine was available, causing the exergy analysis to be limited to one engine only.
4. No available measurement data for mass flow, temperature or pressure of cooling water stream. Assumptions were used to complete the exergy analysis of the cooling water stream, these assumptions are discussed in Section 3.2.5.
5. The uncertainties of the measurement equipment that have been used to measure the data on the case vessel used for the exergy analysis in this work have been unknown. This made it impossible to evaluate the quality of the measurement data and give a proper judgement of the certainty of the exergy calculation.
6. No gas chromatograph was installed in the case vessel to analyze the exhaust stream of the main generator engine. Due to this it was necessary to assume complete combustion in order to find the chemical composition of the exhaust stream.

1.4.2 Limitations to Organic Rankine Cycle Thermodynamic Analysis

1. Equations of state for the fluids R-152a, Propyne, R-601, R-245ca, R-1270, FC-4-1-12 and HC-270 were not available in the EES simulation program, and therefore the fluids had to be excluded from the thermodynamic analyses.
2. Difficulties with finding information regarding environmental and safety characteristics of hydrocarbons made it challenging to do a proper evaluation of the feasibility of using hydrocarbons as working fluid.
3. No available data for mass flow of exhaust stream made it challenging to do proper pinch point analysis for the evaporator heat exchanger in the Organic Rankine cycle.

1.4.3 Limitations to Stirling Engine Thermodynamic Analysis

1. None of the available thermodynamic analyses of the SE found by the author included the effects the choice of working fluid has on the Stirling engine performance. A discussion on potential working fluids based on availability and thermodynamic properties was done instead.
2. High level of idealization in the Schmidt cycle thermodynamic analysis made it difficult to do a proper evaluation of the true potential of harvesting waste heat with Stirling engine technology.

1.4.4 Limitations to Cost and Space Analysis

1. No available data for size of Stirling engines with power output above 250 kW was found. Assumptions were made based on dimension data for engines up to 250 kW.
2. Cost of Stirling engine is based on assumed production and prototype prices from companies developing Stirling engines. Very few prices of commercial Stirling engines are available since there are so few companies producing Stirling engines today (Thombare and Verma, 2008).

1.5 Structure of the Report

The rest of the report is organized as follows. Chapter 2 gives a brief overview of the case vessel's machinery system. Chapter 3 explains the exergy analysis, the assumptions that were done previous to the analysis and a discussion of the measurement data that were available in order to calculate the exergy. At the end of Chapter 3, a discussion and a presentation of the results of the exergy analysis are given.

In Chapter 4 the thermodynamic models used for the Organic Rankine systems are presented. An evaluation on working fluids is given in order to chose which substances to include in the thermodynamic analysis. At the end the results are presented and discussed.

Chapter 5 contains the thermodynamic analysis of the Stirling engine. The main difficulties with the thermodynamic model of the engine is presented and discussed. Same as for the other chapters, the results are given at the end together with a discussion.

Chapter 6 comprises a technical feasibility discussion on both Stirling engine and ORC systems. General challenges of both systems are presented and evaluated in addition to implementation into existing machinery, space requirement and finally a cost analysis.

The final chapter includes summary and conclusion for the entire thesis and the main findings from this work.

Chapter 2

Case Study

2.1 BW GDF Suez Paris

The case study of this master thesis is the liquefied gas carrier BW GDF Suez Paris that operates on intercontinental routes. A picture of the vessel can be seen in Figure 2.1. The ship has a diesel-electric architecture with four dual fuel generator engines supplying electrical power to the ship (BW Gas, 2009). The Main Generator Engines (MGE) No. 1 and No. 4 are Wärtsilä 12V50DF type with 11400 kW power output, and MGE No. 2 and 3 are Wärtsilä 6L50DF rated at 5700 kW. The engines are always operating with boil-off gas from the liquefied natural gas (LNG) storage tanks as fuel (C. Chryssakis DNV GL, 2015). The engines are turbocharged, intercooled, 4-stroke diesel with direct fuel injection (BW Gas, 2009), see Table 2.1 for general information about the generator engines.

Engine syst. part	Unit	12V50DF	6L50DF
Engine Output	kW	11400	5700
Cylinder Bore	mm	500	500
Stroke	mm	580	580
Swept Volume	dm^3	1367	683
Mean Effective Pressure, *(Engine Speed 500/514 rpm)*	bar	20 / 19.5	20 / 19.5
Mean Piston Speed, *(Engine Speed 500/514 rpm)*	m/s	9.7 / 9.9	9.7 / 9.9

Table 2.1: Main parameters, Wärtsilä engines aboard case vessel (BW Gas, 2009).

Figure 2.1: Liquefied gas carrier BW GDF SUEZ Paris (BW Gas, 2009)

2.1.1 Operational Profile of Ship

The operational profile of the ship is based on data from a 4 month operating period. It will be assumed in this study that the ship is operating more or less in the same mode over a 1 year period as it has done for the measured 4 month period. The average operating time in each operational mode (loaded, ballast and port) and the adjacent propulsion and hotel power can be seen in Table 2.2. It is further assumed that the hotel power is produced by a single small generator, while the propulsion power by the two large ones or by only one of the large ones if the propulsion power is very small for each engine. In Table 2.3 and Table 2.4 the time spent at loaded and ballast mode can be seen respectively. With the data from Table 2.3 and 2.4, the complete operational profile for MGE No. 1 and No. 4 for 4 months operation of BW GDF Suez Paris can be seen in Figure 2.2.

Operational mode	Time [hrs]	Time [%]	Propulsion [kW]	Hotel [kW]	Total [kW]
Loaded	1600	52.9	11951	2871	14822
Ballast	806	26.7	10894	2802	13696
Port	618	20.4	0	2608	2608

Table 2.2: Four month operating period of BW GDF Suez Paris (C. Chryssakis DNV GL, 2015).

Speed [kn]	Duration [hrs]	Percent of tot time [%]	Propulsion [kW]	No. of Engines	Load each Engine [%]
0-10	20	1.3	12000	2	52.6
10.-15	80	5	13500	2	59.2
15-16	180	11.3	14500	2	63.6
16-17	210	13.1	15000	2	65.8
17-18	650	40.6	17500	2	76.8
18-19	450	28.1	18500	2	81.1
19-20	10	0.6	19500	2	85.5

Table 2.3: Operational profile, loaded mode (C. Chryssakis DNV GL, 2015).

Speed [kn]	Duration [hrs]	Percent of tot time [%]	Propulsion [kW]	No. of Engines	Load each Engine [%]
0-10	10	1.2	6000	1	52.6
10.-15	145	18.0	8300	1	72.8
15-16	120	14.9	5500	1	48.2
16-17	235	29.2	11000	2	48.2
17-18	205	25.5	13000	2	57
18-19	85	10.6	17000	2	74.6
19-20	5	0.6	19000	2	83.3

Table 2.4: Operational profile, ballast mode (C. Chryssakis DNV GL, 2015).

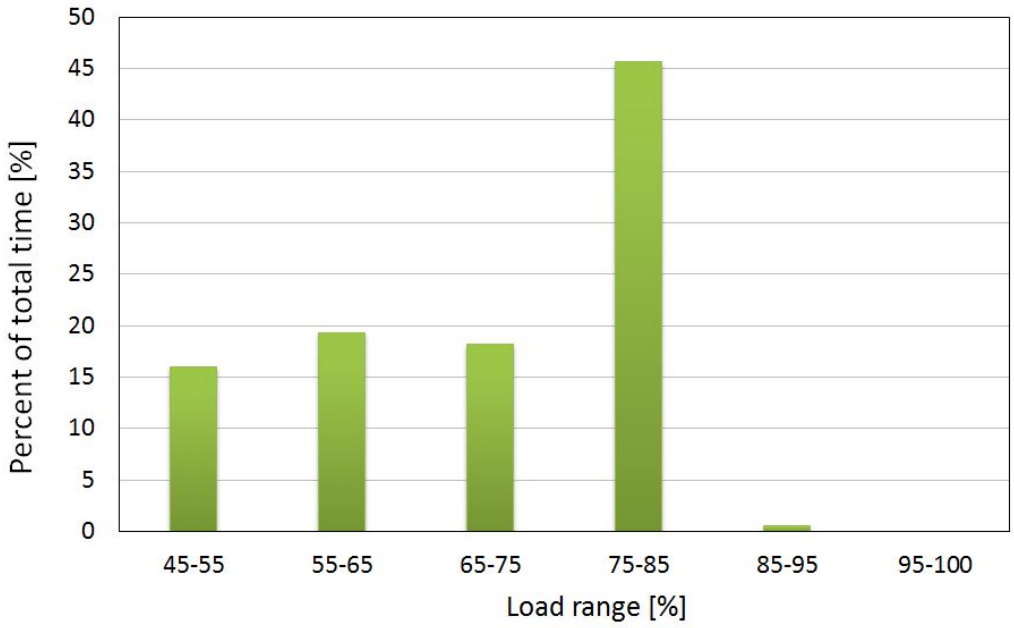

Figure 2.2: Operational profile, loaded and ballast mode of MGE1 and MGE4 (C. Chryssakis DNV GL, 2015).

2.1.2 Fresh Water Cooling System

Each generator engine installed in the case vessel have their own fresh water cooling system which are divided into High Temperature (HT) and Low Temperature (LT) cooling circuits (BW Gas, 2009). It will only be the HT circuit that will be evaluated in this work due to the LT circuits low grade energy (Bianchi and Pascale, 2011). The HT circuit has a circulation pump that supplies cooling water to the jacket, cylinder head and HT air cooler (BW Gas, 2009). The HT system is controlled by an engine driven circulation pump and a three way control valve set to regulate the temperature of the water leaving the engine at 91°C. The data for the HT cooling water circuit can be seen in Table 2.5.

HT cooling syst. part	Unit	12V50DF	6L50DF
Pressure after pump (514 rpm)	bar	3.15	2.8
Temperature before engine, approx	°C	74	74
Temperature after engine, nom.	°C	91	91
Pump capacity, nom.	m^3/h	270	135
Pressure drop over engine	bar	0.5	0.5
Water volume in engine	m^3	1.7	0.95
Pressure from expansion tank	bar	0.7-1.5	0.7-1.5
Pressure drop over central cooler, max	bar	0.6	0.6

Table 2.5: High Temperature cooling water system (BW Gas, 2009).

Chapter 3

Exergy Analysis

A conventional energy analysis is only based on the first law of thermodynamics that states that energy and mass are always conserved (Kalyan Annamalai, 2001). This means that by performing an energy balance on an ICE, the available waste heat from the engine will be the difference between the energy added to the system by the fuel, and the work produced by the engine. This is a highly idealized analysis and in order to do a more realistic evaluation of the engine under investigation, an exergy analysis will be performed (Kalyan Annamalai, 2001). Exergy is measured in the same unit as energy, but in contrary to energy, it is based on both the first and the second law of thermodynamics (Moran et al., 2010). The second law accounts for entropy production, also called irreversibilities, within the system. Irreversibilities are spontaneously processes that can not be brought back to their initial states without doing work on the system of interest. Typical irreversibilities according to (Moran et al., 2010) include:

- Heat transfer through a finite temperature difference.
- Unrestrained expansion of a gas or liquid to a lower pressure.
- Spontaneous chemical reactions.
- Spontaneous mixing of matter at different compositions or states.
- Friction; sliding friction as well as friction in the flow of fluids.

When including the second law of thermodynamics into engineering, it is possible to evaluate the best theoretical performance of a system (Moran et al., 2010). By doing so, one is able to evaluate the potential for improvement in performance for an existing system, or to have a

realistic performance target for a system or product under development.

Exergy is often explained as available and useful energy (Kalyan Annamalai, 2001). An example of this is a hydropower station with a dam filled to its limit with water. This is an immense resource of available energy. However, if the floodgates are opened so the water can run freely down the river path, the energy will still be conserved in the water, but the available energy in the water has significantly decreased. The water running down the river path has a lower exergy than what it had behind the dam. It will no longer be possible to utilize the water to create electricity without adding work by pumping it back up to the dam.

In this chapter it will be performed an exergy analysis on two of the waste heat sources of the main engine; the jacket cooling water and the exhaust stream.

3.1 Assumptions for Exergy Analysis

3.1.1 Exergy Reference Environment

When calculating exergy it is necessary to define a reference environment because exergy is always evaluated relative to the environment surrounding the system of interest (Moran et al., 2010). The exergy of a system is the maximum theoretical obtainable work when the system is brought to thermal, mechanical and chemical equilibrium with the reference environment (Moran et al., 2010).

In this analysis, the reference environment will be set to $T_0 = 25°C$ and $P_0 = 1$ atm which is a common reference environment used in literature (Kalyan Annamalai, 2001) (Moran et al., 2010) (Bejan and Moran, 1996). Since the machinery system under investigation is aboard a ship that operates on global shipping routes, the temperature of the environment will of course vary. Since there is no accessible weather data for the ship, the variation of the temperature will not be considered. It should, however, be noted that the exergy will be higher when the ship is sailing in colder areas, and lower in warmer regions of the world (Kalyan Annamalai, 2001) (Etele and Rosen, 1999).

3.1.2 Combustion Model

The chemical composition of the combustion products has to be determined before the exergy of the exhaust stream can be calculated. The only way of determining the real chemical composition of combustion products, is by measurement (Moran et al., 2010). The composition of the exhaust stream has not been measured on the case vessel. Because of that, complete combustion has to be assumed in order to determine the combustion products (Moran et al., 2010). When complete combustion is assumed, the only components present in the products will be carbon dioxide (CO_2), water (H_2O), nitrogen (N_2) additionally to oxygen (O_2) when the air/fuel ratio is above the theoretical amount of air[1] (Moran et al., 2010). Complete combustion is an idealized model, and an actual combustion process is a result of complicated chemical reactions and a number of uncontrollable factors (Moran et al., 2010) (Heywood, 1988) (Woodyard, 2009);

- Pressure and temperature of the fuel and air.
- The mixing of the fuel and air inside the cylinders vary for every power cycle.
- Traces of carbon monoxide (CO), unreacted fuel and unburned oxygen can appear in the exhaust even though the air supplied is above the theoretical amount of air. Reasons for this can be;
  - Incomplete mixing of fuel and air.
  - Too little time for complete combustion.
  - Misfiring and flame quenching due to cold cylinder walls.

As mentioned in Chapter 2, the engines under consideration are always running on boil-off gas from the LNG tanks (C. Chryssakis DNV GL, 2015). Diesel is used in small amounts (less than 1% of full-load fuel consumption) as pilot fuel for ignition (Wärtsilä, 2014). To decrease the complexity of the analysis, the pilot fuel contribution to the chemical reaction balance will be neglected. If this was included, sulphur oxides (SOx) would be present in the combustion products where the amount would be dependent on the amount in the diesel fuel. However, only very small traces would be present considering diesel fuels have a sulfur content less than 3.5%

[1] The minimal amount of air that supplies sufficient oxygen for the complete combustion of the fuel (Moran et al., 2010).

in global areas, and less than 0.1% in the Emission Control Areas (ECA) after new regulations were implemented in January 2015 (Pedersen, 2015).

Further, it will be assumed that the nitrogen is inert and can not react chemically with the combustion air to form nitrogen oxides (NO_x). For the Wärtsilä 12V50DF engine, the NO_x content in the fuel would typically be around 2 g/kWh (Wärtsilä, 2014). Since this is a study of exergy and not emissions, neglecting NO_x will not give a great impact on the exhaust exergy except complicate the calculations (Kalyan Annamalai, 2001) (Moran et al., 2010). Additionally, it is assumed that the engine is heated up and has reached steady state operation. Effects from motion and gravity will be neglected.

3.1.3 Fuel and Combustion Air Composition

The molar composition of the natural gas fuel will be based on measurement data. The fuel composition will be modeled as an ideal gas mixture. The ideal gas law is accurate at relatively low pressures and high temperatures, which suits well the stoichiometric combustion reaction balance (Moran et al., 2010).

The combustion air will be modeled as dry air with 21% oxygen and 79% nitrogen on molar basis. The dry air signifies that there is no water vapor present in the air (Kalyan Annamalai, 2001). In real applications, the combustion air would contain almost 1% argon, and some small traces of carbon dioxide, neon, helium, methane and others (Moran et al., 2010). However, to decrease the complexity when calculating the chemical reaction balance, these substances will be left out. This idealization gives a molar ratio of nitrogen to oxygen to be $0,79/0,21 = 3,76$ kmol N_2 per kmol O_2.

3.1.4 Summary of Assumptions

1. The reference environment set to $T_0 = 25°C$ and $P_0 = 1$ atm.
2. Complete combustion.
3. The fuel mixture is modeled as an ideal gas.
4. The combustion products act as an ideal gas mixture.
5. Nitrogen is inert.

6. Combustion air will be modeled as 1 mole of oxygen and 3.76 mole of nitrogen.
7. Effect from diesel pilot injection to the combustion products will be neglected.
8. Effects of motion and gravity will be neglected.
9. Engine is operating in steady state.

3.2 Discussion on Available Data

3.2.1 Molar Analysis of Fuel

The gas chromatograph installed in the case vessel measures the molar analysis of methane (CH_4), ethane (C_2H_6), propane (C_3H_8) and nitrogen. The measurement data for methane and nitrogen can be seen in Figure 3.1, and ethane and propane in Figure 3.2. The case vessel was reloaded with LNG at Hammerfest LNG plant early in October 2014 (C. Chryssakis DNV GL, 2015). This can be seen in Figure 3.1 at the point where the nitrogen content increases from about 0% to 23-25%. Since LNG is stored at -162°C, nitrogen will evaporate faster than methane, propane and ethane due to nitrogen's lower normal boiling point (Kidnay et al., 2011). The NBP's of the LNG substances can be seen in Table 3.2. The data from the gas chromatograph in Figure 3.1 verifies this, where it is evident that the content of nitrogen is decreasing, and therefore causing the molar concentration of methane to increase. Despite the fluctuations in the measurement data, both methane and nitrogen show a more or less linear change in the composition.

The content of ethane and propane are very low compared to methane and nitrogen as can be seen in Figure 3.2. Ethane is between 0.1-1 mol% and propane is below 0.2 mol%. A small increase in the mol% for both ethane and propane can be seen due to the previous mentioned boil-off of nitrogen.

Based on measurement data from the gas chromatograph, a varying composition (see Table 3.1) is decided in order to investigate how the fuel composition influences the exhaust exergy. For analysis on how other parameters influence the exhaust exergy, a fixed fuel composition as presented in Table 3.1 will be applied. Since the content of nitrogen decreases, the calorific value of the fuel is expected to increase during the ship voyage due to nitrogens zero lower heating value (LHV), (see Table 3.2). This will in all likelihood cause the exergy of the exhaust to increase

towards the end of the ship voyage since it is directly influenced by the fuel composition (Moran et al., 2010).

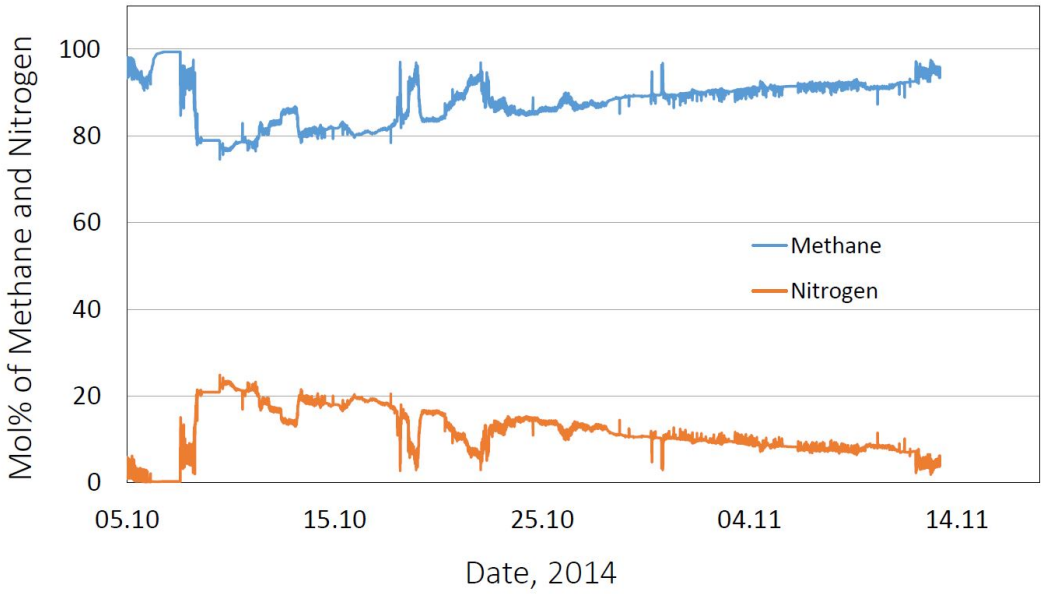

Figure 3.1: Molar analysis of Methane (top) and Nitrogen (bottom) from gas chromatograph (C. Chryssakis DNV GL, 2015).

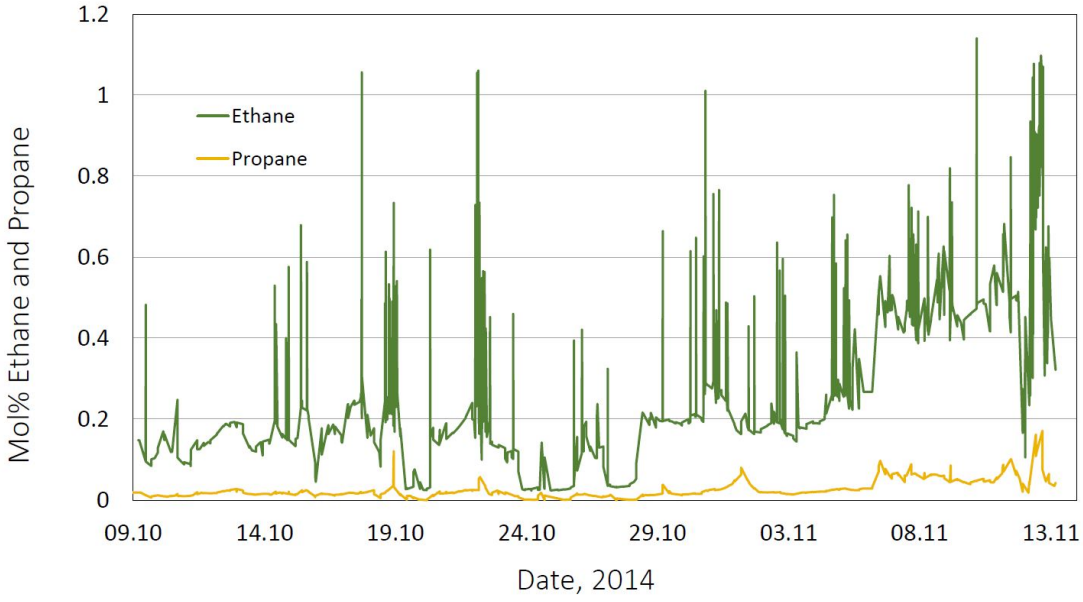

Figure 3.2: Molar analysis of Ethane (top) and Propane (bottom) from gas chromatograph (C. Chryssakis DNV GL, 2015).

Reactants		Varying comp.	Fixed comp.
		%mol	%mol
Methane	CH_4	75→ 95	86,58
Nitrogen	N_2	24.88→ 4.1	12,85
Ethane	C_2H_6	0.1 → 0.8	0,5053
Propane	C_3H_8	0.02 → 0.1	0,06632

Table 3.1: Composition of fuel for exergy analysis (C. Chryssakis DNV GL, 2015).

Substance		LHV [kJ/kg]	NBP [°C]
Methane	CH_4	50010	-161.6
Nitrogen	N_2	0	-195.5
Ethane	C_2H_6	47484	-88,6
Propane	C_3H_8	46353	-42

Table 3.2: Lower heating values for fuel substances (Kidnay et al., 2011).

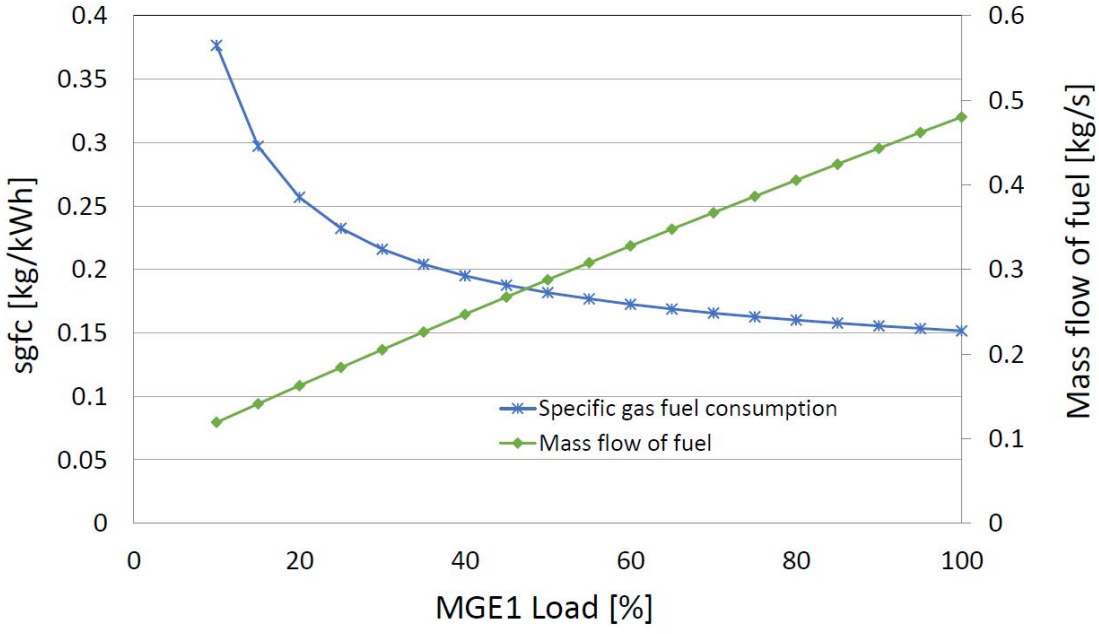

Figure 3.3: Specific gas fuel consumption and mass flow of fuel based on load (C. Chryssakis DNV GL, 2015).

3.2.2 Mass Flow of Fuel

No measurement data has been available for the mass flow of fuel for the engine in the case vessel. The values for the mass flow of fuel will be based on available data from other similar engines (see Figure 3.3) and the Machinery Operating Manual (BW Gas, 2009). A value of 0.35 kg/s will be used as fixed value when evaluating other parameters influence on the exergy.

3.2.3 Amount of Excess Air

The engine is operating with very lean combustion (Wärtsilä, 2013). No measurement data for the air flow to the MGE has been available for this analysis. Values for the air/fuel ratio will be based on data from the Wärtsilä 50DF Product guide as can be seen in Figure 3.4. Based on this information, the fixed air/fuel ratio, λ, will be set to $\lambda = 2.2$. Additionally, an evaluation of the effect of λ will be given for the operational window; $\lambda = 2.0 - 2.3$. This equals 200-230% excess air.

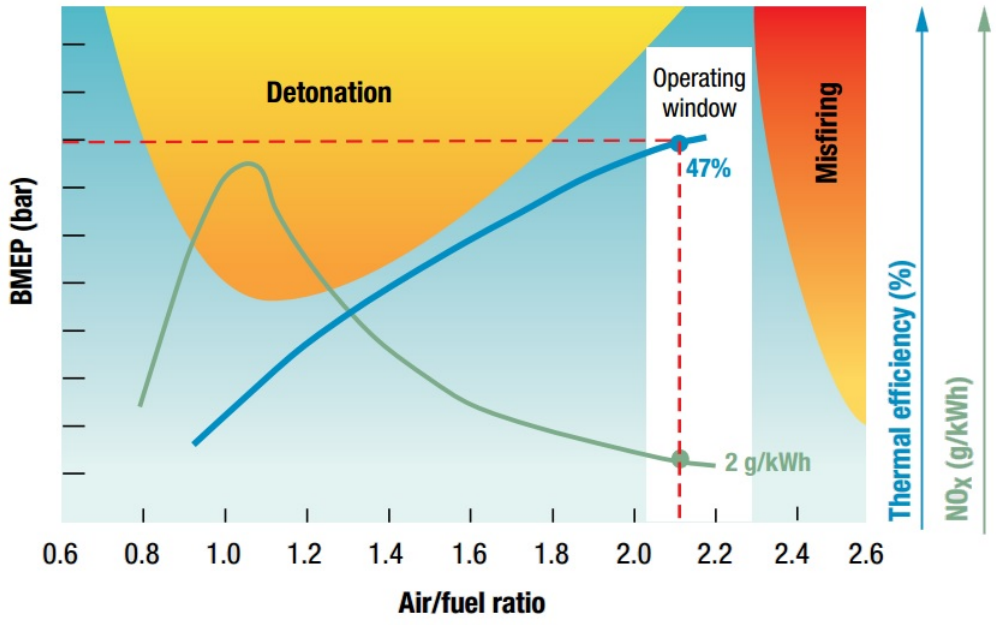

Figure 3.4: Air/fuel ratio operating window for Wärtsilä 50DF engines (Wärtsilä, 2014).

3.2.4 Exhaust Temperature

The exhaust temperature after the turbocharger [TC] has been measured in two different periods; one from May to June 2014 (Figure 3.5), and one from June to August 2014 where the temperature is measured versus load (Figure 3.6) (C. Chryssakis DNV GL, 2015). According to the Machinery Operating Manual, the exhaust temperature should vary between $T_{exh} = 400-450°C$ for 100-50% load respectively which agrees well with the measured data in Figure 3.6 and 3.6. The temperature increases as the load decreases because less air is supplied at lower loads and this causes the temperature to go up (Woodyard, 2009). For the temperature that is plotted versus load in Figure 3.6, it is obvious that the data is very volatile. Even so, it seems as the temperature increases as the load drops until about 40% load.

In order to model the exhaust temperature vs load, a linear regression line has been calculated in Matlab[2] (Equation 3.1) from 40-100% load. The data below 40% is excluded because the engine rarely operates at this load (see operational profile in Chapter 2). This regression equation will be used to investigate how the variation in exhaust temperature based on load influences the exergy.

$$T_{exh}[K] = -0.8039x + 483.14 + 273.15 \tag{3.1}$$

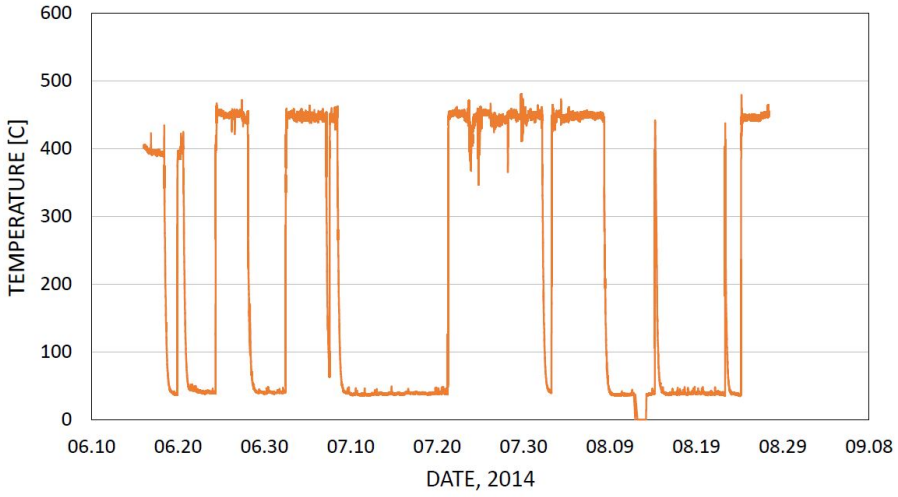

Figure 3.5: Exhaust temperature for MGE1, June to August, 2014 (C. Chryssakis DNV GL, 2015).

[2]MATLAB® is a high-level language for numerical computation, visualization, and application development (MATLAB, 2014).

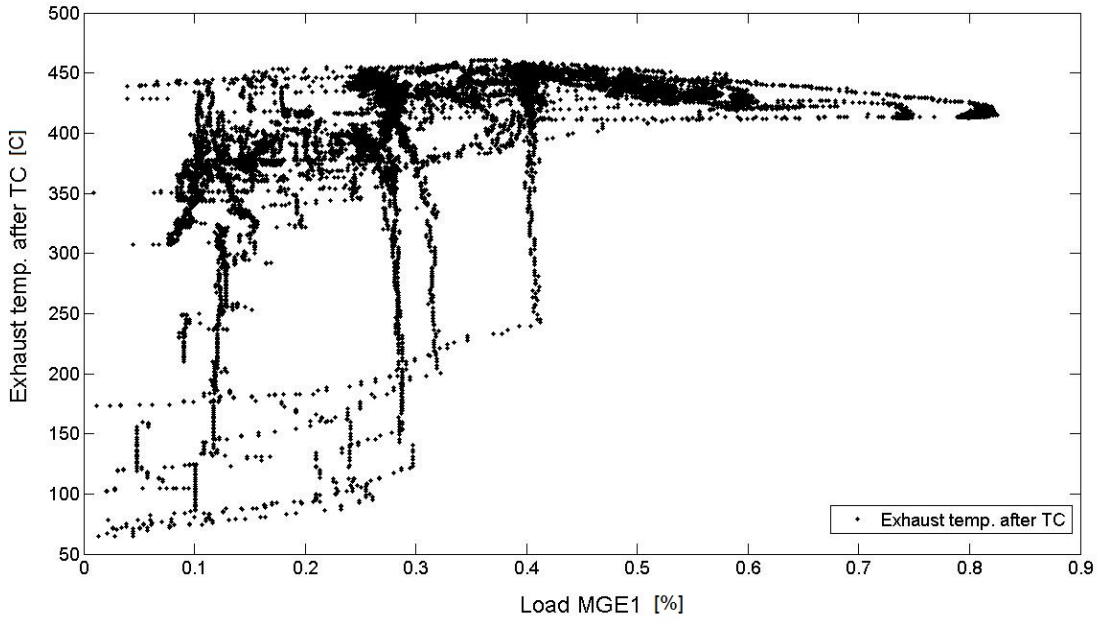

Figure 3.6: Exhaust temperature for MGE1 after Turbo Charger vs load (C. Chryssakis DNV GL, 2015).

Condensation of some of the water vapor in the combustion products will occur when the products are brought to equilibrium with the reference environment (Bejan and Moran, 1996). This can cause corrosion on equipment, and should by all means be avoided (Bejan and Moran, 1996). Due to this, the exhaust should not reach a temperature below $T_{exh,out} = 120°C$.

3.2.5 Cooling Water Measurement Data

No data has been accessible for the CW, so assumptions are necessary. Assumptions will be taken for mass flow, temperature and pressure of cooling water. These assumptions will be based on information given for the high temperature CW system in the ship's Machinery Operating Manual as presented in Chapter 2.

3.2.6 Summary of Data Evaluation and Model Parameters

Property	Fixed value	Varying comp.	Unit
Reference environment pressure, P_0	≥1		atm
Reference environment temperature, T_0	25		°C
Air/fuel ratio, λ	2.2	2.0-2.3	
Fuel mass flow, $\dot{m}_{fuel}$	0.35	≈0.1-0.5	kg/s
Exhaust temperature, T_{exh}	430	Equation 3.1	°C
Exhaust pressure, P_{exh}	1		atm
Exhaust outlet temperature, $T_{exh,out}$	120		°C
Universal gas constant, R	8.314		kJ/kmol K
HT CW inlet temperature, $T_{cw,in}$	91		°C
HT CW outlet temperature, $T_{cw,out}$	≈74		°C
HT CW volumetric flow, $\dot{V}_{cw}$	270	≈200-270	m^3/h
HT CW pressure, $P_{cw,out}$	3.15		bar
Natural gas fuel molar composition	Table 3.1	Table 3.1	ratio

Table 3.3: Parameters for the exergy analysis.

3.3 Exergy Model of Exhaust Stream

3.3.1 Determining Products of Combustion

Before calculating the exergy of the exhaust stream, the combustion products in the exhaust stream need to be known, these are calculated with Equation 3.2. The underlined part is the molar analysis of the natural gas fuel. The q, x, y and z are the molar fractions for each substance in 1 kmol of fuel. The amount of kmol of oxygen is denoted with a. The notations b, c and d are the amount of kmol for each substance in the combustion products based on 1 kmol of fuel.

$$\underline{qCH_4 + xN_2 + yC_2H_6 + zC_3H_8} + a(O_2 + 3.76N_2) \quad \rightarrow \quad bCO_2 + cH_2O + dN_2 \tag{3.2}$$

Equation 3.2 is balanced with Equation 3.3 to 3.6. The amount of kmol for each substance, i, in the combustion products based on 1 kmol of fuel, are denoted with n_i:

$$\text{CARBON}: \quad b = \frac{q + 2y + 3z}{2} \quad \rightarrow \quad b = n_C \tag{3.3}$$

$$\text{HYDROGEN}: \quad c = \frac{4q + 6y + 8z}{2} \quad \rightarrow \quad c = n_H \tag{3.4}$$

$$\text{OXYGEN}: \quad a = \frac{2b + c}{2} \quad \rightarrow \quad a = n_O \tag{3.5}$$

$$\text{NITROGEN}: \quad d = \frac{2x + 2 \cdot 3.76a}{2} \quad \rightarrow \quad d = n_N \tag{3.6}$$

The theoretical air/fuel ratio on a molar and mass basis is calculated with Equation 3.7 and 3.8 respectively.

$$\overline{AF}_{theoretical} = \frac{a + 3.76a}{q + x + y + z} \tag{3.7}$$

$$AF_{theoretical} = \overline{AF}_{theoretical}\left(\frac{MW_{air}}{MW_{fuel}}\right) \tag{3.8}$$

Amount of Excess Air

As mentioned in Section 3.2.3, the engine will always operate in lean mode. This will cause oxygen to be present in the combustion products in addition to an increase in the amount of nitrogen (Kalyan Annamalai, 2001). In order to include the effect of excess air, the reaction equation has to be balanced once more after the theoretical amount of air has been calculated. The quantity of CO_2 and H_2O in the products will not change due to no increase in hydrocarbons (Moran et al., 2010).

$$\text{Lean combustion}: \lambda = \frac{AF}{AF_{theoretical}} > 1 \tag{3.9}$$

Second balancing of reaction equation;

$$qCH_4 + xN_2 + yC_2H_6 + zC_3H_8 + \lambda a(O_2 + 3.76N_2) \quad \rightarrow \quad bCO_2 + cH_2O + d_2N_2 + eO_2 \tag{3.10}$$

Applying conservation of mass principle to the of amount of oxygen and nitrogen to the reaction balance;

$$\text{OXYGEN}: \quad e = \frac{\lambda 2a - 2b - c}{2} \quad \rightarrow \quad e = n_{O,p} \tag{3.11}$$

$$\text{NITROGEN}: \quad d_2 = \frac{2x + \lambda a(2 * 3.76)}{2} \quad \rightarrow \quad d_2 = n_{N,p} \tag{3.12}$$

Calculation of final molar analysis of the exhaust;

$$y_{CO_2} = \frac{b}{b + c + d_2 + e} \tag{3.13}$$

$$y_{H_2O} = \frac{c}{b + c + d_2 + e} \tag{3.14}$$

$$y_{N_2} = \frac{d}{b + c + d_2 + e} \tag{3.15}$$

$$y_{O_2} = \frac{e}{b + c + d_2 + e} \tag{3.16}$$

3.3.2 Exergy Calculation

Exergy consists of both thermomechanical and chemical exergy (Kalyan Annamalai, 2001). In Equation 3.17, the chemical contribution to the exergy is denoted with $\boldsymbol{e}^{ch}$, and the thermomechanical contribution is denoted with $\boldsymbol{e}^{mech}$. Equation 3.18 shows the total specific flow (f) exergy for a specific substance, i, with the thermomechanical contrubution underlined. The $\bar{h}$ and $\bar{s}$ refer to the specific enthalpy and entropy of the fluid, respectively, while the $\bar{h}_0$ and $\bar{s}_0$ refer to the corresponding values of the fluid when it goes to equilibrium with the environment. The bar over the symbols signifies that the exergy is calculated on a molar basis. As previously mentioned, the effect of motion and gravity will be neglected. The amount of kmol of a specific substance, i, in the combustion products is denoted with n_i.

$$\boldsymbol{e}_{tot} = \boldsymbol{e}^{mech} + \boldsymbol{e}^{ch} \tag{3.17}$$

$$\bar{\boldsymbol{e}}_{f,i} = \Big[\underline{\bar{h}_i - \bar{h}_{i,0} - T_0(\bar{s}_i - \bar{s}_{i,0}) + \frac{V_i^{\cancel{2}}}{\cancel{2}} + \cancel{g z_i}} + \bar{\boldsymbol{e}}^{ch}\Big] n_i \tag{3.18}$$

The chemical exergy is calculated with Equation 3.19. T_0 is the temperature of the reference

environment, y_i is the mole fraction of component i in the exhaust at T_0 and p_0, and y_i^e is the mole fraction of component i in the environment at T_0 and p_0.

$$\bar{\boldsymbol{e}}^{ch} = \bar{R}T_0 \sum_i y_i \ln\left(\frac{y_i}{y_i^e}\right) \tag{3.19}$$

When evaluating entropy by using tables, as is normal in thermodynamic learning books, it is only the absolute entropy[3], $\bar{s}_i^\circ(T)$, that is available for a specific temperature and a constant pressure, p=1 atm (Moran et al., 2010). In order to calculate the specific entropy when using tables, it is necessary to extend the entropy part of Equation 3.18 to Equation 3.20 to include the effect of a specific pressure.

$$\bar{\boldsymbol{e}}_i^{mech} = \left[\bar{h}_i - \bar{h}_0 - T_0\underline{\left(\bar{s}_i^\circ(T) + \bar{s}^\circ(T_0) - \overline{R}\ln\left(\frac{y_i p}{p_0}\right)\right)}\right] n_i \tag{3.20}$$

However, for this analysis it will not be necessary to change the equations in order to account for pressure effects. This is because the exergy model built for this analysis has been built by the use of EES. In EES, the built-in entropy function used in the model returns the specific entropy of a substance based on both a specific temperature and pressure (Klein and Alvarado, 2002). The entire exergy analysis built in EES can be reviewed in Appendix A.

When a difference in flow exergy between different states of the same composition is evaluated, there will be no chemical contribution because there will be no chemical reactions between to similar mixtures, leaving just the difference in the thermomechanical contribution, see Figure 3.7.

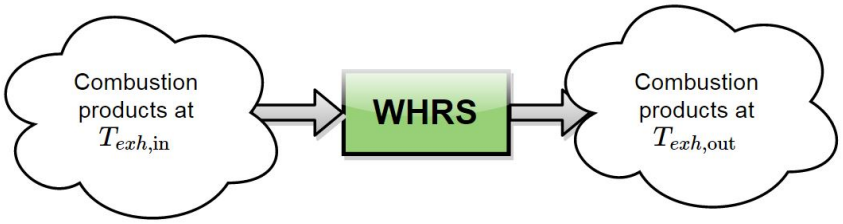

Figure 3.7: Net rate of thermomechanical exergy contribution in and out of WHRS (Figure developed in Draw.io (2015)).

[3]The change of entropy of a substance between absolute zero and any given state. $\bar{s}_i^\circ(T)$ (Moran et al., 2010).

As discussed in Section 3.2.4, the exhaust should not reach a temperature below $T_{exh,out}$ = 120°C. Therefore, it is more correct to calculate the net rate of exergy carried into the waste heat recovery system (the ORC or the SE), because the exhaust gas mixture will not be allowed to reach the temperature of the environment and react with the surrounding air, see Figure 3.7 (Moran et al., 2010).

Due to this, the chemical exergy contribution that would occur if the gas mixture from the combustion products was allowed to react with the surrounding air will not be added to the total exergy calculation. The chemical contribution will therefore not give additional exergy to the exhaust flow, and will be considered as a loss. Equation 3.17 is then reduced to Equation 3.21:

$$\bar{\boldsymbol{e}}_{f,i} = \left[\bar{h}_{in,i}(T_{exh,in}) - \bar{h}_{out,i}(T_{exh,out}) - T_0\big(\bar{s}_{in,i}(T_{exh,in}) - \bar{s}_{out,i}(T_{exh,out})\big)\right] n_i \tag{3.21}$$

In Equation 3.21, enthalpy, $h_{in,i}$ and entropy, $s_{in,i}$ values at $T_{exh,in}$ account for the enthalpy and the entropy of substance i of the combustion products at the exhaust inlet temperature to the waste heat recovery system. Enthalpy, $h_{out,i}$ and entropy, $s_{out,i}$ values at $T_{exh,out}$ account for the specific enthaply and entropy values as the exhaust outlet temperature; $T_{exh,out}$ = 120°C.

The exergy is changed from molar to mass basis by dividing the molar exergy with the molar weight of the fuel, MW_{fuel}. The molar weight of the fuel is calculated in EES based on the fixed fuel composition presented in Table 3.1.

$$\boldsymbol{e}_{f,i}[\text{kJ/kg fuel}] = \frac{\bar{\boldsymbol{e}}_{f,i}}{MW_{fuel}} \tag{3.22}$$

The total exergy in kW in the exhaust is calculated by multiplying the exergy on a mass basis by the mass flow of fuel, $\dot{m}_{fuel}$.

$$\dot{\boldsymbol{e}}_{f,tot}[\text{kW}] = \dot{m}_{fuel} \sum_i \boldsymbol{e}_{f,i} \tag{3.23}$$

3.4 Exergy Model of CW

The exergy of the cooling water will be calculated in the same way as the exhaust exergy. Since it is only possible to utilize the energy in the temperature range of 91-74°C, it is only necessary to account for the net flow rate of exergy, as discussed in the previous section.

$$\bar{\boldsymbol{e}}_{f,cw} = \left[\bar{h}_{in,i}(T_{cw,in}) - \bar{h}_{out,i}(T_{cw,out}) - T_0\left(\bar{s_{in,i}}(T_{cw,in}) - \bar{s}_{out,i}(T_{cw,out})\right)\right]_{cw} \tag{3.24}$$

The mass flow of the CW is calculated from the volumetric flow rate of the CW, $\dot{V}_{cw}$, and the density of the cooling water at 91°C, $\rho_{cw}[T_{cw}]$.

$$\dot{m}_{cw} = \left[\dot{V}_{cw}\rho_{cw}[T_{cw}]\right]_{cw} \tag{3.25}$$

The total exergy in the CW is calculated by dividing the molar exergy, $\bar{\boldsymbol{e}}_{f,cw}$, with the molar weight of water, MW_{water}, and multiplying it with the mass flow, $\dot{m}_{cw}$.

$$\dot{\boldsymbol{e}}_{f,cw} = \dot{m}_{cw}\frac{\boldsymbol{e}_{f,cw}}{MW_{water}} \tag{3.26}$$

3.5 Results and Discussion of Exergy Analysis

The objective of this chapter was to perform an exergy analysis on the waste heat sources of the MGE1. Both the exhaust stream and the high temperature cooling water stream of the MGE1 were analyzed. The influence of input parameters such as variation in hydrocarbon content in fuel, the exhaust temperature, the air/fuel ratio and the mass flow of both fuel and CW were investigated.

Exhaust Stream

In Figure 3.8 the results on how the various parameters affected the exergy in the exhaust can be seen. The values are calculated by keeping all parameters fixed at the values presented in Table 3.3, and then each parameter; HC content, T_{exh}, air/fuel ratio, λ, and finally the mass flow of fuel, $\dot{m}_{fuel}$ are changed withing the range presented in Figure 3.8. The figure shows that an increase in every parameter will give an positive change in the exhaust exergy. Especially the fuel flow affects the exergy to a great extent compared to the other parameters. The variation in the air/fuel flow gives the smallest impact.

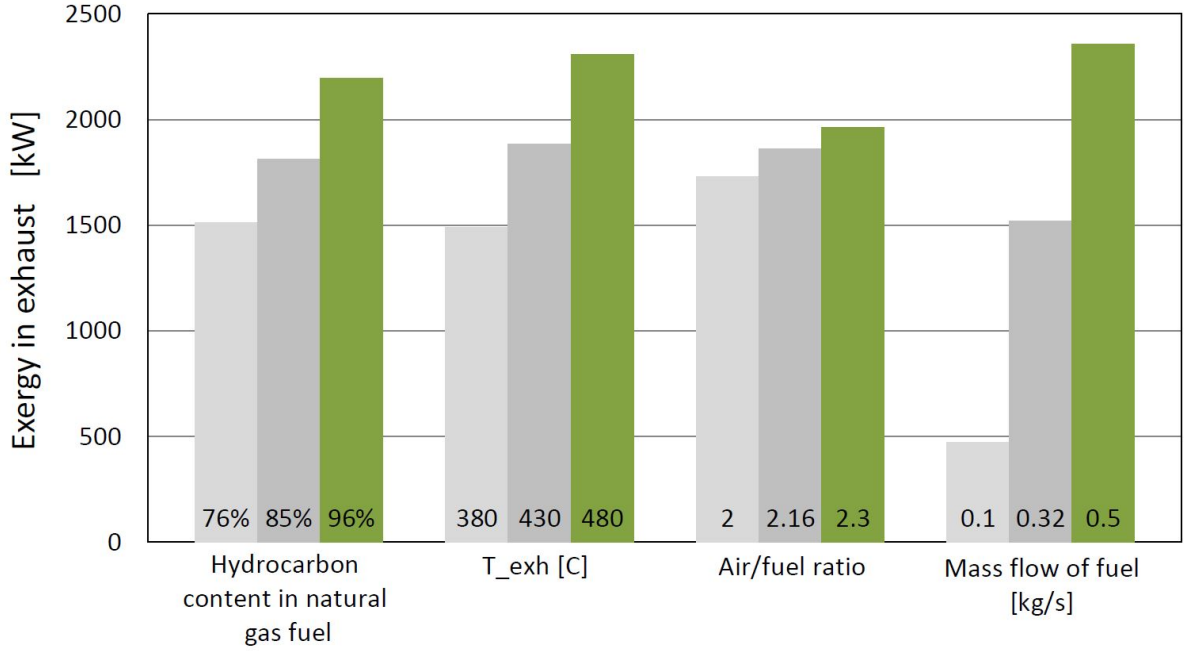

Figure 3.8: Exergy in exhaust vs air/fuel ratio, λ, T_{exh}, $\dot{m}_{fuel}$ and HC content in fuel.

The parameters in Figure 3.8 are not corrected for engine load. The hydrocarbon content in the fuel does not get influenced by the engine load, since this is only based on the boil-off gas from the LNG storage tanks as discussed in Section 3.2.1. The content of hydrocarbons in the fuel is on the highest at the end of a voyage. This implies that the potential of energy recovery will be significantly better dependent on how long the LNG has been stored. As can be seen in Figure 3.8, the exergy varies from 1500 kW to around 2200 kW dependent on the hydrocarbon content, which is almost equal to 50% increase in the exergy.

The mass of fuel flow and the temperature of the exhaust do however get influenced by the engine load as have been discussed in Section 3.2.2 and Section 3.2.4. Mass flow is the highest at highest load, however, the temperature of the exhaust is higher at loads around 40-50% (see Figure 3.6). The combined effect of the variation of both the temperature and the mass flow of fuel based on load gives a variation in the exergy as can be seen in Figure 3.9. The air/fuel ratio, $\lambda = 2.2$, and the fixed fuel composition presented in Table 3.1 were used in this calculation. Even though the temperature has a decrease of approximately 50°C from 40-100% load, the exergy increases. This is due to the fact that the mass flow of fuel increases as the load increases, and since this parameter has such an extensive effect on the exergy, the exergy will increase even though the temperature has a drop of ≈50°C.

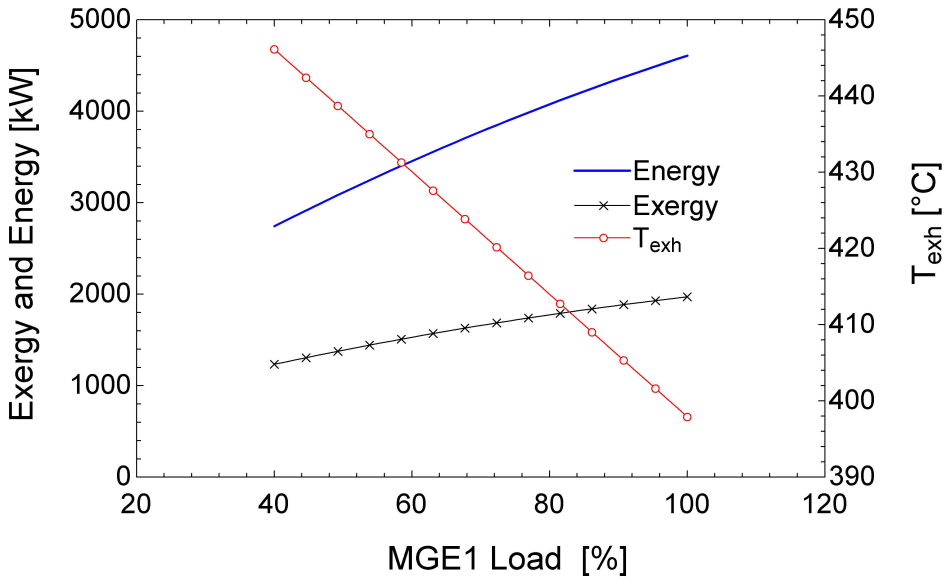

Figure 3.9: Exergy and energy in exhaust vs MGE1 load

In Figure 3.9, a conventional energy calculation is plotted together with the exergy. Not surprisingly, the energy analysis gives more or less the double amount of exhaust exergy. This is caused by the fact that a conventional energy analysis does not account for the second law of thermodynamics and entropy production due to irreversibilities (Kalyan Annamalai, 2001) (Moran et al., 2010). This agrees well with former comparative studies between energy and exergy analyses (Dimopoulos and Kakalis, 2014) (Sayin et al., 2007) (Al-Najem and Diab, 1992) (Fu et al., 2013). This also shows the importance of performing thorough and detailed evaluations of available waste heat before discussing waste heat recovery alternatives.

The exergy in the exhaust stream is about 1300-2000 kW for 40-100% load respectively, which corresponds to 28-18% of the engine's power output as can be seen in Figure 3.10. The percentage of waste heat to the MGE1 power output is higher at lower loads. This is expected considering the specific gas fuel consumption decreases as the load increases as was presented in Figure 3.3.

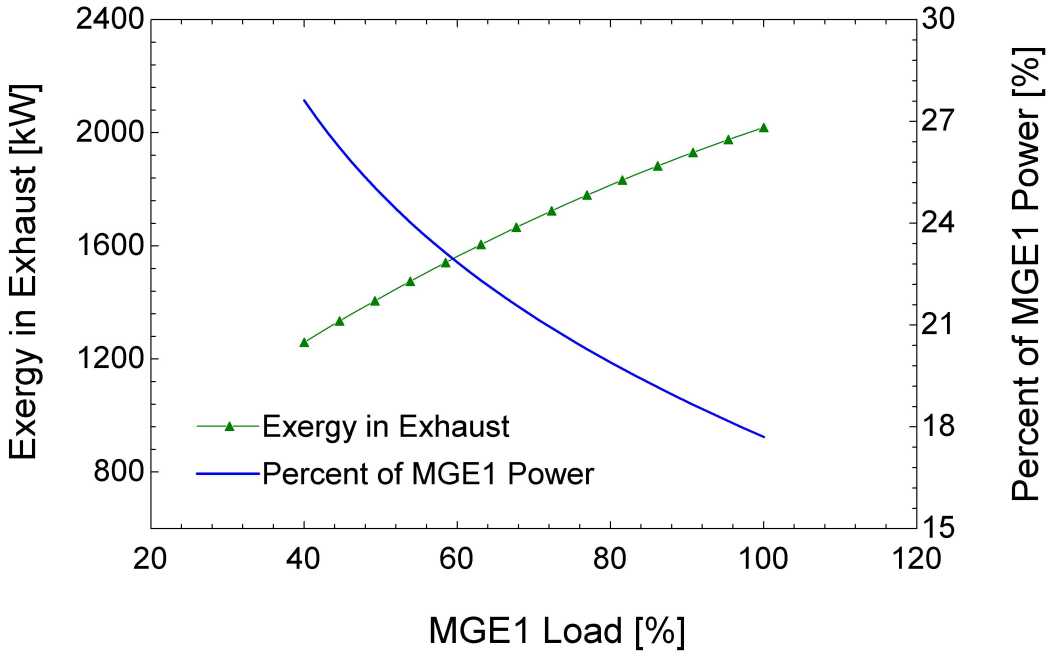

Figure 3.10: Exergy in Exhaust and Percent of MGE1 Power

The highest exergy values are found at maximum load. When evaluating the numbers together with the operational profile of the ship in Figure 2.2 in Section 2.1.1, it is evident that

the ship operates very rarely above 85% load. At 85% the exergy is around 1800 kW. It should be noted that on the case vessel there are two Main Generator Engines of 11.4 MW. That means that if the exhaust could be exited through the same piping, that would signify that the exergy would double. This would mean that one WHR system could benefit from the waste heat from both engines. Further discussion on how the WHR system can be implemented into the existing machinery will be discussed in the technical feasibility section in Chapter 6.

Cooling Water Stream

In Figure 3.11 the results of the exergy analysis of the cooling water can be seen. For this analysis, it was only the mass flow of CW that varied. The temperature was fixed between 91 to 74°C. The exergy in the CW is about 40-50% lower than the value given for energy in the heat balance in the Machinery Operating Manual (Wärtsilä, 2014). The heat loss to the HT jacket water circuit is stated to be 1440 kW in the Machinery Operating Manual (Wärtsilä, 2014).

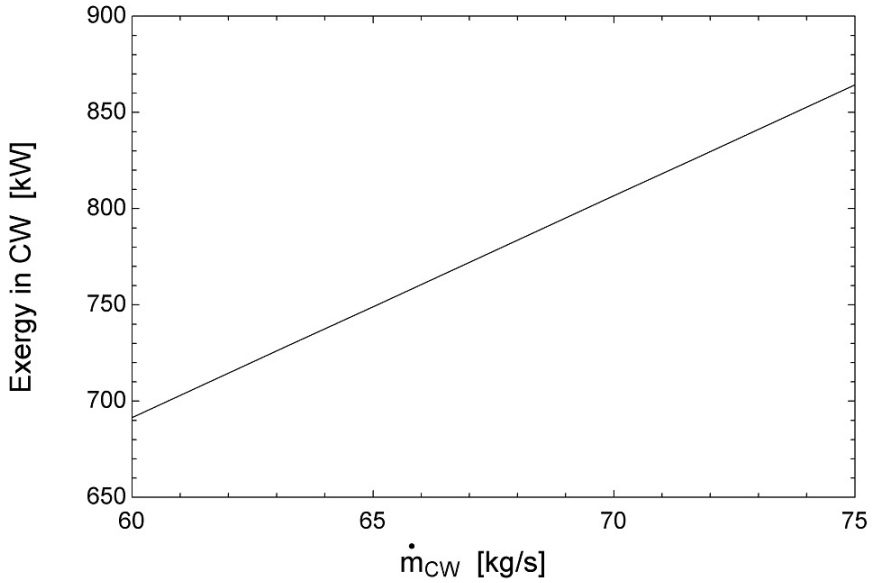

Figure 3.11: Exergy in CW vs mass flow of CW.

In the performance analysis of the Organic Rankine system and the Stirling Engine, the potential of harvesting the calculated exergy in the exhaust and the CW from this section will be evaluated.

Chapter 4

Performance Analysis of Organic Rankine Cycle

4.1 System Design

A significant number of variations of the Organic Rankine cycle exist (Klein and Nellis, 2012). Generally, they are divided into two categories; subcritical and trans-critical cycles. In this analysis, two versions of the subcritical cycle in addition to one trans-critical cycle will be modeled (Klein and Nellis, 2012). The subcritical and the trans-critical Organic Rankine cycles are differentiated dependent on where the four thermodynamic processes take place relative to the critical pressure of the working fluid.

4.1.1 Subcritical ORC

Figure 4.1 shows the schematics of the subcritical cycle which includes an expander, a condenser, a pump and the evaporator. In this cycle all the four different processes; evaporation, expansion, condensation and pressure increase, take place below the critical pressure of the working fluid. This is the most conventional form of an ORC (Kalyan Annamalai, 2001). The four processes in the subcritical ORC are as follows (Kalyan Annamalai, 2001) (Moran et al., 2010):

TURBINE, Process 1-2: The working fluid enters the turbine as saturated vapor with high pressure and high temperature where it expands from the evaporating pressure to the con-

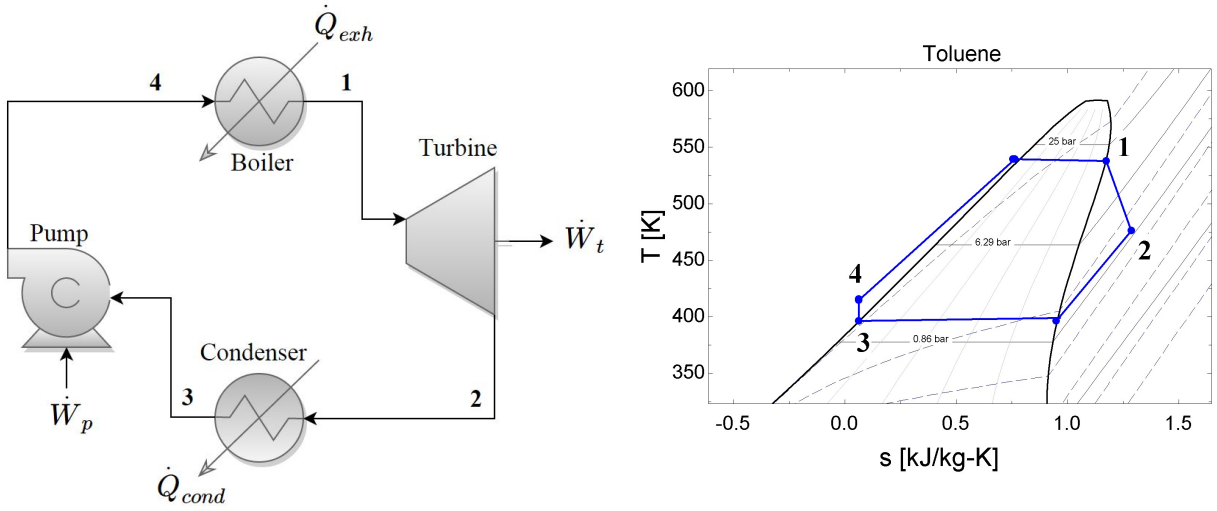

Figure 4.1: Subcritical and Trans-critical ORC, Flowchart and T-s diagram (Flowchart developed in Draw.io (2015) and T-s diagram in EES).

densing pressure. The thermal energy is converted to mechanical energy.

CONDENSER, Process 2-3: In the condenser the heat from the vapor will transfer to the heat sink, which is a heat exchanger with sea water. The working fluid is condensed to saturated liquid.

PUMP, Process 3-4: The working fluid goes trough the pump and the pressure increases from the condensing pressure, P_{cond}, to the evaporation pressure, P_{evap}.

BOILER, Process 4-1: The working fluid is heated by the exhaust from the MGE1 and evaporated to saturated vapor.

4.1.2 Subcritical ORC with Superheat and Regeneration

Figure 4.2 shows the flow chart for the subcritical cycle with superheat and regeneration. Two turbine stages are included, a high pressure turbine, and a low pressure turbine. Additionally, an open feed water heater is implemented between point 5 and 6 to mix the small part of the fluid mixture that does not go through the second turbine stage.

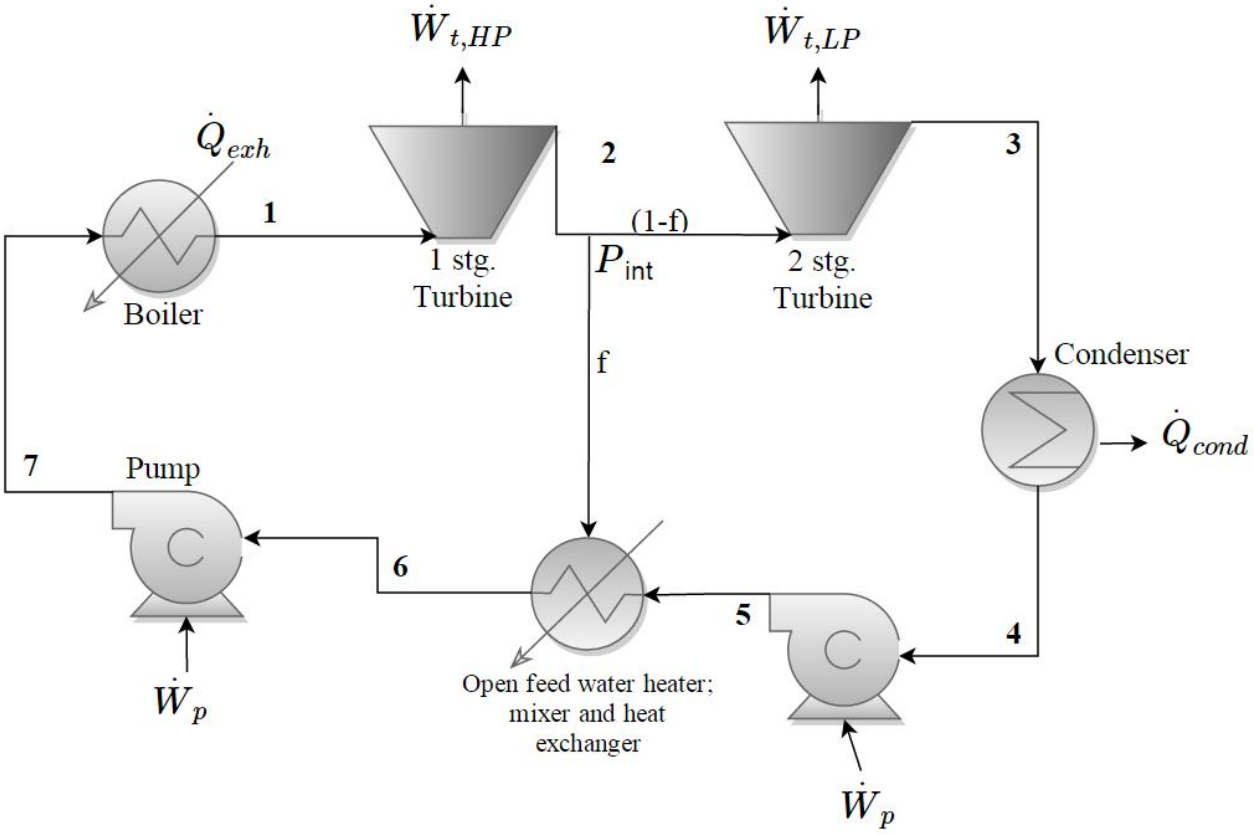

Figure 4.2: Flowchart of subcritical ORC with superheat and regeneration (Flowchart developed in Draw.io (2015)).

4.1.3 Trans-critical ORC

In a trans-critical ORC, or by many researches called supercritical ORC, the heat is added at a pressure higher than the critical pressure for the working fluid (Ladam and Skaugen, 2007). The condensation occurs at a pressure lower than the working fluid's critical pressure, as can be seen i Figure 4.3. The schematics for the trans-critical ORC will be the same as for the subcritical ORC in Figure 4.1. In contradiction to the subcritical cycle, no phase change occurs during heat absorption. Trans-critical cycles give a better temperature match and enhance heat transfer between the heat source and the working medium that will cause less irreversibilities as can be seen in Figure 4.4 (Chen et al., 2010) (Ladam and Skaugen, 2007).

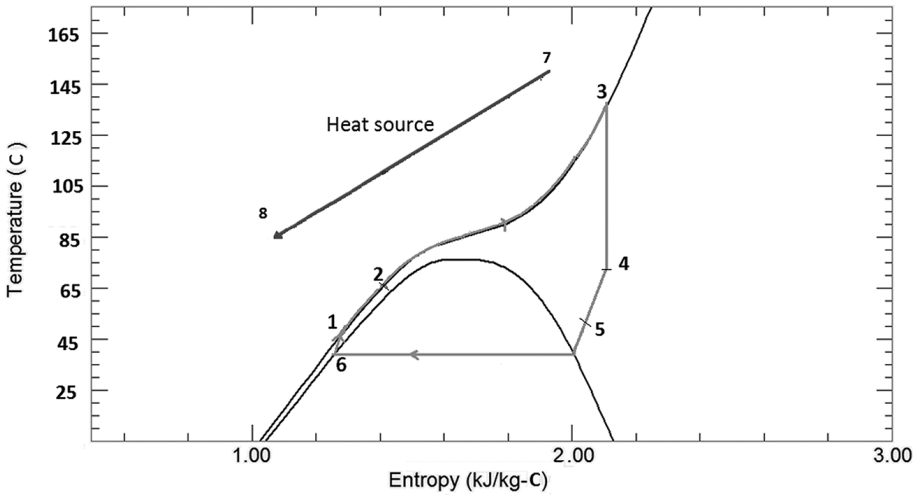

Figure 4.3: T-s diagram of trans-critical ORC (Chen et al., 2006).

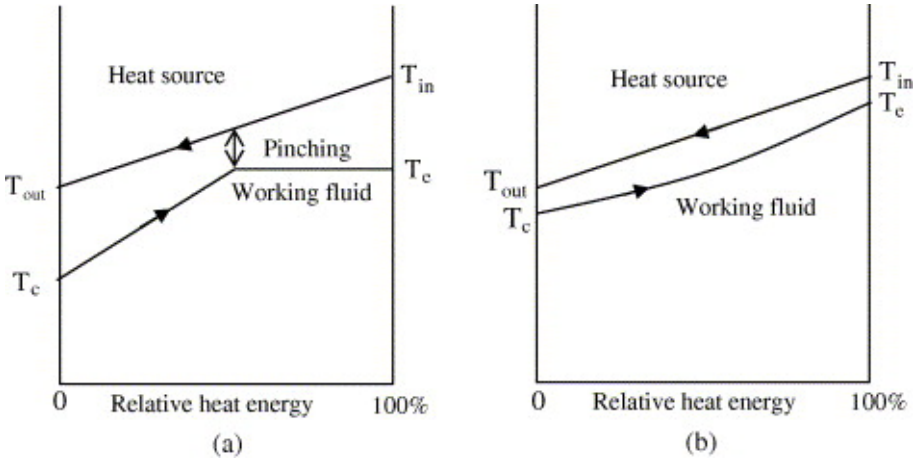

Figure 4.4: Pinch point in subcritical (a) and trans-critical cycles (b) (Chen et al., 2006).

4.2 Selection of Parameters for Thermodynamic Models

The thermodynamic models will be based on the conservation of mass and conservation of energy principles. In order to make the thermodynamic model of the Rankine cycle more realistic, the most important irreversibilities that are present in a real system have to be accounted for. Additionally, limitations due to thermophysical properties of the various working fluids and limitations on pressure levels to reduce the need for complex and expensive systems need to be taken into account.

4.2.1 Pressure Levels

The condensing pressure will be set to $P_{cond} \geq 1$ atm in order to remove the risk of vacuum in the condenser. The condensing pressure should be higher than the atmospheric pressure to avoid leakage of air into the condenser (Guillen et al., 2011). This problem can be avoided with special vacuum equipment, but the equipment is often very expensive and will require more maintenance time and down time (Badr et al., 1985) (Guillen et al., 2011). The condensing pressure is dependent on the condensing temperature which is set to $T_{cond} \geq 330$ K (57°C). The choice of the condensing temperature is discussed in Section 4.4.3. The limit for P_{evap} will be the critical pressure of the working fluids in the subcritical cycles. In the trans-critical cycle, P_{evap} will be set to 150 bar since heat exchangers at this operating pressure have been developed for refrigeration systems and should therefore be feasible (Ladam and Skaugen, 2007).

4.2.2 Pinch Point

The pinch point leads to an important limitation in ORCs by not allowing the exhaust temperature to be lowered far below the temperature where the evaporation takes place (Guo et al., 2014). Limitations will be set in the regenerative ORC EES model to avoid that the temperature at the evaporator limit is above the exhaust exit temperature. For a subcritical ORC, the minimum temperature difference in the evaporator heat exchanger, the pinch point, will take place within the heat exchanger. This will give limitations to the exit temperature of the working fluid and affecting the thermal efficiency (Chen et al., 2006). For working fluids that has a critical temperature far below the exhaust inlet temperature, the location of the pinch point may move to the cold end of the evaporator (Bolland, 2013). A criteria of minimum temperature difference will be set to $T_{exh} - T_{wf,evap} \approx 10$°C at all points in the evaporator to ensure that the temperature of the exhaust and the working fluid never cross.

4.2.3 Effects of Dry, Isentropic and Wet Fluid

For an ORC, the slope of the saturation vapor curve of the working fluid is of high importance (Chen et al., 2006). This curve is the boundary between the superheated vapor state and the two-phase state in a T-s diagram (Kalyan Annamalai, 2001). The curve effects the stage of the

fluid after the expansion process (Kalyan Annamalai, 2001). There are three different saturation vapor curves; a negative (wet), a positive (dry) and an vertical saturation vapor curve as can be seen in Figure 4.5.

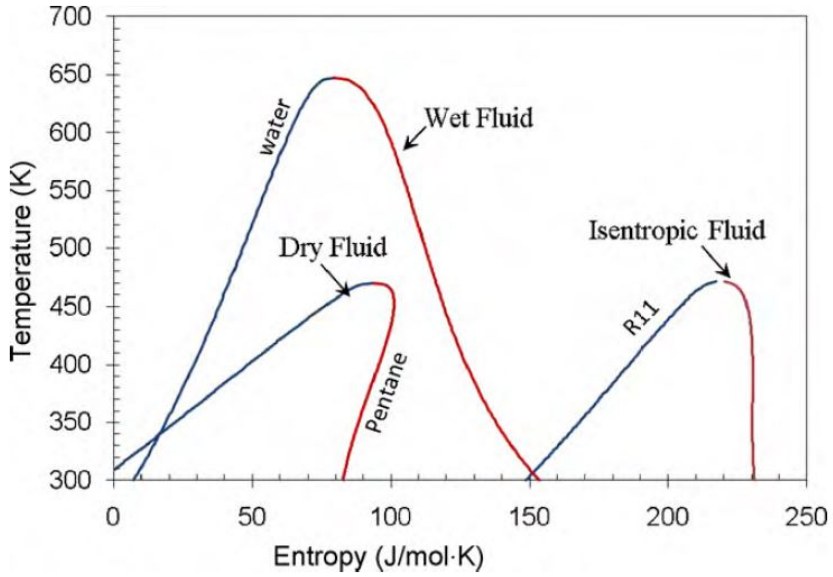

Figure 4.5: T-s diagram for wet, dry and isentropic fluids (Chen et al., 2010).

Negative Saturation Curve: Fluids with a negative saturation curve are often called wet fluids. When a wet fluid is expanded from saturated vapor, the state of the fluid will always be in the two-phase region after expansion and the vapor quality, x, will be less than 1 (Klein and Nellis, 2012). Nozzels within the turbine will convert the high pressure in the working fluid to high velocity (Klein and Nellis, 2012). In case of liquid droplets in the fluid, the droplets will hit the turbine blades with high velocity and cause erosion (Klein and Nellis, 2012). Due to this issue, wet fluids will not be included in the conventional subcritical cycle in this work. The normal solution to avoid this issue it to provide superheating of the fluid, so that the fluid will end in the superheated vapor region after expansion (Chen et al., 2010). Considering this, wet fluids will be included in the subcritical ORC with superheat.

Isentropic Saturation Curve: An isentropic fluid has a near vertical vapor saturation curve. Since there will always be some entropy production in the expansion turbine, the fluid will be in the saturated vapor state after expansion (Klein and Nellis, 2012). Isentropic fluids will be

included in all of the thermodynamic analyses of this work.

Positive Saturation Curve: Fluids with positive saturation curve are called dry fluids. The fluid will always end up in the saturated vapor state after an expansion process and therefore eliminate the issue of erosion on turbine blades (Klein and Nellis, 2012). Additionally, an ORC with a dry fluid can have a cheaper and smaller heat exchanger since there is no need for superheating the vapor before expansion (Sprouse and Depcik, 2013).

4.2.4 Effects of Irreversibilities

Pressure loss: In a real cycle, there will be pressure loss in the condenser heat exchanger, the boiler heat exchanger and in the systems piping due to frictional effects, as can be seen in Figure 4.6 (Kalyan Annamalai, 2001). The pressure loss will be set to 2% in both the condenser and the boiler for the thermodynamic models of the ORCs in this work. Pressure drop in the systems piping will be neglected for simplicity due to low impact on thermal efficiency (Moran et al., 2010) (Kalyan Annamalai, 2001).

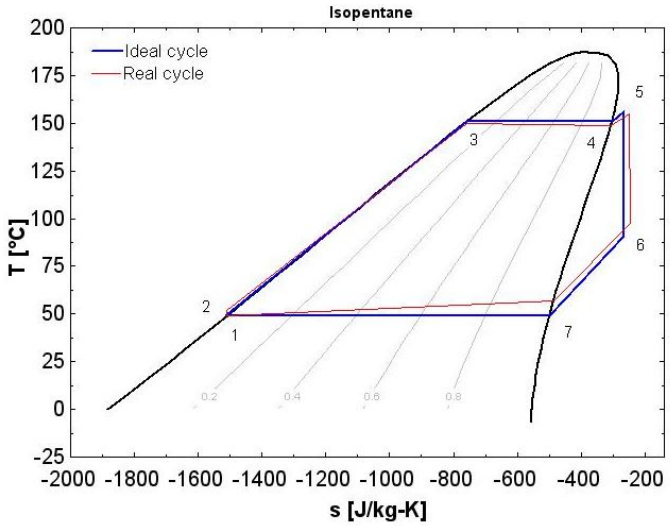

Figure 4.6: Illustration of the effects of pressure losses in an ORC (Klein and Alvarado, 2002).

Entropy Production: Entropy production will be present in both the turbine and the pump (Moran et al., 2010). Entropy production will be accounted for in the form of isentropic efficiencies. The isentropic efficiency of the pump will be set to $\eta_p = 75\%$ and $\eta_t = 80\%$ for the turbine

which are common values reported in literature (Kalyan Annamalai, 2001) (Moran et al., 2010) (Bejan and Moran, 1996).

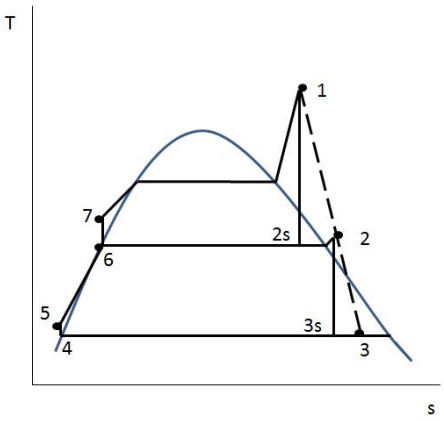

Figure 4.7: Effects of entropy production in a subcritical ORC (Kalyan Annamalai, 2001).

Other Losses: Heat transfer from the components to the surroundings will reduce the amount of heat that can be converted to work (Moran et al., 2010). However, heat losses are not a major source of irreversibilities compared to the previously mentioned losses (Moran et al., 2010), and will therefore not be included in this thermodynamic model. Another loss is the energy carried away with the cooling water. The cooling water under consideration is considered to hold a temperature 10-20°C above the sea water surrounding the ship. Due to this the energy transfer from the working fluid to the CW will only cause a temperature increase of a few degrees, and the utility of the energy loss to the CW will therefore be very low (Kalyan Annamalai, 2001).

4.2.5 Summary of Selection of Thermodynamic Model Parameters

Property	Value	Unit
Minimum condensing pressure, P_{cond}	≥1	atm
Maximum evaporating pressure, subcritical, $P_{evap,sub}$	P_c	bar
Maximum evaporating pressure, trans-critical, $P_{evap,trans}$	150	bar
Evaporator min. temperature difference, $T_{exh} - T_{wf,evap}$	≈10	K
Pressure loss in heat exchangers, dp	2	%
Isentropic efficiency, pump, η_p	75	%
Isentropic efficiency, turbine, η_t	80	%
Condensing temperature, T_{cond}	≥330	K
Minimum vapor quality, expander, x	100	%

Table 4.1: Parameters for the thermodynamic models.

4.3 Thermodynamic Models

4.3.1 Thermodynamic Model of Subcritical ORC

The thermodynamic model presented here is a brief explanation of the model built in EES. See Appendix B for the complete model.

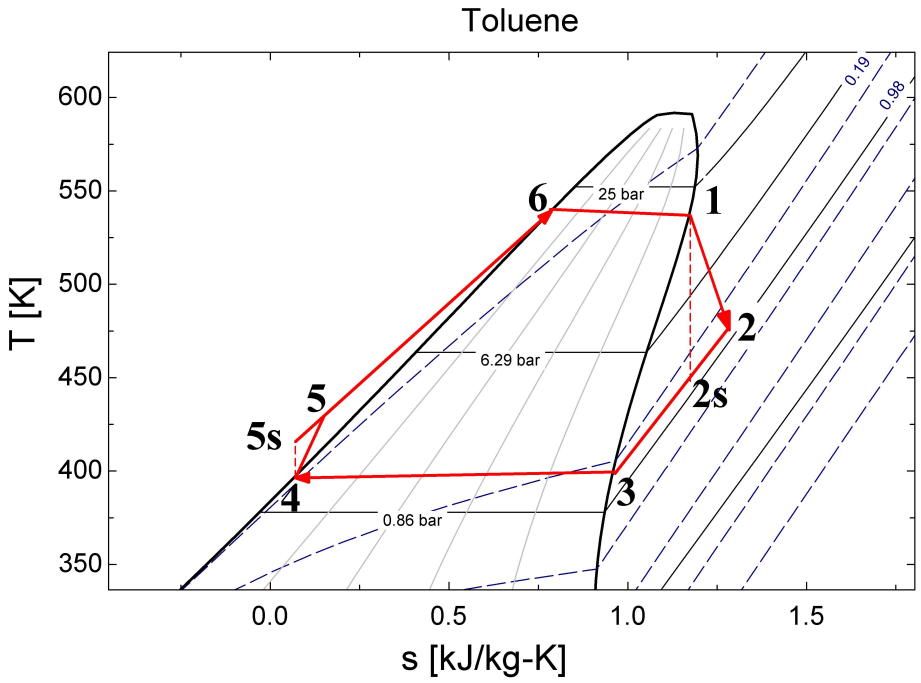

Figure 4.8: Sketch of T-s diagram for subcritical ORC Rankine cycle.

TURBINE, Process 1-2: By neglecting kinetic and potential energy changes and assuming steady state, the energy rate balance in Equation 4.1 reduces to Equation 4.2. The enthalpy values h_1 and h_2 are the specific enthalpies at point 1 and 2 respectively. The enthalpy, h_1, is found in EES by the evaporation pressure and the temperature, T_1.

$$\frac{\cancel{dE}}{\cancel{dt}} = \cancel{\dot{Q}} - \dot{W}_t + \sum_{in} \dot{m}_{wf}\left(h_{in} + \frac{V_{in}^2}{\cancel{2}} + \cancel{g z_{in}}\right) - \sum_{out} \dot{m}_{wf}\left(h_{out} + \frac{V_{out}^2}{\cancel{2}} + \cancel{g z_{out}}\right) \tag{4.1}$$

$$\frac{\dot{W}_t}{\dot{m}_{wf}} = h_1 - h_2 \tag{4.2}$$

$$h_1 = h_1[P_{evap}, T_1] \tag{4.3}$$

Similarly, by applying the steady state form of the entropy balance and neglecting heat transfer, the entropy production in the turbine reduces to the right side of Equation 4.4. The entropy production, $\dot{\sigma}_t/\dot{m}$, can never be negative, and therefore $s_2 > s_1$ (Kalyan Annamalai, 2001). The turbine exit pressure is fixed by the condensing pressure, and the specific enthalpy will decrease as the specific entropy decreases. The difference between $h_2 > h_{2s}$ can therefore be applied with Equation 4.5.

$$\cancel{\frac{dS}{dt}} = \cancel{\sum_j \frac{\dot{Q}_j}{T_j}} + \sum_{in} \dot{m}_{wf} s_{in} - \sum_{out} \dot{m}_{wf} s_{out} + \dot{\sigma}_t \quad \rightarrow \quad \frac{\dot{\sigma}_t}{\dot{m}_{wf}} = s_2 - s_1 \geq 0 \tag{4.4}$$

$$\eta_t = \frac{(\dot{W}_t/\dot{m})}{(\dot{W}_t/\dot{m})_s} = \frac{h_1 - h_2}{h_1 - h_{2s}} \tag{4.5}$$

The enthalpy value at stage 2 can then be calculated with Equation 4.6 in order to include the effects of entropy production.

$$h_2 = h_1 - \eta_t(h_1 - h_{2s}) \tag{4.6}$$

CONDENSER, Process 2-4: The specific enthalpy at point 4 is based on the condensing pressure, and the vapor quality, x.

$$h_4 = h_4[P_{cond}, x = 0] \tag{4.7}$$

When the specific enthalpy at point 4 is calculated, the heat transfer in the condenser, Q_{cond}, can be decided with Equation 4.8.

$$\frac{\dot{Q}_{cond}}{\dot{m}_{wf}} = h_2 - h_4 \tag{4.8}$$

PUMP, Process 4-5: The pump work, $\dot{W}_p$, is calculated with Equation 4.9, 4.10 and 4.11. It is assumed that the specific volume does not vary significantly from point 4 to 5 (Moran et al., 2010).

$$\frac{\dot{W}_p}{\dot{m}_{wf}} = h_5 - h_4 \tag{4.9}$$

$$\frac{\dot{W}_p}{\dot{m}_{wf}} = \int v \mathrm{d}p \approx v_4(p_{evap} - p_{cond}) \tag{4.10}$$

$$v_4 = v_4(P_{cond}, x = 1) \tag{4.11}$$

Same as for the turbine, the enthalpy value at point 5 will be calculated with help of Equation 4.12 in order to include the effects of entropy production.

$$\eta_p = \frac{(\dot{W}_p/\dot{m})_s}{(\dot{W}_p/\dot{m})} = \frac{h_{5s} - h_4}{h_5 - h_4} \tag{4.12}$$

$$h_5 = h_4 + (\dot{W}_p/\dot{m})_s \tag{4.13}$$

BOILER, Process 5-1:

$$\frac{\dot{Q}_{evap}}{\dot{m}_{wf}} = h_1 - h_5 \tag{4.14}$$

Overall Thermal Efficiency

$$\eta = \frac{\dot{W}_t/\dot{m} - \dot{W}_p/\dot{m}}{\dot{Q}_{evap}/\dot{m}} = \frac{(h_1 - h_2) - (h_5 - h_4)}{h_1 - h_5} \tag{4.15}$$

Back Work Ratio

The back work ratio, bwr, is the ratio between the pump work input to the turbine work output (Moran et al., 2010). It is a good parameter to describe the performance of the ORC (Moran et al., 2010).

$$\text{bwr} = \frac{\dot{W}_p/\dot{m}}{\dot{W}_t/\dot{m}} = \frac{(h_5 - h_4)}{(h_1 - h_2)} \tag{4.16}$$

There is only 1 degree of freedom in this model when the objective is to obtain the highest possible efficiency; the evaporating pressure; P_{evap}. The optimal evaporator pressure in order to reach the highest efficiency will calculated in EES.

4.3.2 Thermodynamic Model of Subcritical ORC with Superheat and Regeneration

The T-s diagram of the subcritical cycle with superheat and regeneration can be seen in Figure 4.9. Compared to the conventional subcritical cycle, there are not any major changes to the thermodynamic model. The main difference is the introduction of an open feed water heater. The fraction of the working fluid that goes from point 2 to point 7, can be calculated with Equation 4.17. This is obtained by taking a mass flow rate balance over the first and second turbine stage.

$$f_{wf} = (h_7 - h_6)/(h_2 - h_6) \tag{4.17}$$

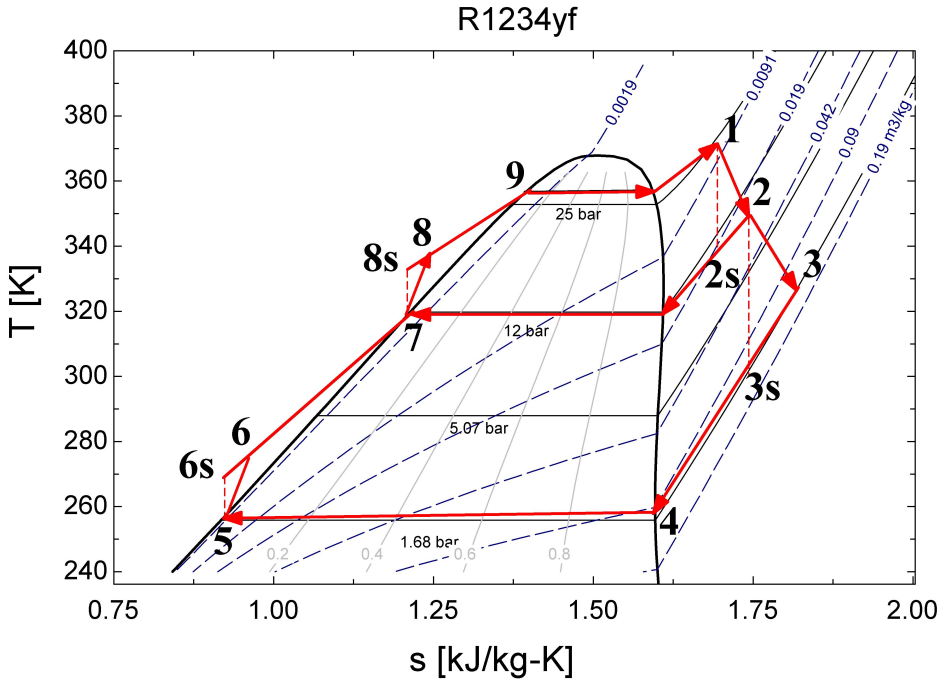

Figure 4.9: Sketch of T-s diagram for subcritical ORC with superheat and regeneration.

The change in the mass flow rate balance of the working fluid affects the calculation of turbine and pump work, and heat transfer in the evaporator and in the condenser.

$$\frac{\dot{W}_t}{\dot{m}_{wf}} = (h_1 - h_2) + (1 - f_{wf})(h_2 - h_3) \tag{4.18}$$

$$\frac{\dot{W}_p}{\dot{m}_{wf}} = (h_8 - h_7) + (1 - f_{wf})(h_6 - h_5) \tag{4.19}$$

The heat from the exhaust gas is only added between point 1 and 8, since the regeneration heats the working fluid from point 6 to 7.

$$\frac{\dot{Q}_{evap}}{\dot{m}_{wf}} = (h_1 - h_8) \tag{4.20}$$

$$\frac{\dot{Q}_{out}}{\dot{m}_{wf}} = (1 - f_{wf})(h_3 - h_5) \tag{4.21}$$

There are 3 degrees of freedom in this model when the objective is to obtain the highest possible efficiency; P_{evap}, P_{int} and T_1. The three parameters will be optimized in EES. In case the best efficiency is gained with only regeneration or only superheat and not both, the model will account for this. The complete EES model for the subcritical ORC with superheat and regeneration can be seen in Appendix C.

4.3.3 Thermodynamic Model of Trans-critical

The thermodynamical model of the trans-critical cycle will be based on the same equations as the conventional subcritical cycle, except for the fact that no phase change has to be modeled in the evaporator. Some minor alterations were necessary in EES to model the supercritical equations of state for the working fluids. The complete EES model can be seen in Appendix D.

4.3.4 Optimization of Thermodynamic Models

For the optimization of pressure and temperatures the Conjugate Directions method and Variable Metric Optimization Method were used. Both these methods are implemented in the EES computer program within the Min/Max calculation command function and are recommended by EES for multidimensional optimization (Klein and Alvarado, 2002). Finite lower and upper bounds were set for each independent variable dependent on the thermophysical properties of the selected fluid under investigation and the range of the equation of state in EES for each fluid. The equation of state ranges can be seen in Table 4.4.

4.4 Choice of Organic Rankine Cycle Working Fluids

The selection of the working fluid of an Organic Rankine cycle is a cumbersome and complex process. As briefly discussed in Chapter 1, the choice of correct working fluid for a specific ORC is one of the most important design considerations due to its high influence on the ORC performance. Even though there exist a high number of scientific reports on research with the goal to find the best working fluid over the hundred different fluids that are available, literature conclude that there is no optimal fluid for each area of application or for a given temperature level

(Quoilin et al., 2011). The choice has to be based on a variety of thermodynamic properties, the heat source temperature in addition to evaluate the working fluids from a practical, economical and environmental perspective. A pre-screening of avalible working fluids is necessary in order to reduce the number of working fluids that will be included in the thermodynamic analyses in this work. Based on previous studies, a significant number of working fluids have been chosen for pre-screening as can be seen in Table 4.2.

In Table 4.2, ODP and GWP stands for Ozone Depletion Potential and Global Warming Potential. The ODP of a chemical substance, is the ratio of the relative impact on degradation of the ozone layer that a substance can have compared to a similar mass of the reference substance, R-11, which has a ODP of 1 (ASHRAE, 2010). GWP is a value used to compare greenhouse gases ability to trap heat in the atmosphere (IPCC, 2013). GWP of all greenhouse gases is measured in comparison to carbon dioxide ($GWP_{CO_2} = 1$). The GWP is given for different time horizons, usually 20, 100 or 500 years, and gives an estimate of the impact the specific substance will have considering their decay rate in the atmosphere (ASHRAE, 2010). Na stands for not available.

The Safety classification in Table 4.2 is based on The ASHRAE refrigerant safety classification as can be seen in Figure 4.10. The classification is a good indicator of a fluid's level of toxicity and flammability (Chen et al., 2010). A2L and B2L are lower flammability refrigerants with a maximum burning velocity of ≤ 10 cm/s (ASHRAE, 2010).

CFC, HCFC, PFC, HFO, HFC and HC stands for chlorofluorocarbons, hydrochlorofluorocarbons, perfluorocarbons, hydrofluoroolefin, hydrofluorocarbons and hydrocarbons respectively.

	Safety group	
Higher Flammability	A3	B3
Lower Flammability	A2	B2
	A2L*	B2L*
No flame Propagation	A1	B1
	Lower Toxicity	Higher Toxicity

Figure 4.10: Safety classification of refrigerants (ASHRAE, 2010).

ASHRAE	Name	T_c [K]	P_c [MPa]	GWP_{100}	ODP	Type	Safety Cl.
R-11	Triclogofluormethane	471.1	4.41	4750	1	CFC	A1
R-114	1,2-dichloro-1.1.2.2-tetrafluorethane	418.8	3.26	9180	0.58	CFC	A1
R-115	Chloropentafluoroethane	353.1	3.13	7230	0.57	CFC	A1
R-116	Hexafluoroethane	293.0	3.05	10000	0	PFC	A1
R-12	Dichlorodifluoromethane	385.1	4.14	10900	0.82	CFC	A1
R-123	2,2-Dichloro-1,1,1-trifluoroethane	456.8	3.66	77	0.01	HCFC	B1
R-1234yf	2,3,3,3 -tetrafluoro-1 -propene	367.9	3.38	4.4	0	HFO	A2(L)
R-1234ze	Trans-1,3,3,3 -tetrafluoro-1 -propene	382.5	3.64	6	0	HFO	A2(L)
R-124	2-Chloro-1,1,1,2-tetrafluoroethane	395.4	3.62	619	0.02	HCFC	A1
R-125	Pentafluoroethane	339.2	3.62	3420	0	HFC	A1
R-1270	Propene	365.6	4.66	20	0	HC	A3
R-134a	1,1,1,2-Tetrafluoroethane	374.2	4.06	1370	0	HFC	A1
R-141b	1,1-Dichloro-1-fluoroethane	477.5	4.21	725	0.12	HCFC	na
R-142b	1-Chloro-1,1-difluoroethane	410.3	4.06	2310	0.065	HCFC	A1
R-143a	1,1,1-Trifluoroethane	345.9	3.76	4470	0	HFC	A2
R-152a	1,1-Difluoroethane	386.4	4.52	133	0	HFC	A2
R-161	Fluoroethane	375.3	5.09	12	na	HFC	A2
R-170a	Ethane	305.3	4.87	3	0	HC	A3
R-21	Dichlorofluoromethane	451.5	5.18	210	0.01	HCFC	B1
R-218	Octafluoropropane	345.0	2.64	2600	0	PFC	A1
R-22	Chlorodifluoromethane	369.3	4.99	1790	0.04	HCFC	A1
R-227ea	1,1,1,2,3,3,3-Heptafluoropropane	375.9	3.00	3580	0	HFC	A1
R-236fa	1,1,1,2,3,3-Hexafluoropropane	412.4	3.50	9820	0	HFC	A1
R-23a	Trifluoromethane	299.3	4.83	14200	0	HFC	A1
R-245fa	1,1,1,3,3-Pentafluoropropane	427.2	3.64	1050	0	HFC	B1
R-290	Propane	369.8	4.25	3	0	HC	A3
R-3-1-10	Decafluorobutane	386.3	2.32	8860	0	PFC	na
R-32	Difluoromethane	351.3	5.78	650	0	HFC	A2(L)
R-402A	R-125/290/22 (60.0/2.0/38.0)	348.2	4.23	2700	0.015	HFC-blend	A1
R-402B	R-125/290/22 (38.0/2.0/60.0)	356.2	4.53	2400	0.024	HFC-blend	A1
R-404a	R-125/143a/134a (44.0/52.0/4.0)	345.2	3.73	3700	0	HFC-blend	A1
R-407c	R-32/125/134a (23.0/25.0/52.0)	359.9	4.62	1700	0	HFC-blend	A1
R-408A	R-125/143a/22 (7.0/46.0/47.0)	356.2	4.42	3000	0.019	HFC-blend	A1
R-409A	R-22/124/142b (60.0/25.0/15.0)	385.2	4.11	1600	0.038	HFC-blend	A1
R-41a	Fluoromethane	317.3	5.90	92	0	HFC	na
R-507a	R-125/143a (50.0/50.0)	344.2	3.8	3800	0	HFC-blend	A1
R-600	Butane	425.1	3.80	20	0	HC	A3
R-600a	Isobutane	407.8	3.63	20	0	HC	A3
R-601	Pentane	469.7	3.37	20	0	HC	A3
R-717	Ammonia	405.4	11.33			Inorganic	B2(L)
R-718	Water	647.1	22.06			Inorganic	A1
R-744a	Carbon dioxide	304.1	7.38	0	0	Inorganic	A1
R-C318	Octafluorocyclobutane	388.4	2.78	10300	0	PFC	A1
	Toluene	591.8	4.09	na	0	HC	na
	Butene	419.3	4.01	na	0	HC	na
	Neopentane	433.7	3.20	na	0	HC	na

Table 4.2: Potential working fluids for ORC (ASHRAE, 2013) (BITZER, 2012) (UNEP, 2012) (The Linde Group, 2015) (Tchanche et al., 2011) (Sprouse and Depcik, 2013) (Quoilin et al., 2011) (Brasz and Bilbow, 2004) (Nouman, 2012) (Chen et al., 2010).

4.4.1 Desirable Thermophysical Properties

In order to obtain a good Organic Rankine cycle, several thermophysical properties should be evaluated.

- **High Density, ρ**

  The density of the working fluid should be high in order to decrease the mass flow rate and the volumetric flow rate (Tchanche et al., 2011). This will cause a reduction in the size of the complete system because it will enable use of smaller pipes and more compact machines, something that is preferable due to the limited available space on a ship (Tchanche et al., 2011).

- **High Enthaply of Vaporization, dh_{evap}**

  The enthalpy of vaporization is the necessary change in enthalpy that is required to transform a given amount of a fluid from liquid to gas phase at a specific pressure (Kalyan Annamalai, 2001). The enthalpy of vaporization is dependent on temperature, and decreases for most organic fluids as the temperature increases (Kalyan Annamalai, 2001). The enthalpy of vaporization should be high to ensure that most of the heat is added during phase change to avoid complex ORC systems that need regenerative heating and/or superheating (Maizza and Maizza, 2001).

- **Low Specific Heat Capacity, c_p**

  Badr et al. (1985) and Chen et al. (2010) suggest that the specific heat of the organic fluid should be low because this reduces the necessary amount of heat that is needed to increase the temperature of the working fluid.

- **Low Viscosity, μ**

  The viscosity should be low in both liquid and vapor phases to keep the pump work as low as possible and to increase the heat transfer coefficient (Tchanche et al., 2011).

As one can understand, to achieve all of these thermophysical properties is not easy. It will always be a trade-off between the different parameters, and a decision based on which parameters are the most important for the case under consideration.

4.4.2 Desirable Environmental Characteristics

- **Low ODP and GWP**

  The working fluids that are used in ORCs are often the same as refrigerants used for heating, ventilation and air conditioning (HVAC) and the refrigeration industry (The Linde Group, 2015). A growing focus to ban and replace substances that are environmentally dangerous and increase global warming has forced these industries to do research on new and more environmental friendly fluids. The Montreal Protocol on Substances that Deplete the Ozone Layer has been on the forefront on motivating and influencing all industries to remove dangerous substances that increase global warming (UNEP, 2012).

  - **CFC, Chlorofluorocarbons** CFCs substances, such as R-11, R-12, R-113, R-114 and R-115, are all classified to have high GWP and ODP (The Linde Group, 2015). These substances are under legislation that regards a sales ban for developed countried from 1996, and for developing countries from 2010 reported by the Montreal Protocol (UNEP, 2012). This signifies that there is no point in including these working fluids in the thermodynamic analyses since the fluids will not be available for purchase.
  - **HCFCs, Hydrochlorofluorocarbons** HCFCs, such as R-21, R-22, R-123, R-124, R-142b, R-402A, R-402B, R-408A, and R-409A, were originally the replacement for CFC (The Linde Group, 2015). Their ODP and GWP are lower than CFCs due to lower atmospheric lifetime, but still categorized as high to medium level ODP and GWP (ASHRAE, 2010). The use of virgin HCFCs were phased out from 2010 in EU, and recycled HCFCs have been in use until January 2015. HCFCs will be excluded from this work to assure environmental safety and good availability (see Figure 4.11).
  - **Fluids with too high GWP and ODP** According to the Rules for Classification of Ships published by DNV (2014), the rules for GWP and ODP are:

    CLEAN CLASS

    Section B200, 203: The use of ozone depliting substances is not permitted. The refrigerant may be any HFC or natural refrigerant such as ammonia (NH_3) or CO_2.The used refrigerant shall comply with: GWP<3500.

Section B300, 301: Refrigerants used shall be either a natural refrigerant, or alternatively an HFC complying with: GWP <= 1890 and ODP= 0.

The standards for GWP levels on ships are very high compared to the automobile industry that operates with a maximum GWP of 150 (Comission, 2014). This legislation does not apply to the rest of the HVAC and refrigeration industry. It is decided to set the upper limit of GWP to 3500, and ODP=0 in this work based on the Rules for Classification of Ships published by DNV (2014).

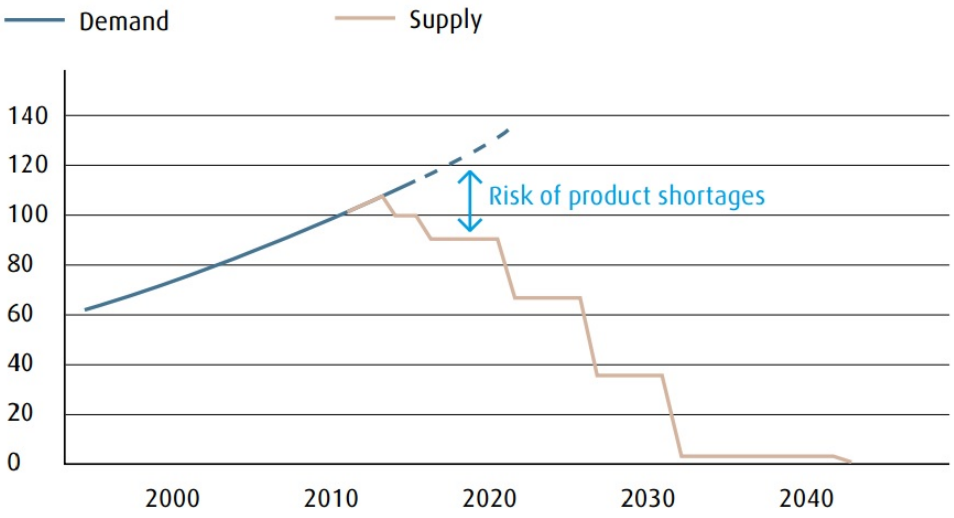

Figure 4.11: HCFC phase-down (in % vs year) (The Linde Group, 2015).

4.4.3 Desirable Safety and Operational Characteristics

- **Good Availability and Low Cost**

  The availability has already been discusses in the previous section. The availability of the working fluid should be good to ensure the possibility to buy the working fluid in various locations around the world in case some of the fluid has leaked and it is necessary to refill the system (Tchanche et al., 2011). For the case vessel that operates globally this is especially important in order to avoid down time of the ORC system. Additionally, it is not economically wise to invest in a ORC whos working fluid might not be available in a couple of years. The performance of an ORC is highly dependent on the working fluid, and retrofitting with another fluid needs substantial work (Tchanche et al., 2011).

- **Low Toxicity and Non-flammable**

  All working fluids with an ASHRAE safety classification A3 or B3 will be excluded from the analysis due to very high flammability and toxicity.

- **Non-corrosive**

  To avoid unnecessary maintenance and failure of system components, a non corrosive working fluid should be chosen (Tchanche et al., 2011).

- **Moderate Operating Pressure**

  The higher the maximun operating pressure, the higher will the efficiency be (Klein and Nellis, 2012). However, very high maximum operating pressure require more expensive, larger and heavier system equipment (Tchanche et al., 2011) (Machinery Spaces, 2010).

- **Too Low Critical Temperature,** T_{crit}

  Condensation is a required process for both the subcritical and the trans-critical ORC. Some working fluids will have critical temperatures above which the fluid gas will not condense. For ships operating in areas with high sea-water temperatures, liquefying working fluids with critical temperatures above the sea-water temperature will not be possible. This is especially a disadvantage with the increasingly popular carbon dioxide that has a low critical temperature of 31°C (Ladam and Skaugen, 2007). With such low temperatures, additional sub-cooling systems will be necessary in order to liquefy the CO_2, something that will increase the complexity of the overall ORC system (Machinery Spaces, 2010). In this work, substances with a critical temperature below 330 K (57°C) will be excluded. The temperature is decided based on the fact that the sea-water temperature in warm areas of the world where the ship operates can reach 35°C (C. Chryssakis DNV GL, 2015). Additionally it is necessary to account for temperature difference in the heat exchanger.

4.4.4 Results from Pre-Screening of Working Fluids

Based on the previous discussed criteria, the working fluids listed in Table 4.3 will be included in the thermodynamic analyses. The thermophysical properties and the range of applicability of the remaining fluids can be seen in Table 4.4. All CFCs, HCFCs are excluded, in addition to working fluids that do not meet the criteria for GWP, ODP, critical temperature and pressure and safety requirements. Lastly, working fluids that are not included in the EES library have been excluded.

ASHRAE	Name	T_c [K]	P_c [MPa]	GWP	ODP	Type	Safety Cl.
R-1234yf	2,3,3,3 -tetrafluoro-1 -propene	367.9	3.38	4.40	0	HFO	A2(L)
R-1234ze	Trans-1,3,3,3 -tetrafluoro-1 -propene	382.5	3.64	6.00	0	HFO	A2(L)
R-125	Pentafluoroethane	339.2	3.62	3420.00	0	HFC	A1
R-134a	1,1,1,2-Tetrafluoroethane	374.2	4.06	1370.00	0	HFC	A1
R-161	Fluoroethane	375.3	5.09	12.00	na	HFC	A2
R-218	Octafluoropropane	345.0	2.64	2600.00	0	PFC	A1
R-245fa	1,1,1,3,3-Pentafluoropropane	427.2	3.64	1050.00	0	HFC	B1
R-32	Difluoromethane	351.3	5.78	650.00	0	HFC	A2(L)
R-407c	R-32/125/134a (23.0/25.0/52.0)	318.3	4.52	1700	0	HFC-blend	A1
	Toluene	591.8	4.13	low	0	HC	na
	Butene	419.3	4.01	low	0	HC	na
	Benzene	562.0	4.89	low	0	HC	na

Table 4.3: Remaining working fluids for ORC thermodynamic analysis (ASHRAE, 2013) (BITZER, 2012) (UNEP, 2012) (The Linde Group, 2015).

Fluid	Range of applicability for Equation of state in EES			Thermophysical properties			
	Min temp [C]	Max temp [C]	Max pressure [bar]	Critical Temperature [C]	Density [kg/m^3]	Molar mass [kg/kmol]	Saturation Curve
R-1234yf	-53.15	136.85	300	94.7	475.55	114.04	wet
R-1234ze	-104.5	146.85	200	109.4	489.24	114.04	wet
R-125	-100.0	226.85	600	66.0	576.58	120.02	wet
R-134a	-53.2	136.85	300	94.7	475.55	114.04	wet
R-161	-143.2	126.85	500	102.2	301.81	48.06	wet
R-218	-147.7	166.85	200	71.9	626.98	627.98	dry
R-245fa	-102.1	166.85	2000	154.0	516.08	134.05	dry
R-32	-136.8	161.85	700	78.1	424.0	52.02	wet
R-407c	-73.2	226.85	500	86.2	453.43	86.20	wet
Toluene	-95.2	426.85	5000	318.6	291.99	92.14	dry
Butene	185.4	251.85	700	146.1	237.89	56.11	isentropic
Benzene	5.5	476.85	5000	288.9	304.79	78.11	dry

Table 4.4: Thermophysical properties of remaining working fluids (Lemmon et al., 2007) (Klein and Alvarado, 2002).

4.5 Discussion and Results of Performance Analysis of ORC

The objective of this study was to perform a thermodynamic analysis of an ORC. Ideal performance have been calculated in addition to identifying the major reasons for losses. Estimations for real performance have been done based on the first and second law of thermodynamics. Three different ORC systems have been analyzed, parametrically optimized and compared in order to find the highest potential for harvesting energy from the waste heat sources of the engine under consideration. A pre-screening process was done of about 50 working fluids, and the remaining fluids in Table 4.3 were studied for each different ORC.

A computer programme in EES was developed to optimize input parameters such as T_1 and P_{evap} (and P_{int} for the regenerative ORC) to achieve the highest thermodynamic performance possible of the various ORC models for each organic fluid under investigation.

4.5.1 Subcritical ORC with Exhaust as Heat Source

In the subcritical ORC, 5 working fluids were tested; R-218, R-245fa, Toluene, Butene and Benzene. These are all dry fluids and do therefore meet the criteria of having a vapor quality equal to 1 after turbine expansion in order to avoid condensing and damage on the turbine blades.

Figure 4.12 shows the thermal efficiency of the subcritical ORC for each working fluid and how the evaporator pressure influences the efficiency. All the fluids show an increase in the efficiency for increased evaporator pressure. For both Butene and R-245a a slight decrease in the efficiency can be seen for the highest pressures. This is because when the pressure increases, the back work ratio will also increase due to increased pump work, causing the efficiency to flatten out and eventually reach the highest possible efficiency before it decreases.

Benzene and toluene show the highest efficiencies with values around 16% to 20%. Toluene is non-toxic and has been used previously in geothermal power systems (Klein and Nellis, 2012). It is important to note that toluene is also highly flammable according to NFPA 704[1] and safety precausions have to be made in order to utilize toluene as a working fluid in an ORC (NFPA, 2015). Benzene inhabits the same hazards as toluene and has the same NFPA 704 coding (NFPA,

[1] NFPA 704 is a standard maintained by the U.S.-based National Fire Protection Association. NFPA 704 provides criteria for assessing the health, flammability instability, and related hazards that are presented by short-term, acute exposure to a material under conditions of fire, spill, or similar emergencies (NFPA, 2015).

2015). However, Benzene is carcinogen[2] and might therefore not be applicable in ships (American Cancer Society, 2015). Based on these facts, the HFC R-245fa might be a better choice than the hydrocarbons considering it is not flammable and has low toxicity. R-245fa gains an efficiency of about 11.5%.

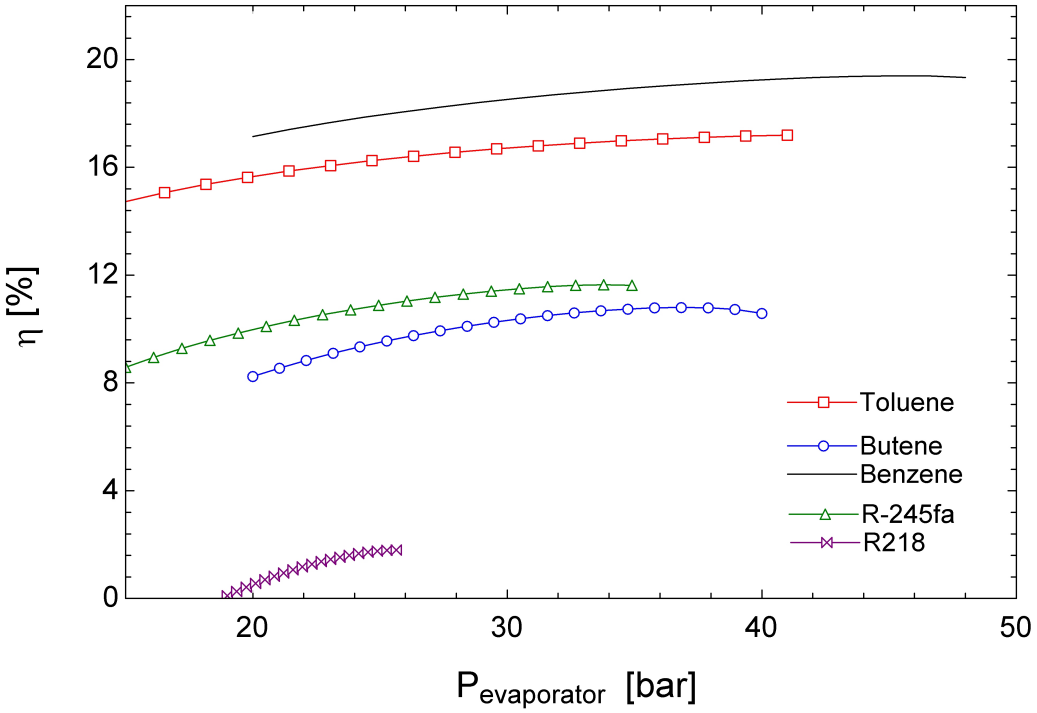

Figure 4.12: Efficiency vs evaporator pressure, subcritical cycle.

In Figure 4.13, the mass flows of the working fluids are plotted against the turbine work output. R-218 is not included since this fluid showed such a poor efficiency in Figure 4.12 due to its low critical temperature. R-218 is probably a better fit for a trans-critical ORC or an ORC with a heat source and heat sink at lower temperatures. All fluids in Figure 4.13 show a tendency where the mass flow increases for the highest work outputs. This is mainly because the enthalpy of vaporization, dh_{vap} [kJ/kg], decreases with increasing pressure, and therefore the mass flow has to increase in order for the working fluid to absorb the same amount of waste heat. Benzene gives a turbine output of about 410 kW for the highest thermal efficiency. This is the highest work output of the subcritical ORC in this study. Benzene also shows a low mass flow which

[2] A carcinogen is any substance that in known to cause cancer (American Cancer Society, 2015).

implies that an ORC with benzene will require a smaller footprint than an ORC with any of the other fluids.

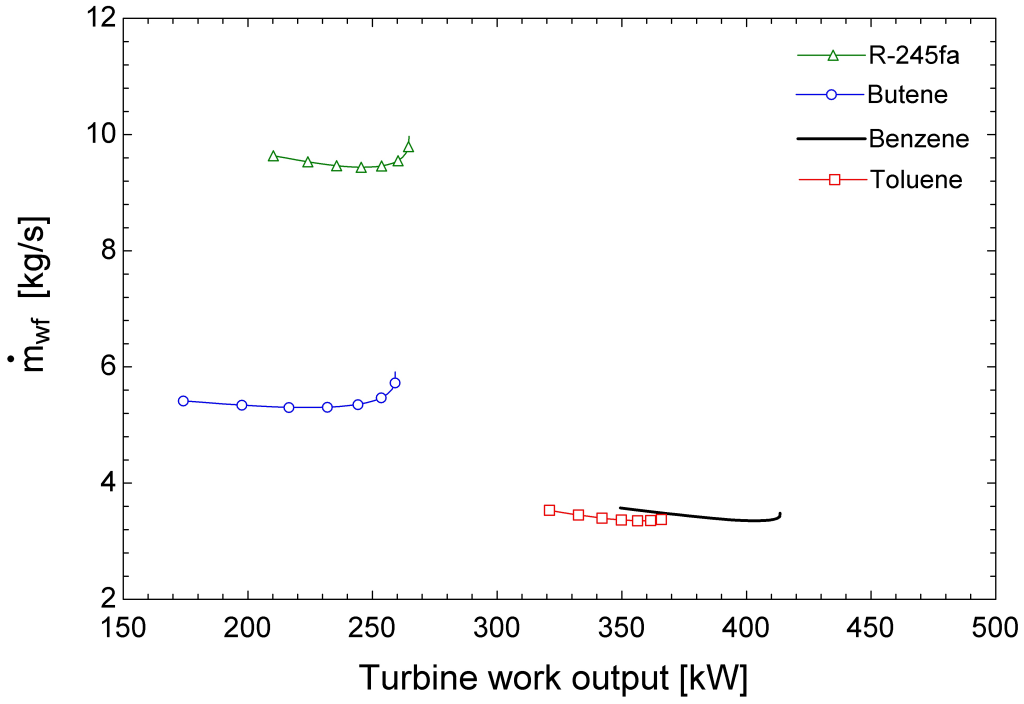

Figure 4.13: Mass flow vs turbine work output with exhaust as heat source, subcritical cycle.

In Figure 4.14 the work output of the subcritical ORC with benzene as the working fluid can be seen versus MGE1 load. The work output increases as the load increases due to increased exergy in the exhaust. The efficiency of the ORC does not get too much affected by the amount of exergy in the exhaust. This is because the EES model is built in such a way that when the exergy decreases, the mass flow of the working fluid in the ORC will also decrease because it will not need as much mass flow to absorb all the exergy. This causes the pump work in the ORC to decrease as the load of the MGE decreases, thus keeping the efficiency of the ORC at a constant level. Between 350-410 kW can be recovered for loads between 70-100%. This equals about 4.4-3.6% of the MGE1 power output.

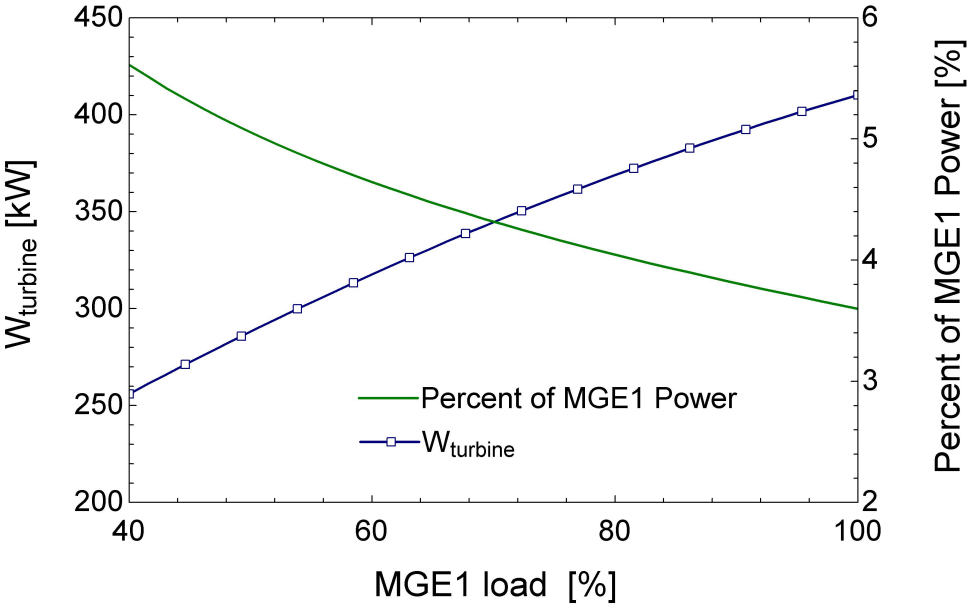

Figure 4.14: Work output subcritical ORC with benzene vs MGE load [%].

4.5.2 Subcritical ORC with Superheat and Regeneration

In the ORC with superheat and regeneration, all fluids except R-218 were tested due to R-218's low critical temperature and pressure.

In Figure 4.15 the thermal efficiency is plotted vs the mass flow of the organic fluids. The parameters T_1, P_{evap} and P_{int} have all been optimized in EES. Same as for the non-regenerated subcritical ORC, benzene shows the best efficiency, however, with more or less the same value as for the conventional subcritical ORC: η = 21%. The cycle for Benzene can be seen in Figure 4.17 with T_1 = 560.3 K, P_{evap} = 48 bar and P_{int} = 2.16 bar. Obviously, the evaporator pressure for benzene is very high. It can also be noted that the expansion process is in the two-phase zone at the beginning of expansion. In order to ensure long operating time of the expansion turbine before failure, the pressure should be lowered down to a level where it stays completely out of the two-phase zone. This can be done without compromising too much on the efficiency. An evaporator pressure of 35 bar gives an efficiency of 20.7%, and an pressure of 25 bar gives an efficiency of 19.7% for benzene. The T-s diagram of the ORC cycle with benzene at 25 bar can be seen in Figure 4.18.

When benzene is used in the EES model, the superheat cancels when the optimizing is performed. This agrees well with the study of (Chen et al., 2010) that shows that superheat has a negative effect on cycle efficiency when dry fluids are used. Butene and R-245fa have both a high increase in the efficiency. This is because the fluids benefit well from the regeneration. Butene and R-245fa have lower critical temperatures, and are therefore able to utilize more regeneration without crossing the temperature of the exhaust exit and violating the pinch constraint. Even though the best performance is achieved with benzene, R-245fa might be the most feasible solution considering benzen is carcinogenic and has high flammability. R-245fa gains an efficiency of ≈15% with regeneration, the cycle can be seen in Figure 4.16. This is with an evaporation pressure of 36 bar. With a more appropriate pressure of 30 bar, the efficiency becomes 14.5%.

The dry fluids with high critical temperatures, such as toluene and benzene, do not show a high increase in efficiency compared to the conventional subcritical cycle. The wet fluids do all show a lower efficiency than the dry fluids when implemented into the model of subcritical ORC with superheat and regeneration. This is mainly due to the fact that the hydrocarbons show a better temperature match with the exhaust waste heat source.

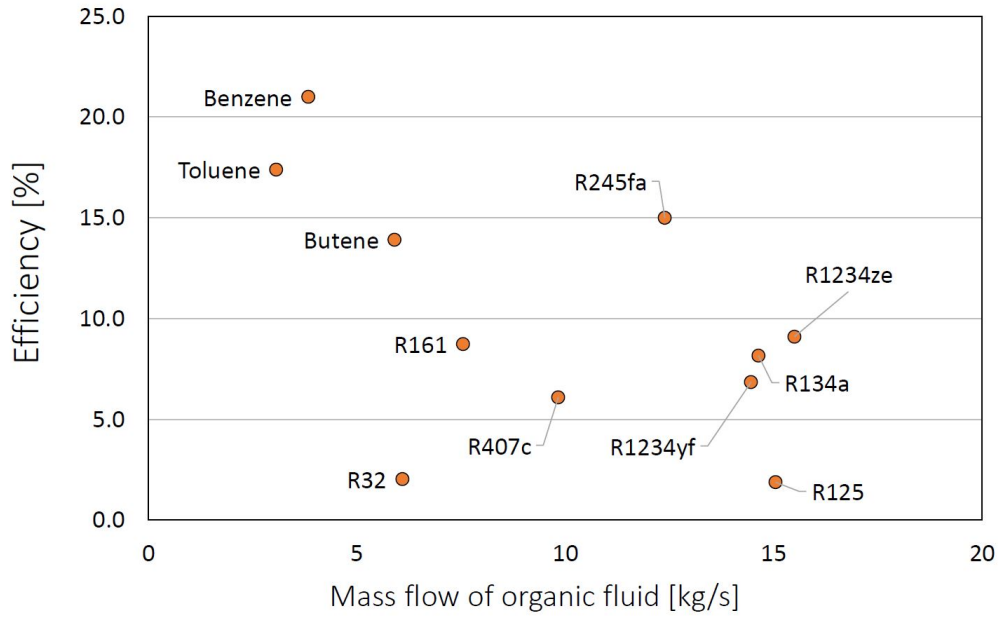

Figure 4.15: Efficiency vs mass flow of organic fluid for superheated and regenerated ORC with exhaust as heat source.

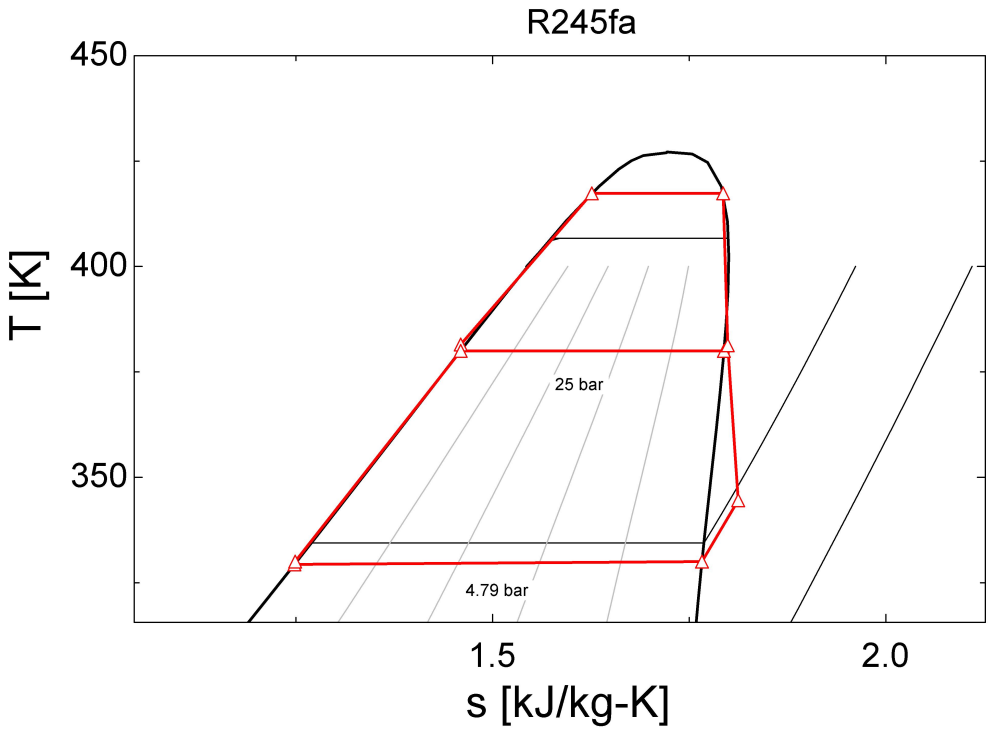

Figure 4.16: Subcritical cycle with regeneration and R-245fa, for P_evap= 30 bar.

4.5.3 Subcritical ORC Systems with CW as Heat Source

When the HT cooling water is applied as heat source, almost all the working fluids will operate in the subcritical zone and it will not be possible with superheat due to the low heat source temperature of 91°C. The wet fluids R-1234yf, R-1234ze, R-134a, R-161 and R-245fa achieve very low efficiencies, around 4-5% for every fluid. This is because the low temperature of the heat source gives small pressure differences in the ORCs that will give low work output in the expander.

The hydrocarbons toluene, benzene and butene can not be used in ORC systems running on waste heat from the CW. This is because the temperature of the CW is almost equal to the condensing temperature of the three hydrocarbons.

R-125, R-218, R32 and R407c do all have critical temperatures below 90°C, so it has the possibility to operate trans-critical even with CW as the heat source. For subcritical applications, the power outputs become insignificant.

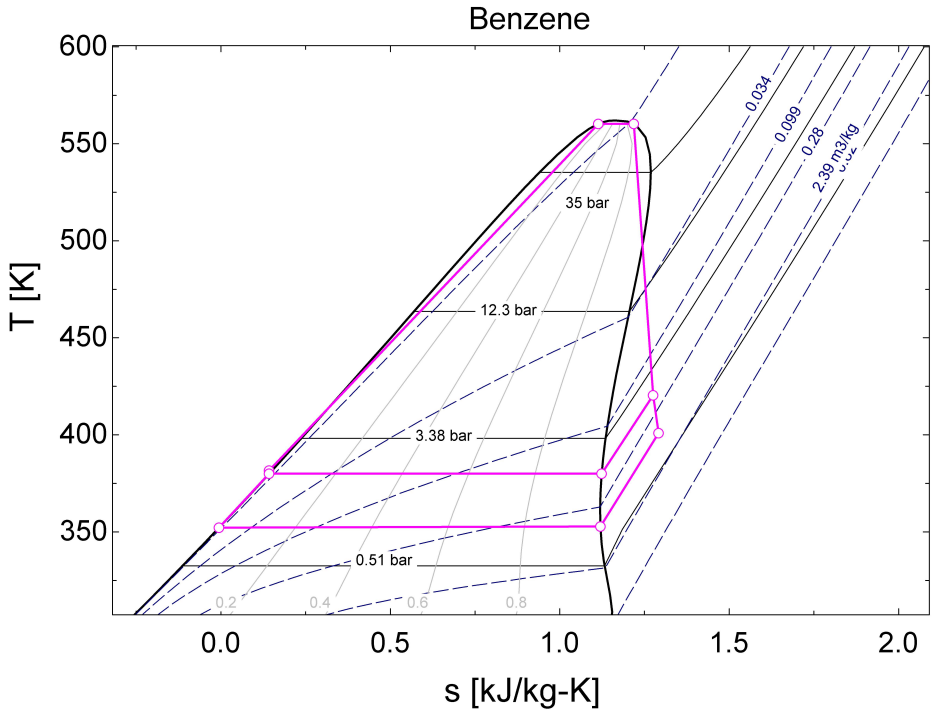

Figure 4.17: T-s diagram Benzene, P_{evap}= 41 bar.

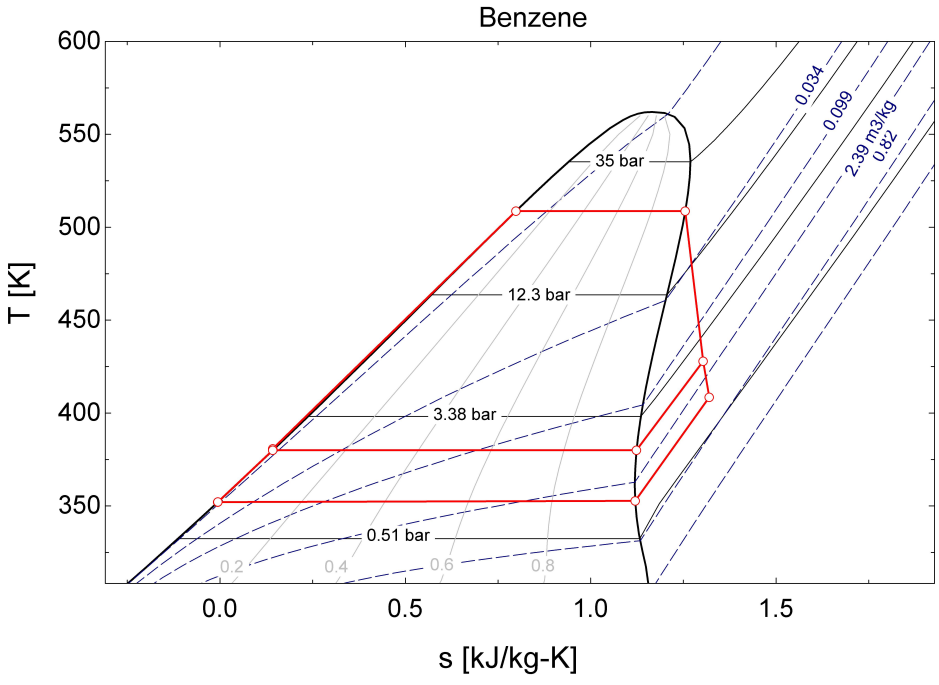

Figure 4.18: T-s diagram Benzene, P_{evap}= 25 bar.

4.5.4 Trans-critical ORC

The results of the dry and isentropic fluids with exhaust as heat source can be seen in Figure 4.20. Neither benzene nor toluene show any specific increase when applied to the trans-critical ORC. Both cycles increase the pump work so much that the efficiecy more or less stay at the same value. Butene reaches an efficiency of 16% at 150 bar. This is quite higher than the sub-critical ORC with regeneration and superheat. Even so, the back work ratio becomes very high due to a pressure ratio of about 21. So high pressure differences are often solved with pump work in two stages, something that would increase cost and complexity of the system in addition to reliability issues that follows with such high operating pressures and is therefore not an interesting solution. Due to R-218 low critical temperature, the fluid shows a great increase in efficiency compared to the two other cycles where the efficiency was more or less negligible. Nevertheless, it still has a much lower efficiency than the other dry and isentropic fluids.

All the wet fluids achieve increased efficiency when applied to the trans-critical cycle as can be seen in Figure 4.21. Especially R-32 and R-125 increase their efficiency significantly due to their low critical temperature. The trans-critical cycle with R-32 can be seen in Figure 4.19. Even though the wet fluids increase their efficiency substantially, the subcritical ORC cycles with hydrocarbons as working fluids still show better potential for energy recovery.

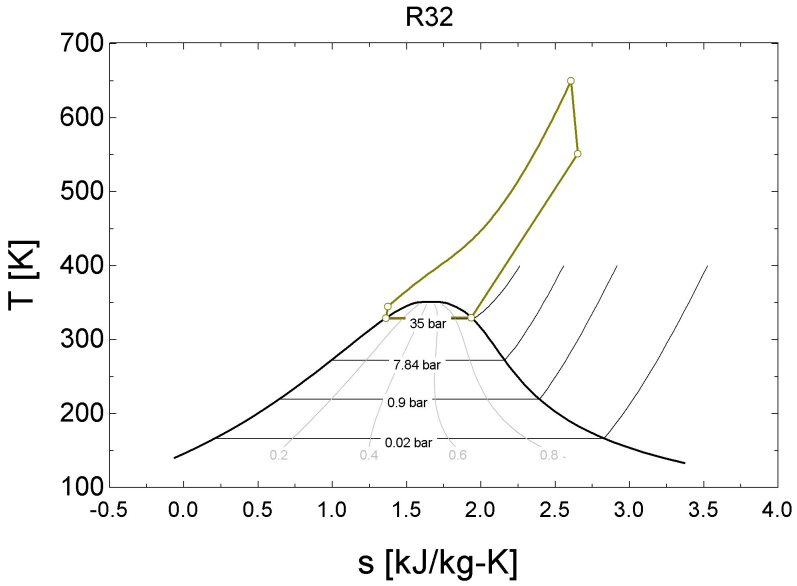

Figure 4.19: Trans-critical cycle with R-32 and exhaust as heat source.

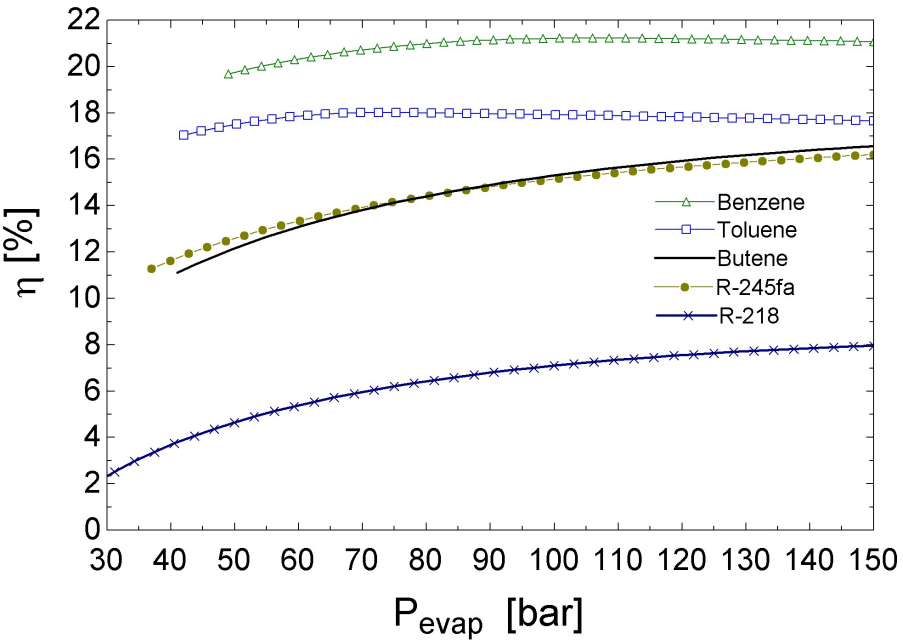

Figure 4.20: Efficiency vs evaporator pressure, dry and isentropic fluids, trans-critical cycle.

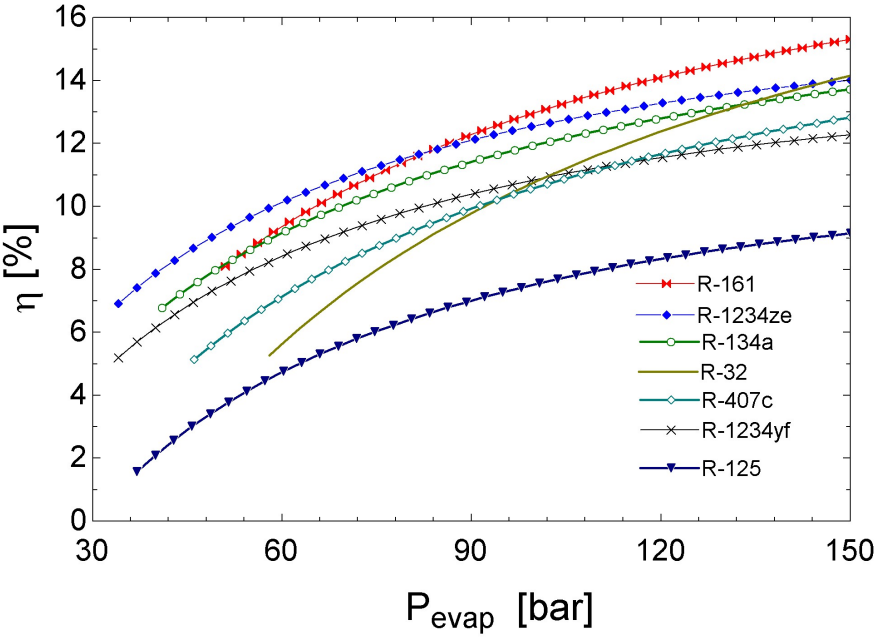

Figure 4.21: Efficiency vs evaporator pressure, wet fluids, trans-critical cycle.

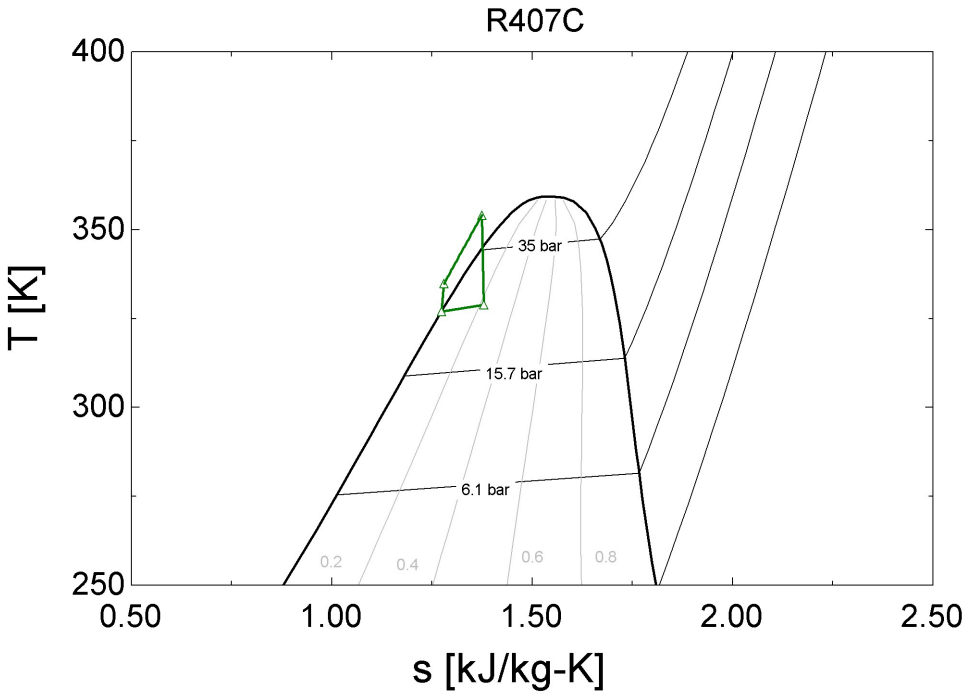

Figure 4.22: Trans-critical cycle with CW heat source.

4.5.5 Trans-critical ORC with CW as Heat Source

As explained in the previous section, it is only the working fluids R-125, R-218, R32 and R407c that are applicable to trans-critical ORC with CW as heat source. All four fluids show very poor efficiencies below 3%. This is because the turbine inlet temperature becomes so low that the fluids ends up in the two phase region after expansion. This issue is plotted in Figure 4.22.

4.5.6 Summary of Results

- Wet working fluids are not applicable to subcritical cycles due to issues with two-phase state in the expansion turbine.
- Working fluids with critical temperature close to the heat sink temperature are not good candidates for subcritical ORCs because the operating area becomes very small and the work output insignificant.
- The efficiency of both subcritical ORC systems do not decrease to much when slightly lowering the operating pressure. It is therefore recommended to choose an operating

pressure around 25-35 bar to get the system to operate in an acceptable pressure range without compromising too much on efficiency. Very high pressures will impact the reliability of the cycle and increase the cost and decrease the life time of the components. An additional positive effect by reducing the operating pressure is an increase in the enthalpy of vaporization, and this will cause a decrease in the mass flow of the working fluid leading to a smaller system.

- The hydrocarbons benzene and toluene show the best efficiencies and work output in both subcritical ORC and subcritical ORC with regeneration and superheat. Benzene and toluene achive 19% and 17.2% efficiency respectively for the conventional subcritical ORC system, and efficiencies of 21% and 17.4% respectively for the subcritical ORC with regeneration and superheat. Benzene and toluene do not gain any additional work output from the superheat, only the regeneration. However, the gain from regeneration is almost nothing for toluene. This is due to two main reasons:
  - The temperature of the outlet of regeneration is restrained by the pinch point for the inlet temperature of the working fluid to the evaporator and the outlet temperature of the exhaust ($T_{out,exh}$= 120°C). This gives a temperature restrain of 110°C for the outlet of regeneration. The condensing temperature of toluene at 1 atm, is approximately the same as the temperature restrain for the regeneration outlet temperature, therefore toluene achieves no increase in the efficiency due to regeneration.
  - Superheat has a negative effect on cycle efficiency when dry fluids are used.
- Toluene, benzene and butene can not be used in ORC systems running on waste heat from the CW. This is because the temperature of the CW (91°C) is too close to the condensing temperature of the three fluids.
- All the wet fluids R-1234yf, R-1234ze, R-134a, R-161 and R-245fa show poor efficiencies in the subcritical cycles with HT CW as the heat source.
- The minimum condensing temperature of 330 K highly affects the efficiency. A decrease in condensing temperature would increase the efficiency of the systems where the working fluid has a condensing pressure above 1 bar for 330 K. Vaccum should be avoided as explained in Section 4.2.1.

- All wet fluids increase their efficiency substantially when implemented into trans-critical ORC with exhaust as the heat source.
- None of the working fluids tested in this work are applicable to be used in trans-critical cycles with CW as the heat source.

This study has showed that the potential of harvesting waste heat with an ORC shows promising results for subcritical ORC arrangements with hydrocarbons as the working fluid and with exhaust as the heat source. Even so, the most practical and feasible solution has shown to be a subcritical ORC with regeneration and R-245fa at a moderate operating pressure of 30 bar. R-245fa has no flammability and low toxicity. R-245fa gains an efficiency of approximately 14.5% at this operating point. This corresponds to 2.5% of the MGE power output at 100% load and 4.1% at 40% load. This cycle will be used in the cost and technical feasibility discussion in Chapter 6.

Chapter 5

Performance Analysis of Stirling Engine

5.1 Stirling Engine Design

5.1.1 Alpha Design

Various Stirling engine designs have been proposed since the first invention. The most common and referred design, is the alpha type, shown in Figure 5.1. Alpha machines are multiple piston machines that have two or more power pistons placed in separated cylinders that are interconnected with a regenerator (Walker, 1980). The regenerator is a heat exchanger made of a mesh pad, a material made of a network of wire or thread, similar to steel wool (Thombare and Verma, 2008). The pistons are mechanically linked together to a crankshaft (Walker, 1980). In a Stirling engine, there are three heat exchangers. One to transfer the heat from the heat source to the working fluid in the first cylinder, one regenerator between the pistons, and one to transfer the heat from the working fluid to the heat sink on the cold side piston cyclinder. The variations and configurations that can be made to a multiple piston machine are more or less endless (Thombare and Verma, 2008).

5.1.2 Beta Design

Beta engines have one power piston and one displacer (Walker, 1980). The displacer and the power piston are in line with each other in the same cylinder, as can be seen in Figure 5.2. The major difference between a displacer and a piston is that the displacer has the same pressure on

both sides, signifying that a seal is not necessary in order to contain the working fluids pressure (Thombare and Verma, 2008). In addition, the displacer is only there to change the volume and the pressure of the working fluid in the different compartments; it does not create mechanical power as do the piston (Walker, 1980). The displacer does not work on the gas, it simply just displaces it from one point to another (Walker, 1980). The displacer can also, in some few engine concepts, be made of a porous material that makes it into a heat exchanger, and in that way replace the regenerator (Thombare and Verma, 2008).

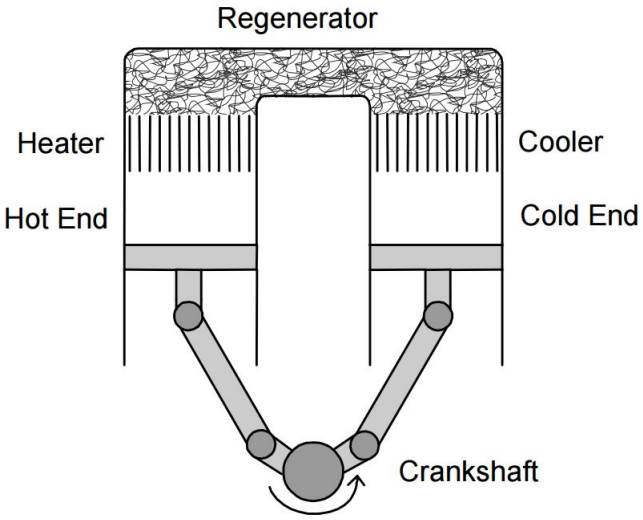

Figure 5.1: The Alpha Stirling engine (Majeski, 2002).

5.1.3 Gamma Design

The gamma engine works in the same way as the beta engine, just that the piston and the displacer operate in separate cylinders (Walker, 1980). In this configuration, it is the power piston that both compresses and expands the working fluid (Walker, 1980).

Even though there exist many configurations to the Stirling engine, all of them work on the same thermodynamic principle (Thombare and Verma, 2008). In the next section, two thermodynamic analyses of the Stirling engine will be presented.

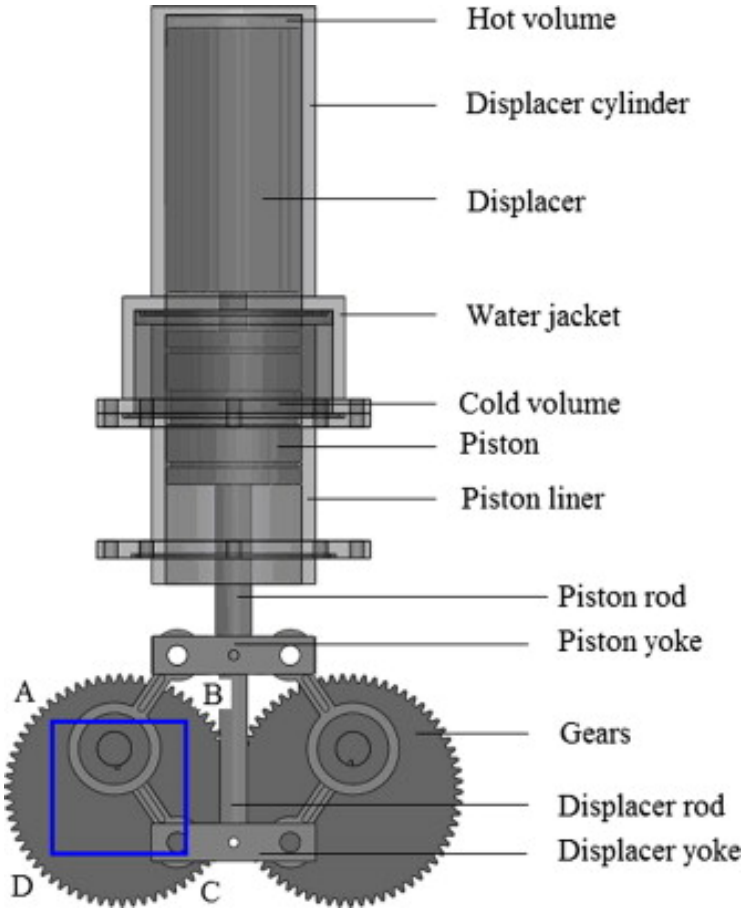

Figure 5.2: Example of Beta Stirling engine (Aksoy, 2013).

5.2 Thermodynamic Models of the Stirling Cycle

5.2.1 Ideal Stirling Cycle

The ideal Striling cycle consists of 4 processes, 2 isothermal and 2 adiabatic processes (Walker, 1980). The P-v and T-s diagram of the cycle can be seen in Figure 5.3. In the following thermodynamic model the heat supplied, the waste heat, and the heat rejected to the heat sink are denoted with Q_{wh} and Q_{hs} respectively. The heat transfer from the working fluid to the regenerator, and the heat transfer from the regenerator to the working fluid, are denoted with $Q_{wf,2-3}$ and $Q_{wf,4-1}$ respectively. Letting the temperature ratio be $\tau = T_{min}/T_{max}$ and the volume ratio be $r = V_{max}/V_{min}$, the 4 processes become (Walker, 1980):

Process 1-2: Isothermal expansion due to heat transfer from waste heat source. Work is done by the working fluid on the piston.

$$p_2 = p_1 V_1 / V_2 = p_1 (1/r); \quad T_2 = T_1 = T_{max} \tag{5.1}$$

$$Q_{wh} = W_{piston} = p_1 V_1 \ln r = R T_1 \ln r \tag{5.2}$$

$$\text{Change in Entropy} = (s_2 - s_1) = R \ln r \tag{5.3}$$

Process 2-3: Adiabatic and isochoric (constant volume) heat transfer from working fluid to regenerator until temperature T_{min}. No work is done, and there is a decrease in the internal energy and entropy of the working fluid.

$$p_3 = p_2 T_2 / T_3 = p_3 \tau, \quad V_3 = V_2 \tag{5.4}$$

$$\text{Heat transfer} = Q_{wf,2-3} = C_v (T_3 - T_2) \tag{5.5}$$

$$\text{Change in Entropy} = (s_3 - s_2) = C_v \ln \tau \tag{5.6}$$

Process 3-4: Isothermal compression. Heat transfer from working fluid at T_{min} to heat sink. Work is done on the working fluid equal in magnitude to the heat rejected from the cycle.

$$p_4 = p_2 T_2 / T_3 = p_3 \tau, \quad V_3 = V_2 \tag{5.7}$$

$$Q_{hs} = W_{3-4} = p_3 V_3 \ln(1/r) = R T_3 \ln(1/r) \tag{5.8}$$

Process 4-1: Adiabatic and isochoric compression of working gas. Heat transfer to working fluid from regenerator, increasing the temperature from T_{min} to T_{max}.

$$p_1 = p_4 T_1 / T_4 = p_1 / \tau, \quad V_4 = V_1 \tag{5.9}$$

$$Q_{wf,4-1} = C_v (T_1 - T_4), \quad W = 0 \tag{5.10}$$

Thermal Efficiency The thermal efficiency of the ideal Striling cycle is the same as the Carnot efficiency (Moran et al., 2010).

$$\eta_{th} = (Q_{wh} - Q_{hs})/Q_{wh} \tag{5.11}$$

$$\eta_{th} = \frac{RT_1 \ln r - RT_3 \ln(1/r)}{RT_1 \ln r} = 1 - \tau \tag{5.12}$$

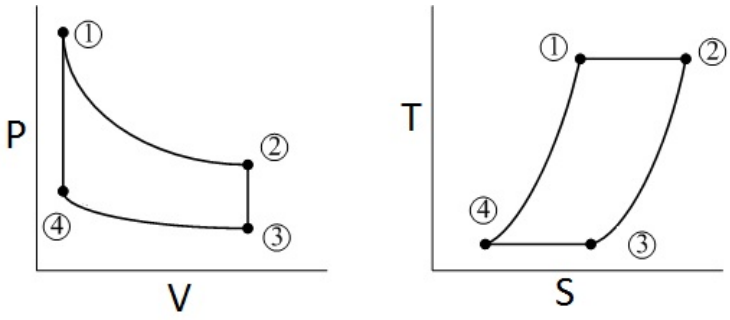

Figure 5.3: P-v and T-s diagram Striling cycle (Sketch made in Draw.io (2015).

The presented Stirling cycle is a highly idealized cycle and is based on thermodynamic reversible processes that are not obtainable in real engines (Walker, 1980). The ideal cycle is so idealized compared to the real Stirling engine that it is only suitable for very elementary and preliminary design calculations (Walker, 1980).

The real thermal efficiency is only a fraction of the ideal, or Carnot, efficiency (Walker, 1980). Walker (1980) expresses the ratio between the actual thermal efficiency and the carnot efficiency, as the relative efficiency (Equation 5.13). According to Walker (1980), a value above 0.4 for the relative efficiency is considered a well designed engine, and a value of 0.7 is considered as the maximum achievable. The term experience factor will also be used for relative efficiency in this work.

$$\eta_{rel} = \frac{\eta_{actual}}{\eta_{Carnot}} \tag{5.13}$$

It is evident that the ideal thermodynamic analysis will not give a good indication of the potential for harvesting waste heat with a Striling engine without multiplying it with an experi-

ence factor (Walker, 1980) (Thombare and Verma, 2008). Other thermodynamic analyses have been made in order to make the theoretical Stirling cycle more realistic. The Schmidts analysis is known to give good indication of the indicated power of a Stirling engine, given that certain design parameters are know (Walker, 1980) (Kongtragool and Wongwises, 2005) (Finkelstein and Organ, 2001). In this work, there is not a prototype engine available, and the design of a Stirling engine is not within the scope of this thesis. However, the Schmidt analysis is a good tool in order to get estimations on how big the piston cylinders of the engine should be and the pressure level of the engine in order to obtain a certain work output (Senft, 2002). The Schmidt analysis will be presented in the next section.

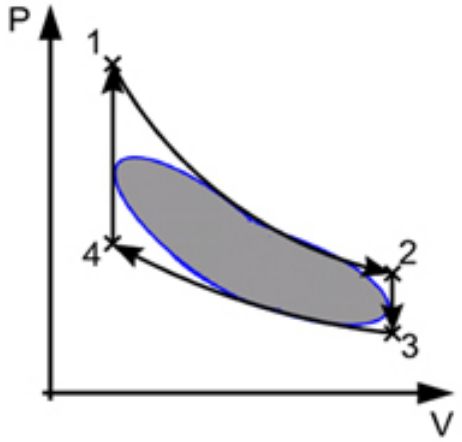

Figure 5.4: The ideal vs real stirling cycle (SunPower, 2015).

5.2.2 Schmidt Analysis

A more realistic cycle and corresponding analysis than the ideal cycle was devised by Gustav Schmidt in 1871 (Walker, 1980). The cycle is based upon sinusoidal volume variations as a function of crank angle, ϕ (Rakesh K. Bumataria, 2013). The analysis has become the common choice for preliminary design analysis of a Stirling cycle and gives a mathematical good estimate of the indicated work per cycle, given that it is followed by an appropriate experience factor to calculate the real thermal efficiency (Kongtragool and Wongwises, 2005) (Rakesh K. Bumataria, 2013). A Stirling engine design manual published by NASA in 1983 recommended calculating the shaft power by reducing the Schmidt analysis by an experience factor of 35% (Martini, 1983). Graham

Thomas Reader (1983) advised a factor between 30-50% for a good designed engine. G. Walker, one of the most cited researcher within the field of Stirling engines, writes in his book;
"To attain the likely performance of a practical engine one simply divides the efficiency and power output of the Schmidt analysis by two (if one is an optimist) or by three (if one is a realist)" (Walker, 1980). When using the Schmidt analysis for this work, an experience factor of 30% will be used. The value is on the low side compared to what the cited researchers report, but a conservative value is chosen to keep the result of the power output at a realistic and obtainable level. An alpha-type Stirling Engine is chosen as the reference model, since that is the most common engine configuration (West, 1986) (Kongtragool and Wongwises, 2005).

Assumptions for Schmidt Analysis

When the volume, the mass of the working gas and the temperature are decided, the pressure is calculated using an ideal gas method as shown in Equation 5.14 to 5.33 (Walker, 1980). The assumptions for the analysis are as follows (Walker, 1980):

1. There is no pressure loss in the heat exchangers and there are no internal pressure differences.
2. The regeneration is perfect.
3. The expansion and compression processes are isothermal.
4. The working gas is modeled as an ideal gas.
5. The regenerator gas temperature is an average of the expansion gas temperature, T_E, and the compression gas temperature, T_C.
6. The expansion space, V_E, and the compression space, V_C, change according to sine curves.

Alpha Design Stirling Engine

The compression and the expansion volume, V_E and V_C, are calculated with Equation 5.14. V_{SE} and V_{SC} are both the swept volume of the piston cylinders. V_{DE} and V_{DC} are the dead volumes of the expansion and compression cylinder respectively. Both volumes are calculated based on

the crank angle, ϕ.

$$V_E = \frac{V_{SE}}{2}(1-\cos\phi) + V_{DE} \qquad V_C = \frac{V_{SC}}{2}(1-\cos(\phi - d\phi) + V_{DC} \tag{5.14}$$

The total volume is calculated with Equation 5.15. V_R is the volume of the regenerator.

$$V_{tot} = V_E + V_R + V_C \tag{5.15}$$

The total mass in the engine is calculated by using the ideal gas law for both cylinder volumes and the regenerator volume.

$$m = \frac{PV_E}{RT_E} + \frac{PV_R}{RT_R} + \frac{PV_C}{RT_C} \tag{5.16}$$

The temperature ratio, t, the swept volume ratio, v, and the dead volume ratios, X_{DE}, X_{DC} and X_R, are found with the following equations:

$$t = \frac{T_C}{T_E}, \qquad v = \frac{V_{SC}}{V_{SE}}, \qquad X_{DE} = \frac{V_{DE}}{V_{SE}}, \qquad X_{DC} = \frac{V_{DC}}{V_{SE}}, \qquad X_R = \frac{V_R}{V_{SE}} \tag{5.17}$$

The temperature in the regenerator, T_R, is calculated based on temperatures in the expansion and compression cylinders.

$$T_R = \frac{T_E + T_C}{2} \tag{5.18}$$

By using the ratios, t and X_R, in addition to the equations for V_E and V_C, then the mass in the engine can be described by the crank angle, ϕ.

$$m = \frac{P}{RT_C}\left(tV_E + \frac{2tV_R}{1+t} + V_C\right) \tag{5.19}$$

$$m = \frac{PV_{SE}}{2RT_C}\Big(S - Bcos(\phi - a)\Big) \tag{5.20}$$

By defining the coefficients, a, S and B, the engine pressure is defined as in Equation 5.24

$$a = \tan^{-1}\frac{v\cdot\sin d\phi}{t+\cos d\phi} \tag{5.21}$$

$$S = t + 2tX_{DE} + \frac{4tX_R}{1+t} + v + 2X_{DC} \tag{5.22}$$

$$B = \sqrt{t^2 + 2tv \cdot \cos d\phi + v^2} \tag{5.23}$$

$$P = \frac{2mRT_C}{V_{SE}(S - B\cos(\phi - a))} \tag{5.24}$$

The mean pressure, P_{mean}, is calculated with Equation 5.25.

$$P_{mean} = \frac{1}{2\pi}\oint P d\phi = \frac{2mRT_C}{V_{SE}\sqrt{S^2 - B^2}} \tag{5.25}$$

By defining the coefficient, c, and using Equation 5.25, the engine pressure can be defined by the mean pressure:

$$c = B/S \tag{5.26}$$

$$P = \frac{P_{mean}\sqrt{S^2 - B^2}}{S - B\cos(\phi - a)} = \frac{P_{mean}\sqrt{1 - c^2}}{1 - c \cdot \cos(\phi - a)} \tag{5.27}$$

By setting $\cos(\phi - a)$ =1 or -1, the minimum and maximum pressure of the Schmidt cycle can be found. Then, it is possible to define the engine pressure based on the maximum or minimum pressure.

$$P_{min} = \frac{2mRT_c}{V_{SE}(S + B)} \tag{5.28}$$

$$P = \frac{P_{min}(S + B)}{S - B \cdot \cos(\phi - a)} = \frac{P_{min}(1 + c)}{1 - c \cdot \cos(\phi - a)} \tag{5.29}$$

$$P = \frac{P_{max}(S - B)}{S - B \cdot \cos(\phi - a)} = \frac{P_{max}(1 - c)}{1 - c \cdot \cos(\phi - a)} \tag{5.30}$$

The indicated work of the engine can be calculated by the area of the P-v diagram. Equation 5.31 to 5.33 are used for the calculation.

$$W_E = \oint P dV_E = \frac{P_{mean} V_{SE} \cdot \pi c \cdot \sin a}{1 + \sqrt{1 - c^2}} \tag{5.31}$$

$$W_C = \oint P dV_C = -\frac{P_{mean} V_{SE} \cdot \pi c t \cdot \sin a}{1 + \sqrt{1 - c^2}} \tag{5.32}$$

$$W_i = W_E + W_C \qquad [\mathrm{J}] \tag{5.33}$$

This analysis will be built in EES in order to investigate the potential for harvesting waste heat from the case vessel's engine with a Stirling engine. The EES model can be seen in Appendix E. The parameters used in the thermodynamic analyses can be seen i Section 5.3.6.

5.3 Selection of Thermodynamic Parameters and Factors that Influence Performance in Stirling Engines

The effects of the practical factors that cause the actual engine cycle to deviate from the ideal case are required to be considered separately in order to highlight their influence.

5.3.1 Mean Cycle Pressure

An increase in the pressure level will directly increase the Stirling engine power output (Walker, 1980). Therefore, commercialized Stirling engines today typically operate with pressures from 50-200 bar (p_{mean}=25-100 bar) (Asnaghi et al., 2012). According to Walker (1980), it is very difficult to increase the volume compression ratio much above V_{max}/V_{min}= 2.5, as a consequence of this, the pressure ratio, p_{max}/p_{min}, in Stirling engines become very low compared to ICEs. The pressure ratio rarely exceeds 2, which will cause both p_{max} and p_{min} to become relatively high for high cycle pressures (Walker, 1980). For such high pressure values, the piston and cylinders need to withstand high stresses, and this will require thick cylinders walls made of expensive materials that will increase the size, weight and cost of the engine (Walker, 1980). Stirling engines with high performance tend to use helium and hydrogen as their working fluid due to their high thermal conductivity and low viscosity (Majeski, 2002). These fluids have very low

molecular weight, so by pressurizing these fluids, the diffusion and lekage out of the engine increase which will reduce performance (Majeski, 2002). Additionally, the greater the difference between the pressure in the expansion space and the compression space, the more difficult it will be to maintain the high pressure in the expansion space, and as a result the power output will decrease (Walker, 1980).

5.3.2 Engine Speed

Same as for the mean cycle pressure, an increase in the engine speed will increase the work output (Thombare and Verma, 2008). Most Stirling engines operate at a high speed (or piston frequency), sometimes up to 2000 rpm (Majeski, 2002). High speeds will cause viscous losses, mechanical friction and wear that will lower the efficiency and the lifetime of the engine (Majeski, 2002). Several companies today are designing low-speed engines to increase the efficiency and lengthen the useful life of the engine (Majeski, 2002). Larger Stirling engines are more likely to have lower speeds, and smaller engines will exhibit higher speeds, similar to the trend seen in IC engines (Majeski, 2002). To reduce viscous losses light molecular weight working fluids with low viscosity are to be used such as helium and hydrogen (Majeski, 2002). However, as mentioned previously, these gases are difficult to contain because of ability to diffuse through solid material.

5.3.3 Dead Volume

In the ideal Stirling cycle, all the working fluid is in the same space at the same condition and time (Walker, 1980). This would be impossible in a real Stirling engine (Walker, 1980). Total dead volume is defined as the sum of Stirling engine void volumes (Walker, 1980). It is evident that a real Stirling engine must have some unavoidable dead volume, and that the presence of dead volume will reduce the efficiency of the engine (Thombare and Verma, 2008). Several researchers report that the dead volume in a Stirling engine is usually within the range from 40-60% (Thombare and Verma, 2008) (Asnaghi et al., 2012). The Schmidt analysis can be used to consider the effect of dead volumes on power output (Thombare and Verma, 2008).

5.3.4 Imperfect Regeneration

Imperfect regeneration is another important cause for poor engine performance. Blockage of the mesh pad used in the regenerator is often caused due to particles that are generated from the rubbing action of piston rings and fouling due to lekage of lubrication oil (Majeski, 2002). Various studies have showed that the regenerator is the most crucial part in terms of increasing the efficiency of a Stirling engine (Thombare and Verma, 2008). The effectiveness of the regeneration process largely depends upon the thermal capacity of the regenerator material (Thombare and Verma, 2008). In order to obtain the best possible performance of the regenerator, it has to be optimized to the specific power requirement and heat source available for the application of interest (Thombare and Verma, 2008).

5.3.5 Stirling Engine Working Fluids

Not any of the thermodynamic analyses presented in the previous sections take into consideration the physical characteristics of the working fluid. There are not as many alternatives for working fluids as there are for ORC applications. Compressible fluids, such as hydrogen, helium, nitrogen, air or vapors are typically used as working fluids (Majeski, 2002). A few scientists have done research on which working fluids are the best for a Stirling engine in order to reach highest possible performance.

Performance of Working Fluids

The thermophysical properties of the fluid will very much influence the performance of the Stirling engine (Thombare and Verma, 2008). The working fluid in a Stirling engine should have the following thermophysical properties (Thombare and Verma, 2008):

- High thermal conductivity.
- High specific heat capacity.
- Low viscosity.
- Low density.
- Low molecular weight.

Any working fluid with high specific heat capacity may be used for Stirling cycle engines (Thombare and Verma, 2008). Air was for many years used as working fluid due to its good availability (Walker, 1980). Helium and hydrogen are mostly used today due to their high thermal conductivity, low molecular weight and low viscosity which result in good performance, as can be seen in Figure 5.5 (Kongtragool and Wongwises, 2005).

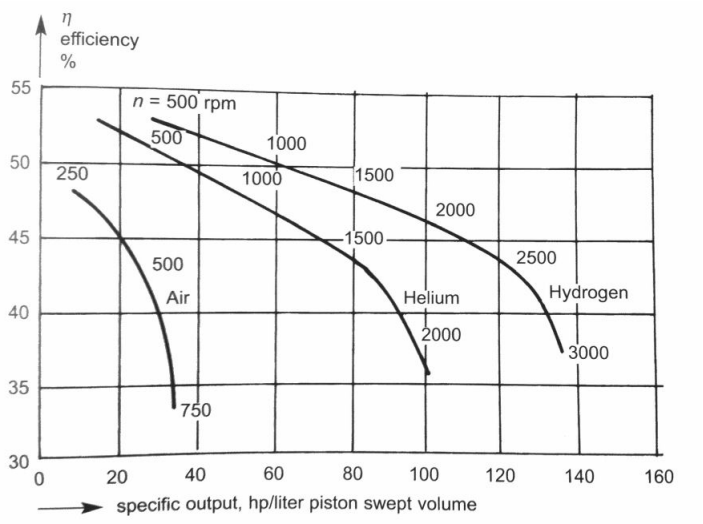

Figure 5.5: Efficiency of air, helium and hydrogen (Finkelstein and Organ, 2001).

From an investigation on power output of gamma-configuration low temperature differential Stirling engines, Bancha Kongtragool and Somchai Wongwises collected data from studies done on various prototype engines, as can be seen in Figure 5.1 (Kongtragool and Wongwises, 2005). It is evident from Table 5.1 that for the ANL (Argonne National Laboratory) engine, helium gives a much higher power output compared to air (Kongtragool and Wongwises, 2005).

	Working fluid	T_H (K)	T_C (K)	P (W)	f (Hz)	V_P (cc)	p_m (bar)
ANL* engine	He	363	283	1.65	2.167	150	1
	Air	363	283	0.7	1.667	150	1
Standard displacer	Air	369	279	0.642	1.75	120	1
Regenerative displacer	Air	369	279	1.05	2.063	120	1
L-27 engine	Air	366	307	0.252	4.5	25	1

Table 5.1: Performance of gamma Stirling engines (Kongtragool and Wongwises, 2005).

A study performed in 1997 on performance differences in a 100 W Stirling engine for helium and nitrogen as the working fluids showed that nitrogen gave the highest power output in a wider range for engine speeds than what helium did (Hirata et al., 1997). It was assumed by the researchers that the high gas leakage of helium was the cause of the low power output for helium (Hirata et al., 1997). Better seals would improve the power output of the engine by using helium, and could increase it to a level higher than what achieved with nitrogen, but this would also imply a more expensive engine (Hirata et al., 1997). Higher leakage rates will also increase maintenance cost since the lost gas will have to be replaced (Majeski, 2002).

Heavier working fluids can be used, such as oxygen, air or nitrogen, that will allow the use of cheaper and more conventional seals, but these fluids will reduce the efficiency (Majeski, 2002). Even though there are some benefits connected to using heavier working fluids, most manufactures today use helium or hydrogen (Majeski, 2002).

Availability, Cost, Safety and Environmental Concerns of Working Fluids

As discussed in Section 4.4.3 regarding working fluids for ORC applications, the availability of a substance chosen as working fluid is highly important. The cost of a fluid is directly influenced by the level of availability (Majeski, 2002).

Hydrogen is all around us. It makes up two thirds of the composition of water and exists in all living things (Olsen, 2006). Even so, the process of converting hydrogen into a usable fluid is very energy demanding, especially if it should be produced without using fossil fuels (Olsen, 2006). About 95% of all hydrogen is produced from fossil sources, making it a non-renewable gas (Olsen, 2006). However, if alternative forms of creating the energy needed to make hydrogen fuel are developed such as solar energy, the process of producing hydrogen fuel can be a pollutant free procedure (Olsen, 2006).

Helium is the second most abundant element in the universe, but on Earth it is relatively rare, found trapped underground with natural gas and in the atmosphere, where it escapes into space due to its low molecular weight (Connor, 2015). On earth there exist a few locations where helium can be harvested; The US National Helium Reserve, which accounts for about 30% of the words helium supply, in addition to recently created helium plants in Russia, Qatar, Algeria and Australia (Connor, 2015). There is a shortage of helium today (Connor, 2015). The major

reason for this is the result of a law from 1996 that forced the US government to sell most of its helium reserves at very low prices (Connor, 2015). Increasing demand for helium, especially from China, together with decreasing availability has caused the price of helium to escalate the last years (Connor, 2015).

The availability of nitrogen is very good (Linde Industrial Gases, 2015). Air contains about 78% nitrogen. For industrial uses, nitrogen is produced in air separation plants (Linde Industrial Gases, 2015). Substantial amounts of nitrogen is also present in natural gas. Nitrogen is also non-flammable, colourless, odourless, tasteless, non-toxic and almost totally inert gas (Linde Industrial Gases, 2015).

The above discussion implies that nitrogen is very promising as working fluid for WHRS in ships operating on global routes, considering it's high availability, low flammability and low cost compared to helium and hydrogen. Nitrogen has a much higher molar weight and will theoretically give lower efficiencies, however, the higher MW would limit the leakage problems often encountered with hydrogen and helium and allow the use of more conventional seals. Conventional seals reduce engine fabrication costs, and make the internal engine components readily accessible for maintenance work, as opposed to hermetically sealed engines that must be designed for little or no maintenance (Majeski, 2002).

5.3.6 Model Parameters for Thermodynamic Analysis

Based on the above discussion and the data from the exergy analysis, the following parameters will be used in the thermodynamic analyses.

Property	Value	Unit
Inlet temp exhaust heat source, $T_{exhaust}$	370-460	°C
Inlet temp CW heat source, T_{cw}	91-82	°C
Mean pressure in SC, p_{mean}	0-100	bar
Total dead volume in SE η_p	0-70	%
Volume of stroke, V_{stroke}	0-0.5	m^3
Temperature of heat sink	50	°C
Speed of engine, n	0-1800	rpm
Volume of regenerator, V_{reg}	0.001-0.1	m^3

Table 5.2: Parameters for thermodynamic analyses of Stirling engine.

5.4 Discussion and Results of Performance Analysis of SE

The objective of this investigation was to perform a thermodynamic analysis of a Stirling engine. Ideal performance has been calculated in addition to identifying main losses. Estimations for real performance have been done based on available methods. A computer program in EES was developed for the Schmidt cycle analysis.

I Figure 5.6 and 5.7 the efficiency results of the ideal analysis vs exhaust temperature and cooling water temperature can bee seen respectively. The curve on the top of both of the graphs represent the Carnot efficiency. The efficiency is plotted for three different relative efficiencies (experience factors); n_{rel} = 0.25, 0.3 and 0.4. The heat sink was set to the same temperature for all calculations; T_{sink} = 360 [K]. The efficiencies vary very little compared to the internal variations in exhaust and cooling water temperature, implying that the Stirling engine efficiency would not be that affected by the engine load. The efficiencies for the Stirling engine operating with cooling water as heat source, obtain much lower efficiencies than the engine operating with the exhaust as heat source. This is because the Stirling engine efficiency is directly dependent on the heat source temperature, and with substantial negative change in the heat source temperature, the efficiency will decrease significantly. However, for the SE operating with CW as the heat source, the efficiencies are higher than what achieved for the best ORC systems with CW as heat source.

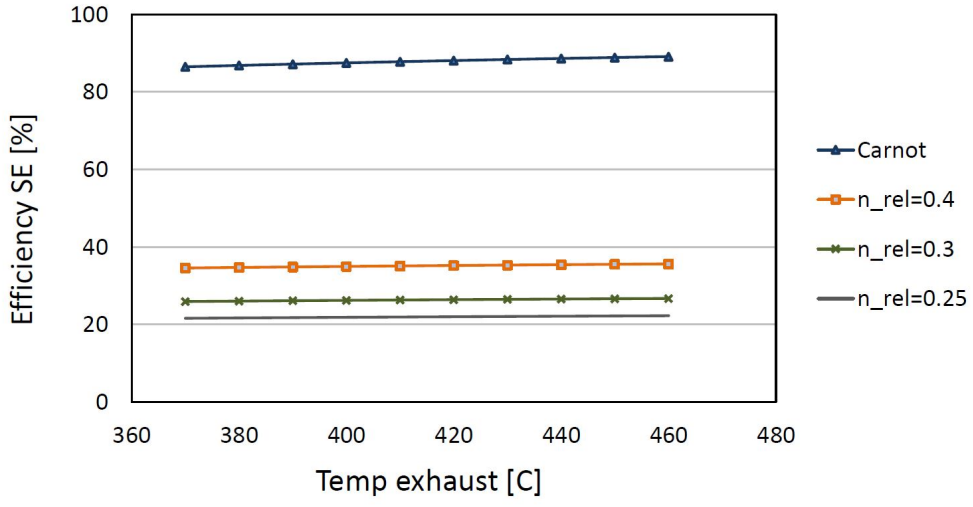

Figure 5.6: Efficiency SE vs exhaust temperature with three different experience factors.

Even for the lowest experience factor of 25%, the actual efficiency of the Stirling engine with

exhaust as heat source is around 22%, which is higher than the best ORC system with benzene as the working fluid, and much higher than the ORC with R-245fa. It should be noted that the values are highly dependent on how well the engine is designed, and that this is only a study of potential performance. To repeat from Section 5.2.1; a Stirling engine with an experience factor of 0.4 is considered a well designed engine (Walker, 1980). Conservative experience factors have been chosen in order to keep the analysis as realistic as possible.

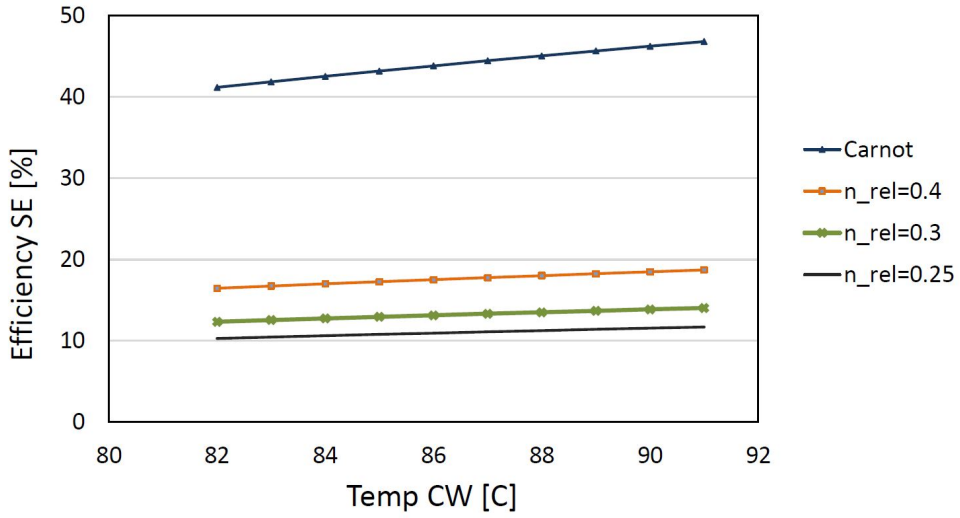

Figure 5.7: Efficiency SE vs CW temperature with three different experience factors.

From this analysis, three different efficiencies from both exhaust and CW heat sources were chosen for further study of the potential for waste heat recovery, these can be seen in Table 5.4. Based on the results in Figure 5.6 and 5.7, it was assumed that the efficiency will stay constant for varying load.

Efficiency SE exhaust		Efficiency SE CW	
n_{rel}	n	n_{rel}	n
0.25	0.22	0.25	0.11
0.3	0.27	0.3	0.13
0.4	0.35	0.4	0.17

Table 5.3: Results of ideal Stirling cycle analysis, efficiencies.

For the efficiencies in Table 5.4, the corresponding power outputs for the exergy in the ex-

haust have been plotted in Figure 5.8 and 5.8. The work outputs for the Stirling engine using the exhaust as heat source are substantially higher than what was achieved with the ORC systems due to the SE's higher efficiency. The efficiencies of 22-35% correspond to 3.9-6.2% of the main generator engine's power output at 100% load for the exhaust as heat source. At 50% load this would correspond to 5.5-8.8% of the engine's power output. For the CW as heat source, the Stirling engine power output corresponds to about 0.75% of the MGE1 power for η = 11%, and about 1.2% of the MGE1 power for η = 17% at approximately 100% load.

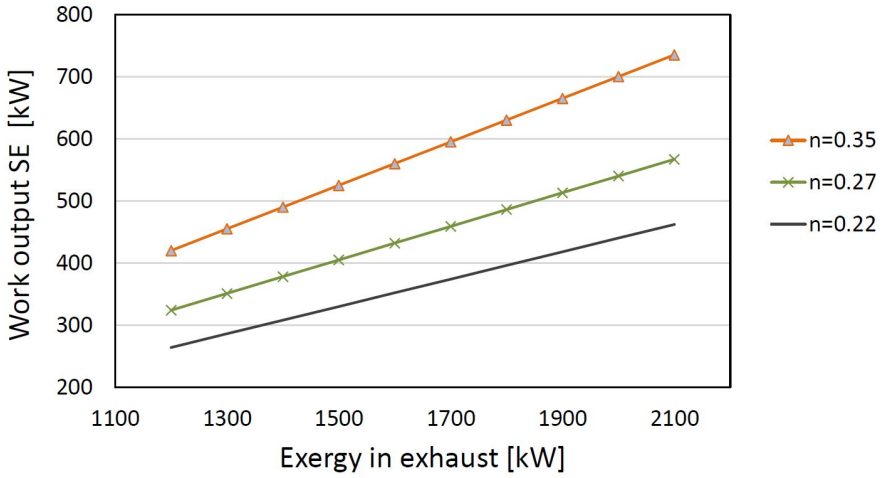

Figure 5.8: Work output SE vs exergy in exhaust for three different efficiencies.

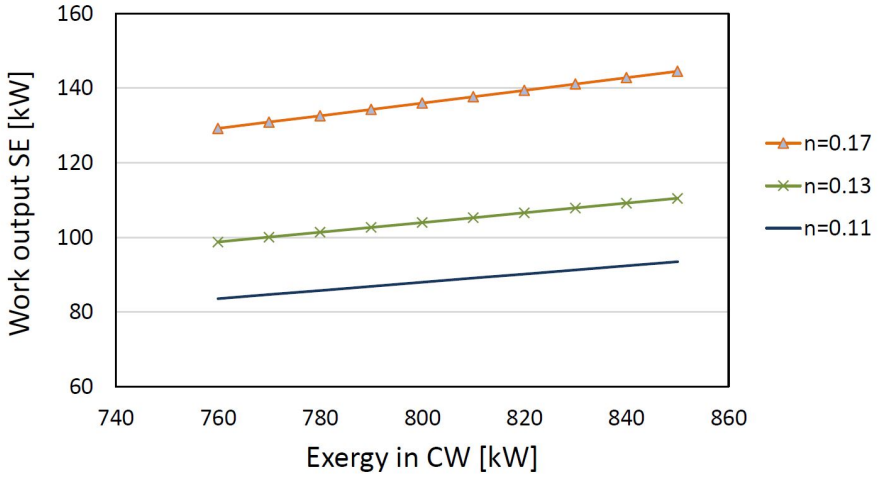

Figure 5.9: Work output SE vs exergy in CW for three different efficiencies.

As discussed in previous sections, the Schmidt cycle is based on linear functions of engine speed, pressure of working fluid and the size of the engine (Walker, 1980). In Figure 5.10, the Schmidt cycle is plotted in a P-v diagram for a randomly chosen engine with a dead volume of 50%, speed of 400 rpm, $V_{stroke} \approx 0.5\ m^3$, a regenerator volume of 0.1 m^3 and p_{mean}= 20 bar. This cycle gives a power output of 446 kW for an experience factor of 0.3.

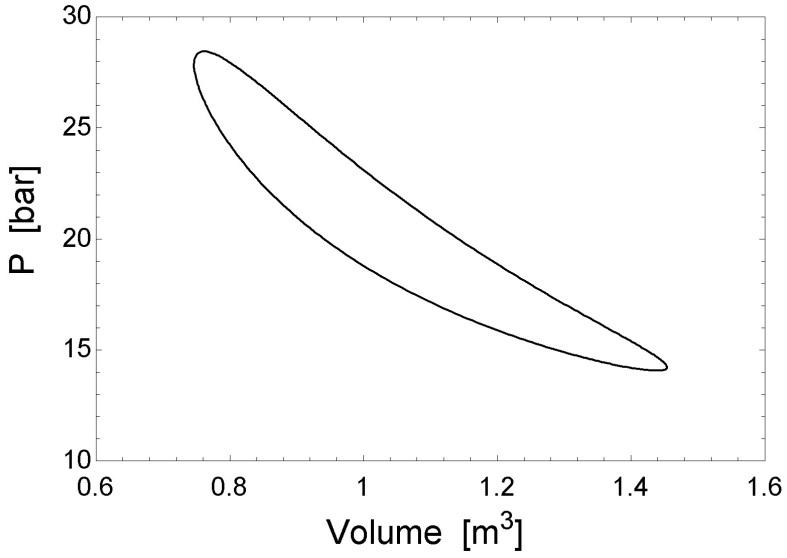

Figure 5.10: Schmidt cycle, V_{dead}= 50%, n= 400 rpm, V_{reg}= 0.1m^3, V_{stroke}= 0.5m^3 and p_{mean}=20 bar.

As can be seen in Figure 5.11, 5.12 and 5.13, the engine work output increases as the engine speed, the mean pressure and the size are increased when running the Schmidt cycle. In Figure 5.14, the work is plotted against the percentage of dead volume in both piston cylinders. It is evident that the dead volume is a significant factor of loss in the engine, and that effort should be made to keep the dead volume as small as possible when preliminary engine design is carried out.

For a Stirling engine aboard a ship, one of the first priorities is the limited space. The Stirling engine should therefore be as small as possible. For the Schmidt cycle plotted in Figure 5.10, the engine has a total internal volume of approximately 1.5 m^3, which would result in a very big engine. In order to decrease the size of a Stirling engine, it is evident that the engine speed or the mean pressure has to be increased. In Figure 5.15, the P-v diagram of the Schmidt cycle is

plotted for an engine with reduced size, but increased pressure and speed; V_{dead}= 50%, n= 1700 rpm, $V_{stroke} \approx 0.01\ m^3$, V_{reg}= 0.001 m^3 and p_{mean}= 100 bar. This cycle gives a power output of 198 kW with an experience factor of 0.3. The power output is quite low even though the pressure and the speed are very high. This implies that the available space on a ship for a Stirling engine implementation should be decided before the Stirling engine is designed. This will enable the designer to maximize the size before considering pressure and speed levels.

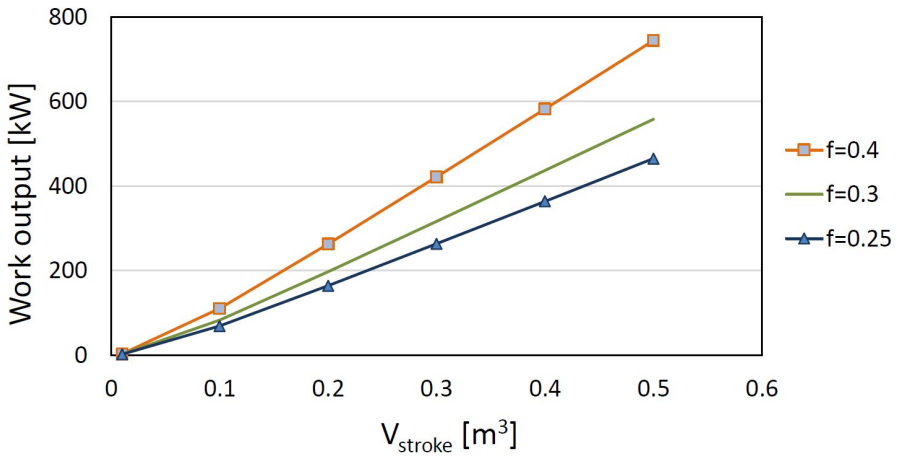

Figure 5.11: Schmidt analysis, Work output vs V_{stroke} for three different experience factors.

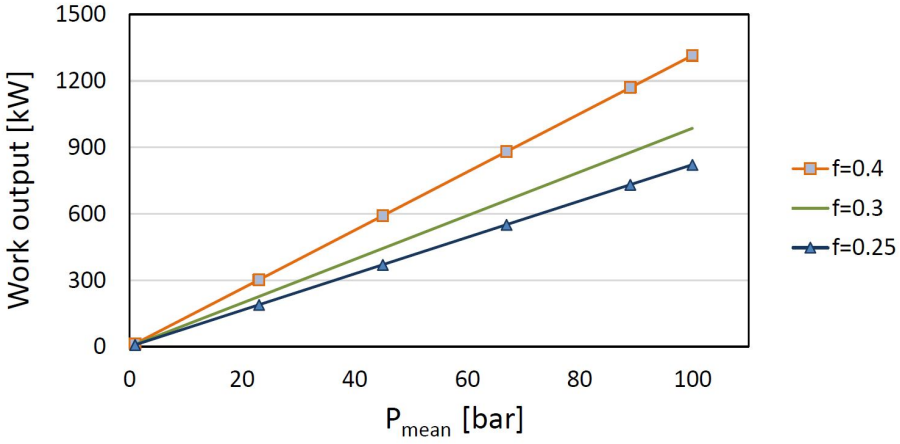

Figure 5.12: Schmidt analysis, Work output vs p_{mean} for three different experience factors.

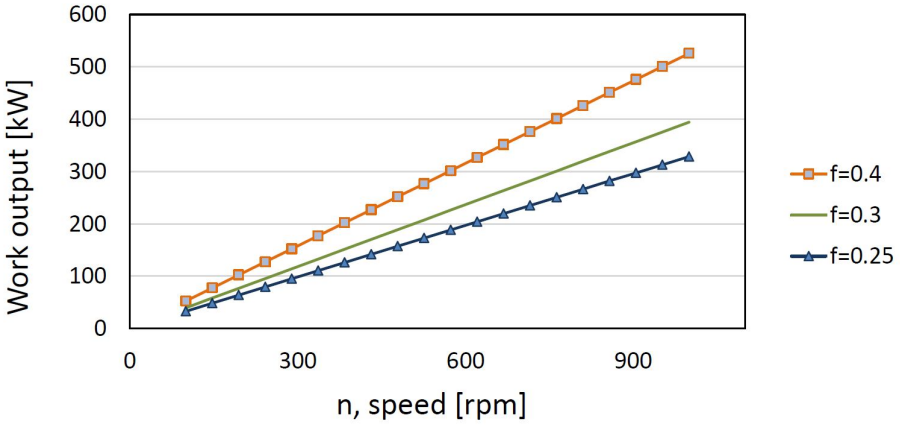

Figure 5.13: Schmidt analysis, work output vs n, speed for three different experience factors.

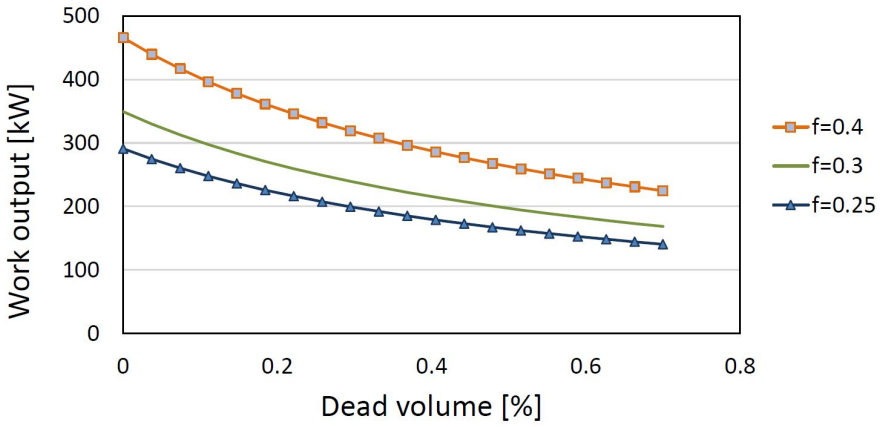

Figure 5.14: Schmidt analysis, work output vs V_{dead} for three different experience factors.

Even though a small Stirling engine is beneficial considering the limited space on a ship, the disadvantages with high speed and high pressure Stirling engines need to be taken into account. According to Majeski (2002), the following advantages are achieved with a low-speed engine:

- Lower wear that gives longer life-time.
- Lower viscous drag losses in the working gas.
- Lower friction losses on seals.
- Smaller heat exchanger and regenerator components.

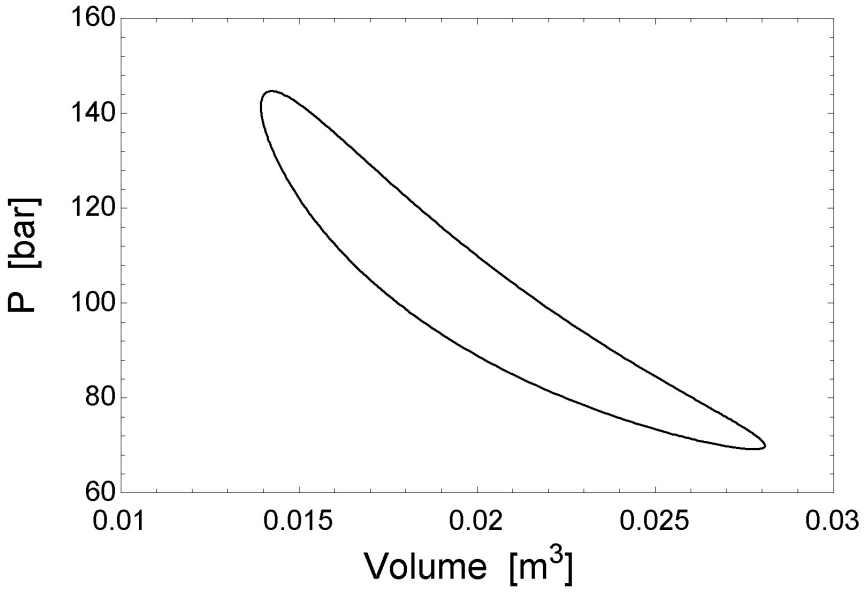

Figure 5.15: Schmidt cycle, V_{dead}= 50%, n= 400 rpm, V_{reg}= 0.1m^3, V_{stroke}= 0.5m^3 and p_{mean}=20 bar.

It is evident from this study that the design of a Stirling engine is a complex and cumbersome procedure where many aspects have to be taken into consideration. The major losses of a Stirling engine that will reduce the engine net work output and the thermal efficiency have shown from this study to be:

- Lekage of working fluid.
- Blockage and fouling of regenerator.
- Dead space in piston cylinders and regenerator.
- Low temperature heat source.

The final design will be a trade-off between speed, size, pressure and work output. This study has showed that the potential of harvesting waste heat with a Stirling engine seems very promising for the exhaust stream as heat source. Using a Stirling engine to harvest waste heat from the CW shows less promising results due to the low temperature of the cooling water. Even so, efficiencies around 11-17 % were calculated. From the discussion on working fluids, it is found that the typical working fluids used in Stirling engines today, such as helium and hydrogen, might

not be the best solution for the future considering the working fluids low availability and high cost compared to more conventional gases such as nitrogen. The study indicates that a Stirling engine working with relatively high temperature heat sources with nitrogen or other safe, cheap and available working fluid is potentially attractive for WHR systems on ships operating on global routes.

A discussion of technical and economical feasibility of the Stirling engine will be given in the next chapter.

Chapter 6

Feasibility Discussion

6.1 Technical Feasibility

In this study, both the ORC and Stirling engine have shown promising results regarding potential for harvesting waste heat from the case vessel's engine. Even though the systems are promising in terms of theoretical efficiencies, there are other factors that need to be discussed to evaluate whether it is feasible to implement these technologies into the case vessel's machinery system.

In this study, the major technological hurdles faced by Stirling engines for WHRS marine applications have shown to be:

1. Leakage from the high-pressure working fluid space to the lubrication in the mechanical drive train and leakage of working fluid out of the cylinder space reduce performance.
2. High material stress and corrosion in the high-temperature and/or high-pressure heat exchangers demands high cost material and frequent maintenance.
3. Low compression ratio due to dead volume reduces efficiency.
4. Blockage of the fine-meshed heat matrices used in the regenerator lowers thermal efficiency and increases maintenance.
5. Large volume and weight demands sufficient available space for implementation.
6. Since Stirling engine design is not fully developed or commercialized the unit cost is high.

Most of the challenges with Stirling engines are related to design. Especially leakage of working fluid has shown to be a great concern. As discussed in Chapter 5, the use of nitrogen or other

heavier fluid would limit that issue, additionally to adding the benefit of higher global availability and enable the use of less expensive seals. However, the higher viscosity and lower thermal conductivity of nitrogen tend to reduce the ability to achieve high cycle efficiencies. According to Stirling engine manufacturers today that utilize nitrogen, the benefits of using working gases with higher molar weight triumphs the potential increase in efficiency received with low molar weight gases (Majeski, 2002).

According to Majeski (2002), the manufacturers that report issues with material stress do operate their Stirling engines with hot end temperatures within the range of 650-800 C. Manufactures that operate with lower temperatures within the range of 90-600 C obtain lower efficiencies, but experience a significant reduction in issues related to material degradation, high cost materials and short life time (Majeski, 2002). Considering the temperature level of the exhaust in this study that is around 400 C, material issues should not be a big concern regarding using Stirling engines for WHRS in the case vessel.

Regarding challenge number 3 related to dead volume, the study by Asnaghi et al. (2012) states that there is still potential for reduction of dead volume in Stirling engines if investment in further research and development is done.

Blockage of the regenerator is often due to fouling or that the regenerator is contaminated with small particles caused from friction and wear between mechanical parts. According to Majeski (2002) and Kongtragool and Wongwises (2005), both these weaknesses should be possible to overcome with sufficient investigation.

Increased investment in Stirling engine development, prototype testing and demonstration is needed in order to determine the possibility to solve these fundamental technical challenges. Challenge 5 and 6 regarding volume, weight and cost will be discussed and elaborated in the next sections.

For ORC systems, the technology is highly developed compared to Stirling engine technology and the ORC systems have therefore not as many challenges as the Stirling engine. The major issue regarding the use of ORC as WHRS has shown to be:

1. To find a proper working fluid that gives good efficiency at the same time as high avail-

ability, high safety and low environmental impact.

Since the choice of working fluid affects the efficiency to such a high extent, it is very important to chose the correct one. In this study benzene gave the best efficiency. However, considering benzen is carcinogenic and its high flammability, it was concluded that an ORC with benzene would not be a feasible solution. As discussed in Chapter 4, many non-flammable and non-toxic refrigerants promoted in the past as attractive working fluids have been outlawed because of their ozone depletion potential, causing the working fluids that are available today to be less thermodynamically efficient. Several refrigerant suppliers are currently doing research in order to develop new refrigerants that have good thermodynamic qualities without compromising on environment or safety (ASHRAE, 2010). If refrigerant suppliers succeed in their goal, then it might be possible to gain efficiencies as high as 20-25% percent for safe and environmental friendly ORC systems. Apart from the working fluid challenge, the ORC system is a highly feasible solution considering it is composed of well known components such as pumps, expansion turbines and heat exchangers.

Further, in this study it was shown that in order to keep the efficiency of the ORC at a more or less constant level, it needs to be possible to control the mass flow of the working fluid. This will enable the mass flow to go down when there is less exergy to be harvested in the exhaust, and in that way reduce the pump work in the ORC at lower loads. This would be possible by installing a liquid receiver for the working fluid, and have a thermostatic control valve that will optimize the fluid flow based on the marine engine load.

In the next section, a comparative study of space requirement, implementation into existing machinery and cost of both systems will be evaluated.

6.1.1 Space Requirement

Space requirement is especially important when implementing WHRS in ships considering the limited space available compared to onshore facilities.

According to Majeski (2002), footprint, volume and weight of the Stirling engine increase with power output. This agrees well with the results in Section 5.4 in Chapter 5, where it was evident that the volume of the piston cylinders increased linearly with the increase in power.

Majeski (2002) has demonstrated this in Figure 6.1. The numbers are based on data from 19 different companies that produced, or did research, on Stiling engine prototypes in 2002. By including the numbers of height of the engines given by Majeski (2002), the volume of the Stirling engines can be plotted. By taking a regression line and do a linear interpolation in Matlab (MATLAB, 2014) to a hypothetical Stirling engine with power output of 800 kW, the volume of the Stirling engine becomes 43.5 m^3, as can be seen in Figure 6.2.

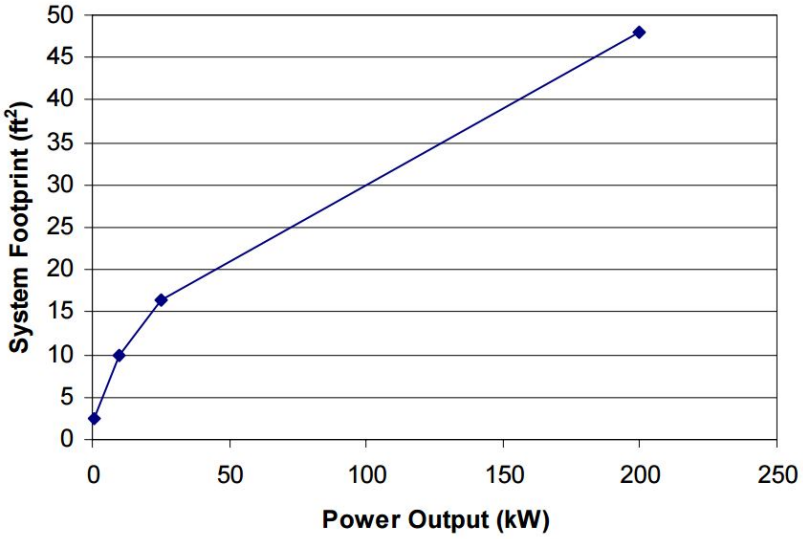

Figure 6.1: Stirling system footprint vs power output (Majeski, 2002).

Figure 6.2: Stirling system volume vs power output.

These numbers can be compared to the volume specifications given by the only company that produces ORC solutions for marine engines today; Opcon (Opcon, 2012). The dimensions of the Opcon ORC Powerbox can be seen in Table 6.1. This is for an Opcon ORC Powerbox with maximum power output of 800 kW.

Dimension	Size
Height [m]	4.6
Width [m]	3.4
Length [m]	8.5
Volume [m^3]	132.94

Table 6.1: Dimensions of Opcon ORC Powerbox (Opcon, 2012).

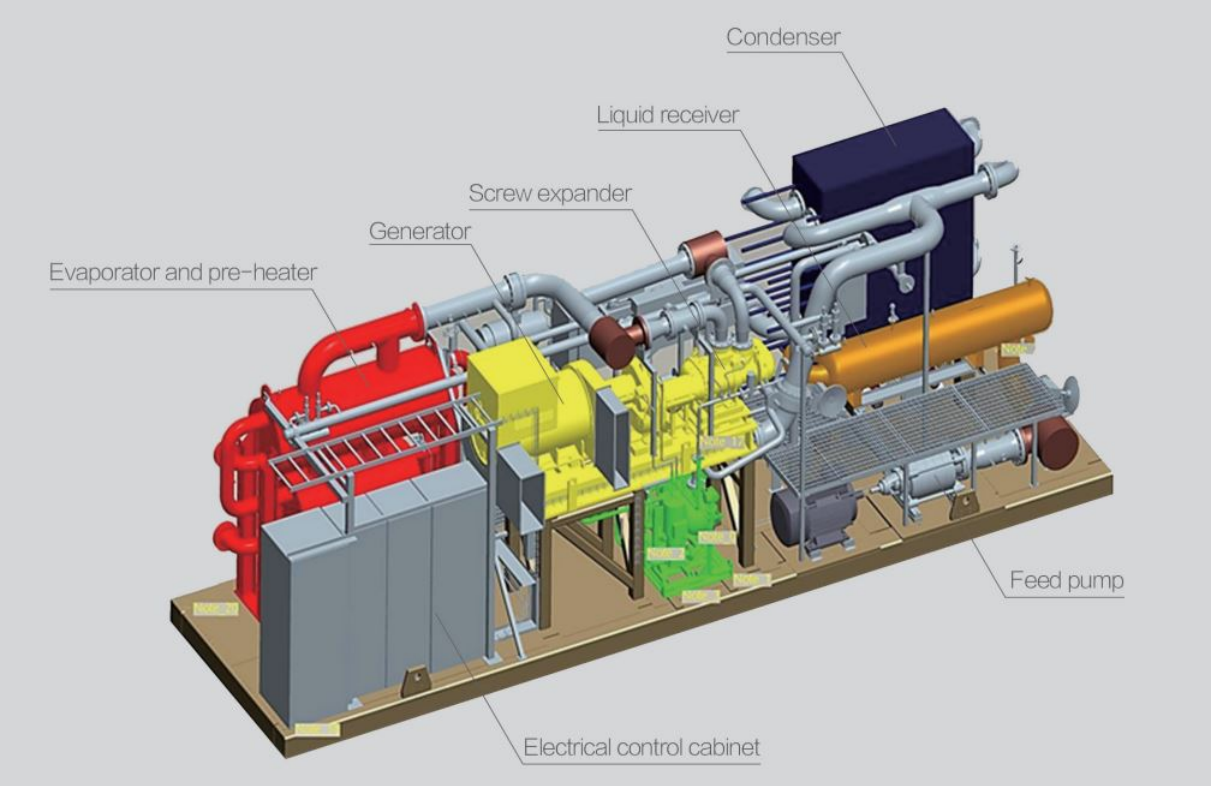

Figure 6.3: Opcon Powerbox ORC (Opcon, 2012).

Suprisingly, the Opcon Powerbox ORC is approximately three times larger than the Stirling engine for the same power output. The reason for this great difference is most likely due to the fact that the size of the Opcon ORC Powerbox is given for the entire system including necessary

piping, power turbine, heat exchangers, pump and generator, see Figure 6.3. The sizes for the Stirling engine do only include the actual engine, and do not account for piping, generator or electrical control unit. Even though, this simple study does indicate that the size issue that is often mentioned when the feasibility of a Stirling engine is discussed in research papers is not as prominent for marine WHR applications compared to an ORC solution.

6.1.2 Implementation Into Existing Machinery

Some suggestions are proposed considering how to implement the WHRS into the existing machinery:

- Both of the systems efficiencies are highly influenced by the temperature of the heat sink. If the heat sink temperature could be lowered, the efficiency would be substantially increased (This does not account for the ORC systems where the working fluids have condensing pressures at 1 bar at the condensing temperature. Lowering the condensing temperature additionally would cause a vacuum in the cold side HX, and this could lead to air leakage into the system). Since the case vessel is transporting LNG stored at cryogenic temperatures, the boil-off gas of the LNG could be used as a heat sink to increase the efficiency of both the Stirling engine and the ORC systems. This would also enable the possibility to use CO_2 as working fluid, which due to its very low critical temperature of 31°C could be applied to a trans-critical cycle and in that way be used to harvest waste heat from the CW. As discussed in Section 1.1.1, CO_2 trans-critical systems have shown very good potential as ORC working fluid in marine applications.
- Since the Stirling engines that are available at the commercial market today do not have higher power outputs than approximately 250 kW, a solution where 2-4 separate engines are installed instead of one big should be considered. This will enable the possibility to choose from several manufacturers and the quality assurance of the engines will be higher since they have been tested for a longer period. However, the complete system would become very complicated with this solution. When one of the main generator engines constantly emits about 1300-2000 kW available energy when operating, it would be necessary to connect 2-3 Stirling engines for each main generator engine in order to utilize the com-

plete potential for energy recovery (See Table 6.3 for calculation of complete potential for energy recovery per year).

- For the ORC system, it could be enough to install only one complete system since this technology is proven for power outputs in the range of 400-800 kW (Opcon, 2012). If the exhaust piping for both the MGEs could be connected, then the ORC system could benefit from the exhaust exergy from both engines at the same time.
- Today, there is already an economizer implemented in the machinery system of the case vessel. The economizer is used for fuel heating and general steam service purposes (BW Gas, 2009). An important question to ask is if the ORC or the SE would give a better potential for WHR than the economizer. Unfortunately, no data for the performance of the economizer has been provided for this work and it is therefore impossible to conclude which solution is the best. This should be evaluated in further studies of this subject.
- As discussed in Section 1.1.1, Shu et al. (2013) evaluated waste heat recovery solutions for two-stroke engines aboard ships. He concluded in his work that combined cycle systems where various technologies are used at the same time to harvest energy from different waste heat sources will be the main research orientation of WHR technology in the future. Although combined cycle systems are not widely used, these will receive more attention for their significant development potential to achieve higher thermal efficiency and to alleviate the atmosphere pollution problem according to Shu et al. (2013). The system proposed by Opcon is also a combined cycle system. The company uses a wet steam turbine to harvest heat from the exhaust, and an ORC to withdraw waste heat from the low-grade energy in the cooling water circuit (Opcon, 2012). Regarding this information, it should be a subject for further study to evaluate if a combined cycle system could give better performance than just one simple technology.

Finally, another important question to evaluate is to decide what the extra electricity produced from the WHR systems should be used for. There is no need for extra electricity if there is no where to use it. Even if the WHR system could produce all the necessary hotel load, auxiliary generator engines are inevitable because a reliable system to produce electricity that are not dependent on the main generator engines are completely necessary according to classification rules (White, 2008). If the main generator engines brake down, a redundancy system

is acquired by classification companies to avoid complete black-out on the ship (White, 2008). However, even though WHR systems operating on waste heat from the main generator engines can not replace the smaller auxiliary engines, the WHRS can significantly reduce the use of these engines, and in that way reduce fuel consumption.

The last years, the focus on hybrid ships has become increasingly popular as a future solution to save fuel (DNV GL, 2013). The additional electricity produced from WHR could be stored in batteries, and in that way be able to prevent loss of electricity if the WHR systems are producing electricity when it is not needed. According to DNV GL, when an offshore supply vessel is operating on dynamic positioning, there will be a significant fuel saving potential (DNV GL, 2013). In port, the vessel can simply use power stored in the batteries, which again will have a positive impact on the environment (DNV GL, 2013). Additional benefits are related to the reduction in the machinery maintenance cost and in noise and vibrations in due to the machinery system (DNV GL, 2013).

Another interesting use for the extra produced electricity, is to use it for re-liquefaction of boil-off gas. The more boil-off gas, the less LNG will be left for sale when the case vessel reach port. By using the waste heat to re-liquefy the boil-off, more LNG can be sold without increasing cost. This potential usage of the WHR electricity production should be further studied in order to evaluate whether the electricity produced from the WHRS would be sufficient in order to re-liquefy the boil-off gas.

6.2 Cost Analysis

A cost analysis based on the current price of fuel and the operational profile of the ship will be performed in this section. As mentioned in the introduction, the exergy has only been calculated for one of the MGEs with power output of 11.4 MW. It is assumed that the two largest MGEs operate in the same way, so the cost analysis will be based on the available heat from these two engines. It is further assumed that the hotel power is produced by the small generators. In Table 6.2, it can be seen that 20.4% of the operating time is when the case vessel is in port, signifying that the two 11.4 MW engines are running 79.6% of the time. The cost analysis will therefore be based on the operational profile for loaded and ballast mode.

The operating hours of the case vessel is based on a 4 month measurement period. Operational time for 1 year is calculated assuming the ship operates in the same mode the rest of the year. This gives a total of 7218 operating hours a year for ballast and loaded mode.

Operating mode	Time for 4 months operation [hours]	Time one year [hours]	Time [%]	Propulsion [kW]	Hotel [kW]
Loaded	1600	4800	52.9	11951	2871
Ballast	806	2418	26.7	10894	2802
Port	618	1854	20.4	0	2608
Total time	3024	9072	100		

Table 6.2: Operational profile for BW Gas Suez Paris (C. Chryssakis DNV GL, 2015).

As can be seen in Figure 2.2 in Chapter 2, approximately 50% of the operating hours of the loaded and ballast mode are between 75-85% load. The remaining hours are between 45-75% load. To simplify the cost analysis, it will be assumed that the two main generator engines are operating at 75% load for 50% of the year, and at 60% load the remaining 50% and that the total amount of operating hours are 7000 hours. This gives the operation of the waste heat recovery system using Stirling engine as presented in Table 6.3. The Organic Rankine system can be seen in Table 6.4. The smallest efficiency achieved for the Stirling engine WHRS systems is chosen to keep the analysis as realistic and conservative as possible. As discussed in Section 4.5, the ORC system with regeneration and R-245fa at a moderate operating pressure of 30 bar was chosen as the best solution to keep the system as cost and space efficient as possible in addition to avoid issues with flammability and toxicity. The efficiency at this operating point is 14.5%. From Table 6.3 and 6.4 the total potential for energy recovery for one year for the Stirling engine and the ORC system can be seen. For the Stirling engine, the total potential for energy recovery is 5019 MWh/year, and for the ORC system 3368 MWh/year.

Engine load	sgfc [kg/kWh]	Engine power [kW]	Exergy in exhaust [kW]	Number of engines	Total exergy in exhaust [kW]	Total operating hours [year]	SE system efficiency	Energy recovered [kW]	Energy recovered [MWh/year]
75%	0.1627	8550	1760	2	3520	3500	22 %	748	2618
60%	0.1726	6840	1560	2	3120	3500	22 %	686	2401

Table 6.3: Potential for waste heat recovery with Stirling engine.

Engine load	sgfc [kg/kWh]	Engine power [kW]	Exergy in exhaust [kW]	Number of engines	Total exergy in exhaust [kW]	Total operating hours [year]	ORC system efficiency	Energy recovered [kW]	Energy recovered [MWh/year]
75%	0.1627	8550	1760	2	3520	3500	14.5%	510	1785
60%	0.1726	6840	1560	2	3120	3500	14.5%	452	1583

Table 6.4: Potential for waste heat recovery with ORC system.

In Table 6.5 the savings in amount of fuel in Tons of LNG and Tons of Oil Equivalent (TOE) can be seen for both systems. The energy conversion factor of 1 tons of LNG = 1.242236 TOE has been used (Hofstrand, 2014).

Engine Parameters		Stirling Engine system			ORC system		
Load	sfgc [kg/kWh]	Energy Recovered [MWh/year]	Tons of LNG Fuel recovered [tons LNG/year]	Tons of Oil Equivalent per year [TOE/year]	Energy Recovered [MWh/year]	Tons of LNG Fuel Recovered [tons LNG/year]	Tons of Oil Equivalent Recovered per year [TOE/year]
75%	0.1627	2618	425.9	529.1	1785	290.4	360.6
60%	0.1726	2401	414.4	514.7	1583	273.2	339.4
Total		5019	840.3	1043.8	3368	563.3	700

Table 6.5: Amount of tons of fuel saved each year for both SE and ORC systems.

Since the engines are operating with natural gas as fuel, the current price of LNG has to be used. Today, there are approximately three different LNG prices in the world, see Figure 6.4. The price in the North America is very low due to the recent discovery of shale gas (Brown, 2013). In Asia the price is high due to increased demand of alternative energy sources after Japan's close-down of reactors after the Fukushima accident in 2011 (Brown, 2013).

With a LHV value of 44.2 MJ/kg calculated from the fixed fuel composition in Table 3.1 in Chapter 3, the price of LNG in $/MMBTU (mmBTU= Million British Thermal Unit) can be changed to $/tonnes LNG by the conversion factor 1 MMBTU = 1.055 GJ. The prices that will be used for this cost analysis can be seen in Table 6.6.

Figure 6.4: Current price of LNG in the world [$/MmBTU] vs year (BP Energy, 2014)

Area	Price [$/MmBTU]	Price [$/tons LNG]	Price [$/TOE]
North America	4	167.6	134.9
Europe	12	461	371.1
Asia	18	713.4	573.5

Table 6.6: Fuel prices used in cost analysis (C. Chryssakis DNV GL, 2015) (BP Energy, 2014).

In Figure 6.5, 6.6 and 6.7 specific prices of Stirling engines and ORC systems can be seen. The graphs are taken from research studies that have collected information from a set of ORC and SE manufacturers and from scientific publications (Quoilin et al., 2011) (Majeski, 2002). For SE, it is decided to use a price of 3000 $/kW. With a potential total power output of the SE of 850 kW for high MGE1 loads, the total price of the SE system then becomes 2,550,000 $. Majeski (2002) comment in his work that Whisper Tech is the only manufacturer of the companies presented in Figure 6.5 that has begun to produce commercialized Stirling engines, and might therefore present the most realistic price. In Figure 6.6 the Beta demonstration price (in 2002) for SE can be seen.

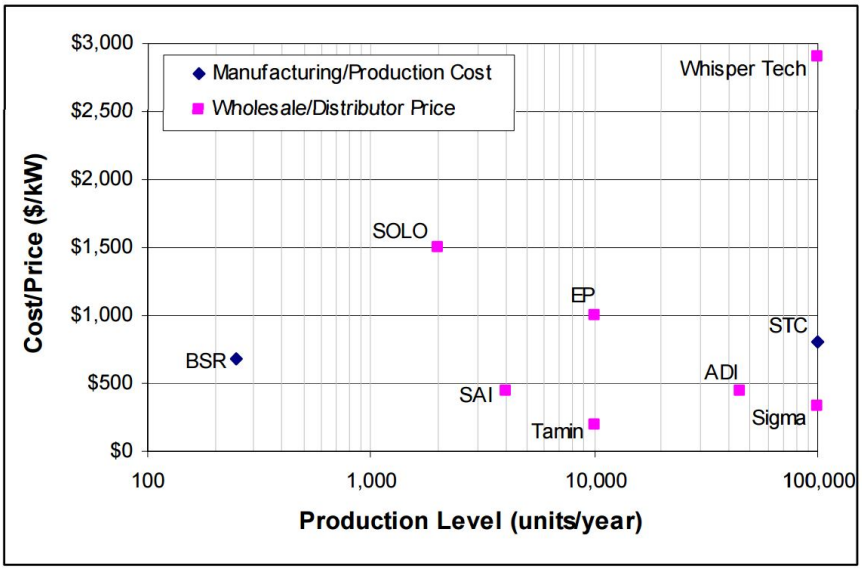

Figure 6.5: Specific cost of SE systems (Majeski, 2002).

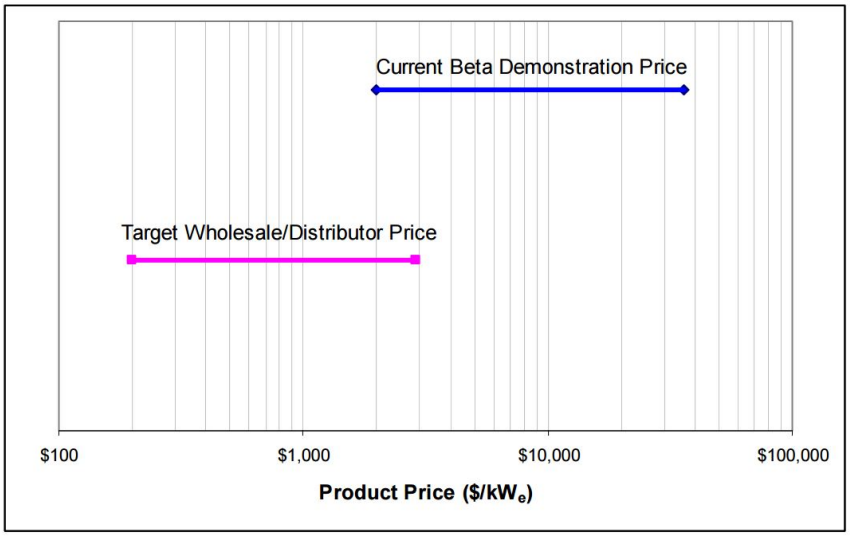

Figure 6.6: Specific cost of SE systems (Majeski, 2002).

The demonstration price is much higher than the target wholesale price. Nevertheless, it is decided to use the target price in this work considering the study is 13 years old, and that the price of today might have decreased due to development. For the ORC system, a price of 1700 $/kW (equivalent to 1600 euro/kW, 15. March 2015) is chosen (see Figure 6.7). This is based on a maximum power output of the ORC system of approximately 600 kW and that it is supposed

for WHR applications. The total price of the ORC system then becomes 1,020,000 $. By applying these prices in addition to the information presented in Table 6.3, 6.4 and 6.5, the potential savings of each system and the number of years until return on investment can be seen in Table 6.7. It has to be emphasized that these specific prices are only assumptions. However, the fact that the specific price of the less commercialized Stirling engine will be higher than the ORC is very likely (Ioannis Vlaskos, 2010) (Thombare and Verma, 2008).

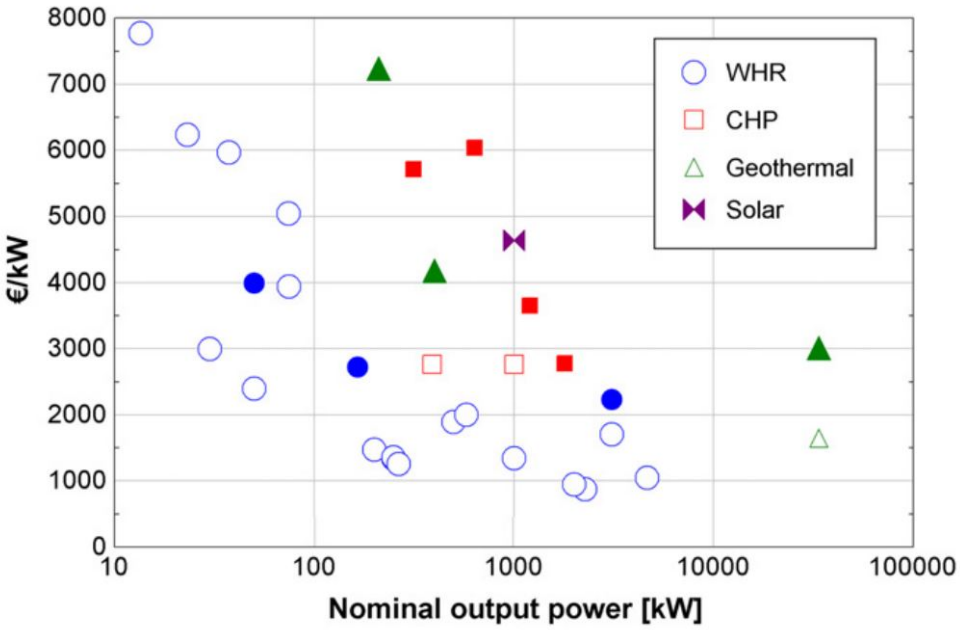

Figure 6.7: Cost of ORC systems depending on target application and net electrical power (Quoilin et al., 2013).

Area	Price [$/MmBTU]	Price [$/TOE]	Potential savings SE [$/year]	Return on Investment SE [years]	Potential savings ORC [$/year]	Return on Investment ORC [years]
North America	4	134.9	141,000	18.1	95,000	10.7
Europe	12	371.1	387,000	6.6	260,000	3.9
Asia	18	573.5	596,000	4.3	405,000	2.5

Table 6.7: Potential savings for SE and ORC WHR systems.

It is evident from Table 6.2 that the ORC has the shortest return on investment period due to the high price of the SE machine. The major reasons for the high price of Stirling machines are

as follows (Majeski, 2002) (Kongtragool and Wongwises, 2005) (Obernberger et al., 2003):

- As of today, Stirling engines are built individually in small numbers for very specific applications or prototypes for research, causing the price to go up.
- The engine requires expensive seals due to the high leakage rate of working fluid.
- High operating pressures and temperatures require complex and expensive materials that can handle high levels of stress, strain and temperature differences.
- The SE consists of less developed and commercialized components than the ORC.

The Stirling engine clearly shows the best theoretical performance and the potential for waste heat recovery, however, bearing in mind that the technology is very little developed, more research is necessary in order to develop the Stirling engine as a viable economical solution to decrease the years until return on investment. Considering the high cost reported by a number of researchers, it is not very likely that any private company will invest in a development of a Stirling engine for marine applications without governmental support (such as the NASA/MTI Stirling project discussed in Chapter 1). The first obstacle is to develop a Stirling engine product that may be produced in batches at a competitive cost while maintaining a performance that is superior to the functionary WHR technologies. As discussed in the first part of this chapter, today's Stirling developers may be able to meet the challenge with improvement in several areas of engine design. If these qualities can be proven through a significant amount of additional field test experience, then Stirling engines may make a significant impact in the WHR market as an economically competitive and environmentally green alternative. However, for the near future perspective, an ORC system seem as a more feasible and economically friendly choice for marine WHRS in the near future for cargo vessels operating on global trading routes considering their number of years until return on investment and proven technology.

The case vessel of this study does not pay anything for the fuel considering it uses boil-off gas from the LNG storage tanks, and are therefore running at relatively high loads during shipping voyages. This causes the available energy for WHR to be higher than most other cargo ships today. This is because it is a common practice now a days to operate ships with so called "slow steaming". This signifies steering the ship at low speeds in order to decrease the fuel consumption. In terms of WHR this is not beneficial. Lower load signifies less exergy in the waste heat.

If it would be possible to increase the speed, but at the same time hold the fuel consumption at the same level with the help of good WHR systems, these ships could probably decrease the time of one voyage without increasing fuel costs.

Chapter 7

Summary and Recommendations for Further Work

7.1 Summary and Conclusions

In this report, the potential for energy recovery from the waste heat in both the exhaust stream and the jacket water of the case vessel's engine has been evaluated. An exergy analysis has been performed on both the exhaust and the high temperature cooling water circuit of the Main Generator Engine No. 1 to quantify the available energy. A comparative study of the potential performance of a Stirling engine and three different Organic Rankine cycles for recovering the waste heat from the MGE1 has been carried out. Lastly, a discussion on technical feasibility including evaluation of technical design obstacles, space requirement, implementation into existing machinery and cost has been elaborated.

Exergy Analysis

The exergy analysis was done on the case vessel's 11.4 MW main generator engine. Only the thermomechanical contribution to the exergy was evaluated. This was because it was only necessary to account for the net exergy carried into the WHR system by the combustion products because a minimum exit temperature from the WHR system was set to 120°C. This was to avoid condensation of exhaust substances that could lead to corrosion on system's components and piping. By taking these precautions, the chemical exergy contribution was canceled. The molar

composition of the exhaust was calculated with an reaction balance between the molar analysis of the fuel composition and the amount of combustion air.

The exergy in the exhaust stream was 1300 kW at 40% load and increased to 2000 kW for 100% load. This corresponds to 28% of the engine's power output at 40% load and 18% of the MGE1 power output at 100% load. For the cooling water, the exergy was approximately 700-850 kW for a mass flow of 60-75 kg/s, or about 6-7.5% of the engine's power output at 100% load. No real measurement data was available for the cooling water circuit, so it was not possible to calculate the exergy based on load.

Performance Analysis of Organic Rankine Cycle

Three different Organic Rankine systems were studied; a conventional subcritical cycle, a subcritical cycle with regeneration and superheat, and a trans-critical cycle. A pre-screening of 50 different working fluids was done based on desirable environmental, safety and operational characteristics. The working fluids that were included in the pre-screening were chosen from available literature and research reports. All CFCs and HCFCs were excluded due to their bad influence on the environment. Additionally, working fluids that did not meet the criteria for GWP<3500, ODP=0, critical temperature above 330 K and pressure and safety requirements had to be removed. Also, fluids that were not included in the EES library had to be excluded. A selection of 12 fluids were chosen to be implemented in the thermodynamic analyses.

The wet working fluids could not be implemented to the conventional subcritical cycle due to issues with two-phase state after expansion. The best performance was calculated for a subcritical cycle with regeneration and benzene as the working fluid and the exhaust as heat source. This resulted in an efficiency of approximately 21%. Considering hydrocarbons high flammability and also the fact that benzene is carcinogen, the safest alternative and most feasible solution was shown to be a subcritical ORC with regeneration and R-245fa as the working fluid. This gave an efficiency of 15%. In order to limit the stress on components due to high pressures, a R-245fa cycle with maximum pressure of 30 bar was chosen, the efficiency of this system solution was 14.5%. This corresponded to a recovery of about 2.5% of the engine's power output at 100% load and 4.1% of the engine's output at 40% load.

Both subcritical ORC systems with cooling water as heat source showed poor efficiencies,

around 4-5% for every applicable fluid. It was only possible to run the EES model for the wet fluids; R-1234yf, R-1234ze, R-134a, R-161 and R-245fa because the other potential working fluids had either too low critical temperature or too high condensing temperature.

It was further proven that all the wet fluids increased their efficiency when implemented into trans-critical ORC with exhaust as the heat source compared to the efficiencies achieved for the ORC with regeneration and superheat. The R-245fa reached an efficiency of about 16%, however, this was at pressure levels between 120-150 bar. It was therefore decided to implement the subcritical ORC cycle with R-245fa to the cost analysis in order to not increase the complexity and cost of the system due to complications that come as a result of high pressure operations. None of the working fluids tested in this work were applicable to be used in trans-critical cycles with cooling water as the heat source because the low grade CW did not manage to heat the working fluid to a sufficient level in order to avoid the two-phase region after the expansion process.

Performance Analysis of Stirling Engine

From the performance analysis of Stirling engine, it was evident that the thermodynamic stirling cycle analyses accessible today are highly idealized. It was therefore necessary to multiply the results with an experience factor. Both an ideal thermodynamic Stirling cycle analysis and a Schmidt cycle analysis of an alpha Stirling engine were carried out. Based on information from literature and research reports, an experience factor of 0.3 was used for the Schmidt cycle analysis, and three different experience factors, 0.25, 0.3 and 0.4, were implemented in the ideal thermodynamic analysis.

With exhaust as the heat source, the efficiency was calculated to be 22-35% with experience factors of 0.25-0.4 respectively. This corresponds to 3.9-6.1% of the main generator engine's power output at 100% load. At 40% load this would correspond to 6.3-10% of the engine's power output. For the CW as heat source, the Stirling engine power output corresponds to about 0.75% of the MGE1 power for an efficiency of 11%, and about 1.2% of the MGE1 power for an efficiency of 17% at approximately 100% load. The efficiencies calculated for the Stirling engine were significantly higher than all the ORC solutions for both waste heat sources.

Based on a review of previous research and studies on Stirling engine working fluids, nitro-

gen seemed to be the best working fluids due to its high availability, low cost and limited leakage and diffusion rate out of the engine.

Feasibility Discussion

In the feasibility discussion, the major technical obstacles for each technology were discussed. The Stirling engine clearly has several more challenges to overcome compared to the ORC before it can be implemented into a marine machinery system as a waste heat recovery system. However, based on available research reports is seems in all probability that these challenges can be resolved with sufficient time for research, development and prototype testing. The main challenge for the ORC system was to encounter a working fluid that showed good thermodynamic properties at the same time as being environmental friendly, safe and globally available.

It was further shown in the feasibility discussion that the size of the Stirling engine might not be such a high concern as is typically stated in accessible literature and research reports. The volume of the Stirling engine was approximately three times smaller than the volume of the ORC for the same power output. However, the ORC size was based on a complete system including all accompanying components such as electrical control units, piping, etc, while the sizing of the Stirling engine was given for the actual engine only. It was therefore not possible to conclude with certainty if the actual size of the Stirling engine would be smaller than the size of the ORC in a real system application.

In the cost analysis, the ORC showed the shortest time until return on investment. Three current prices for Liquefied Natural Gas were used; the price in the USA, the price in Europe (UK) and the Asian (Japan) price. Based on European prices for Liquefied Natural Gas, which was the middle price between the three prices, the Organic Rankine system had 3.9 years until Return on Investment, and the Stirling Engine had 6.6 years. The reason why Stirling engines have a higher investment price, is primarily due to the fact that Stirling engines are not completely commercialized yet, so the unit price is very high.

Based on the literature survey, the exergy analysis, the thermodynamic performance study and the feasibility discussion, the ORC system shows to be the best solution for waste heat recovery system for marine applications in the near future. However, with sufficient investment

in research and development of Stirling engines utilizing working fluids possessing good availability and safety, the Stirling engine might be a better solution considering its superior thermodynamic performance compared to Organic Rankine systems.

7.2 Recommendations for Further Work

The recommendations may be classified as:

- **Short-term**
  - Further studies on working fluids for Organic Rankine systems and Stirling engines in order to find additional alternatives for working fluids with good thermophysical properties that are environmental friendly and show good safety and availability.
  - Improve the thermodynamic analyses of the Organic Rankine systems and the Stirling engine in this work with the objective to make them more realistic. Collect performance data from manufacturers of necessary equipment for both systems, such as heat exchangers, pumps, etc, and include these data in the analyses. Considering the thermodynamic model of the Stirling engine, further research on available analyses including the effects of thermophysical properties of potential working fluids would highly improve the quality of the analysis. Each component in both technologies should be designed and simulated in a simulation IT-tool.
  - Install additional measurement equipment in the case vessel in order to improve the exergy analysis in this work. Especially measurement devices that would give information about the high temperature cooling water circuit, such as mass flow, exact water temperature after engine based on load, pressure of cooling water and so fort. Also, flow meters to measure mass flow of exhaust based on load and chromatograph to evaluate the composition of the combustion products would highly improve the exergy analysis.
  - Calculate performance of the installed economizer in the case vessel with the objective to do a proper comparison between the WHR systems analyzed in this work and the already installed economizer. This would enable the possibility to evaluate which system has the best potential for waste heat recovery. It would be necessary to install additional measurement devices in the case vessel in order to calculate the performance of the economizer.

- **Medium-term**
  - Compare the two technologies in this work to other more conventional waste heat recovery systems that are already common technologies for ships, such as exhaust gas turbines (also called power turbines) and steam turbines, in order to evaluate the thermodynamic potential for WHR for several available systems. Data could be collected from accessible research papers on the subject, or by performing thermodynamic analyses on various power- and steam turbines.
  - Propose combined cycle WHR systems comprising different heat cycles. For example various combinations consisting of Stirling cycle, Organic Rankine cycle, Kalina cycle or Steam power cycle in order to evaluate performance and cost of several systems. This would be helpful in the interest of deciding and quantifying whether a combined cycle systems shows better potential for waste heat recovery than a one-cycle system.
  - Perform a thermodynamic analysis on how the use of LNG boil-off gas as a heat sink would affect the thermal efficiency of the Organic Rankine System and the Stirling engine. Measurement devices to measure temperature and the amount of boil-off gas would be necessary to quantify how much heat could be carried away with the boil-off gas heat sink.
  - Propose a combined cycle WHR system where the electrical power produced by a Stirling engine or Organic Rankine cycle could be used to re-liquefy the boil-off gas from the LNG storage tanks at liquefied gas carriers. A quantification of how much power is necessary in order to re-liquefy the gas, and how much economical savings it is possible to gain by implementing such a system should be determined.
- **Long-term**
  - Develop a prototype for both an Organic Rankine system and a Stirling engine in order to compare these technologies in a realistic waste heat recovery scenario for application in marine machinery systems. This would in all likelihood require an extensive amount of founding and human resources in order to carry out the project

in a good and thorough manner. Especially for the Stirling engine it is important to prove that the system is capable to harvest waste heat from marine engines since the author of this report has not found any examples of Stirling engine prototypes built for this specific type of application.

Bibliography

Aksoy, F. (2013). Thermodynamic analysis of a beta-type stirling engine with rhombic drive mechanism. *Energy Conversion and Management*, 75(0):319 – 324.

Al-Najem, N. and Diab, J. (1992). Energy-exergy analysis of a diesel engine. *Heat Recovery Systems and CHP*, 12(6):525–529.

American Cancer Society (2015). Known and probable human carcinogens. <http://www.cancer.org/cancer/cancercauses/othercarcinogens/generalinformationaboutcarcinogens/known-and-probable-human-carcinogens> Retrived 10.03.2015.

ASHRAE (2010). *Designation and Safety Classification of Refrigerants*. Number ISSN 1041-2336. Approved American National Standard (ANSI).

ASHRAE (2013). *2013 ASHRAE Handbook - Fundamentals (I-P Edition)*. American Society of Heating, Refrigerating and Air-Conditioning Engineers, Inc.

Asnaghi, A., Ladjevardi, S., Saleh Izadkhast, P., and Kashani, A. (2012). Thermodynamics performance analysis of solar stirling engines. *International Scholarly Research Notices*, 2012.

Badr, O., Probert, S., and O'callaghan, P. (1985). Selecting a working fluid for a rankine-cycle engine. *Applied Energy*, 21(1):1–42.

Bejan, A. and Moran, M. J. (1996). *Thermal design and optimization*. John Wiley & Sons.

Bianchi, M. and Pascale, A. D. (2011). Bottoming cycles for electric energy generation: Parametric investigation of available and innovative solutions for the exploitation of low and medium temperature heat sources. *Applied Energy*, 88(5):1500 – 1509.

BITZER (2012). Refrigerant Report 17 BITZER Kühlmaschinenbau GmbH. <http://www.izw-online.de/news/Kaeltemittel_Report_Bitzer_a-501-17.pdf> Retrived 19.01.2015, Informationszentrum Wärmepumpen und Kältetechnik.

Bolland, O. (2013). *TEP4185 Natural Gas Technology*. NTNU.

BP Energy (2014). Bp statistical review of world energy june 2014. <bp.com/statisticalreview> Retrived 13.02.2015, BP Energy.

Brasz, L. J. and Bilbow, W. M., editors (2004). *Ranking of Working Fluids for Organic Rankine Cycle Applications*, volume Paper 722. International Refrigeration and Air Conditioning Conference.

Brown, S. P. (2013). The Shale Gas and Tight Oil Boom, U.S. States Economic Gains and Vulnerabilities. *Council on Foreign Relations Press*.

BW Gas (2009). *Machinery Operating Manual, BW Gas Suez Paris*. BW Gas.

C. Chryssakis DNV GL (2015). Information retrived through telephone conversations and mail correspondance with Phd Christos Chryssakis, Senior Researcher, Maritime Transport Group Leader Greener Shipping at DNV GL Research and Innovation Department.

Chammas, R. E. and Clodic, D. (2005). Combined cycle for hybrid vehicles. In *SAE Technical Paper*. SAE International.

Chen, H., Goswami, D. Y., and Stefanakos, E. K. (2010). A review of thermodynamic cycles and working fluids for the conversion of low-grade heat. *Renewable and Sustainable Energy Reviews*, 14(9):3059 – 3067.

Chen, Y., Lundqvist, P., Johansson, A., and Platell, P. (2006). A comparative study of the carbon dioxide transcritical power cycle compared with an organic rankine cycle with r123 as working fluid in waste heat recovery. *Applied Thermal Engineering*, 26(17-18):2142–2147.

Comission, E. (2014). Refrigerants used in mobile air condition systems (MAC) - State of play. <http://europa.eu/rapid/press-release_MEMO-14-50_en.htm> Retrived 7.01.2015.

Connor, D. E. (2015). Availability of helium. <http://www.peakscientific.com/page/488-availability-of-helium/#.VQwgJI6G-Z8> Retrived 2.02.2015.

Cool Energy (2015). ThermoHeart Engine - Waste Heat Recovery. <http://coolenergy.com/how-it-works/> Retrived 8.01.2015.

DiBella, F. A., DiNanno, L. R., and Koplow, M. D. (1983). Laboratory and on-highway testing of diesel organic rankine compound long-haul vehicle engine. In *SAE Technical Paper*. SAE International.

Dimopoulos, G. and Kakalis, N. (2014). Next generation energy management. Technical Report 05, DNV GL STRATEGIC RESEARCH & INNOVATION.

DNV (2014). Rules for classification of ships, newbuildings, special equipment and systems, additional class, environmental class.

DNV GL (2013). Norway is teaming up in pole position for battery-powered ships. *DNV GL Research Blog*, <http://www.dnv.com/press_area/press_releases/2013/norway_is_teaming_up_in_pole_position_for_battery_powered_ships.asp> Retrieved 2015.04.09.

Draw.io (2015). Diagram editor. *JGraph Ltd.*, <https://www.draw.io/>.

Ernst, W. D. and Shaltens, R. K. (1997). Automotive stirling engine development project. *NASA*.

Etele, J. and Rosen, M. A. (1999). The effect of reference-environment models on the accuracy of exergy analyses of aerospace engines. In *SAE Technical Paper*. SAE International.

Finkelstein, T. and Organ, A. (2001). *Air Engines*. Professional Engineering Publishing Ltd.

Fu, J., Liu, J., Feng, R., Yang, Y., Wang, L., and Wang, Y. (2013). Energy and exergy analysis on gasoline engine based on mapping characteristics experiment. *Applied Energy*, 102(0):622 – 630. Special Issue on Advances in sustainable biofuel production and use - {XIX} International Symposium on Alcohol Fuels - {ISAF}.

Graham Thomas Reader, C. H. (1983). *Stirling engines*. E. and F. Spon, New York, NY, USA.

Guillen, D., Klockow, H., Lehar, M., Freund, S., and Jackson, J. (2011). Development of a direct evaporator for the organic rankine cycle. *Energy Technology 2011: Carbon Dioxide and Other Greenhouse Gas Reduction Metallurgy and Waste Heat Recovery*, pages 25–35.

Guo, C., Du, X., Yang, L., and Yang, Y. (2014). Performance analysis of organic rankine cycle based on location of heat transfer pinch point in evaporator. *Applied Thermal Engineering*, 62(1):176–186.

Heywood, J. B. (1988). *Internal combustion engine fundamentals*, volume 930. Mcgraw-hill New York.

Hirata, K., Iwamoto, S., Toda, F., and Hamaguchi, K. (1997). Performance evaluation for a 100 w stirling engine. In *Proceedings of Eighth International Stirling Engine Conference*, pages 19–28.

Hofstrand, D. (2014). Natural Gas and Coal Measurements and Conversions. *Iowa State University*.

Ioannis Vlaskos, Peter Feulner, A. A. I. K. (2010). Exhaust gas heat recovery on large engines, potential, opportunities, limitations. In *CIMAC World Congress on Combustion Engine, 26th, Bergen, NO, 2010-06-14*.

IPCC (2013). Climate change 2013: The physical science basis. contribution of working group i to the fifth assessment report of the intergovernmental panel on climate change. Technical report, Stocker, T.F., D. Qin, G.-K. Plattner, M. Tignor, S.K. Allen, J. Boschung, A. Nauels, Y. Xia, V. Bex and P.M. Midgley (eds.).

Kalyan Annamalai, I. K. P. (2001). *Advanced thermodynamics engineering*. CRC Press.

Katsanos, C., Hountalas, D., and Pariotis, E. (2012). Thermodynamic analysis of a rankine cycle applied on a diesel truck engine using steam and organic medium. *Energy Conversion and Management*, 60(0):68 – 76. Special issue of Energy Conversion and Management dedicated to {ECOS} 2011 - the 24th International Conference on Efficiency, Costs, Optimization, Simulation and Environmental Impact of Energy Systems.

Kidnay, A. J., Parrish, W. R., and McCartney, D. G. (2011). *Fundamentals of Natural Gas Processing*, volume 218. CRC Press.

Klein, S. and Alvarado, F. (2002). Engineering equation solver. *F-Chart Software, Madison, WI*.

Klein, S. and Nellis, G. (2012). *Thermodynamics*. Cambridge University Press.

Kongtragool, B. and Wongwises, S. (2005). Investigation on power output of the gamma-configuration low temperature differential stirling engines. *Renewable Energy*, 30(3):465 – 476.

Ladam, Y. and Skaugen, G. (2007). Co2 as working fluid in a rankine cycle for electricity production from waste heat sources on fishing boats. Technical report, SINTEF.

Lemmon, E., Huber, M., and McLinden, M. (2007). Reference fluid thermodynamic and transport properties, refprop, nist standard reference database 23, version 8.0. *National Institute of Standards and Technology, Gaithersburg, MD*.

Linde Industrial Gases (2015). Nitrogen. <http://www.linde-gas.com/en/products_and_supply/gases_atmospheric/nitrogen.html> Retrived 20.02.2015.

Machinery Spaces (2010). Modern refrigerants for cargo ships. <http://www.machineryspaces.com/refrigerants.html> Retrived 19.01.2015.

Maizza, V. and Maizza, A. (2001). Unconventional working fluids in organic rankine-cycles for waste energy recovery systems. *Applied thermal engineering*, 21(3):381–390.

Majeski, J. (2002). Stirling engine assessment. Technical Report 1007317, EPRI, Palo Alto, CA.

Martini, W. R. (1983). *Stirling engine design manual*. National Aeronautics and Space Organization, NASA, second edition.

MATLAB (2014). MATLAB and Statistics Toolbox Release 2014a. *The MathWorks, Inc., Natick, Massachusetts, United States*.

Millikin, M. (2012). First reference installation of Opcon Waste Heat Recovery technology for ships; potential for 5 to10% fuel savings. <http://www.greencarcongress.com/2012/08/opcon-20120826.html> Retrived 12.01.2015.

Moran, M. J., Shapiro, H. N., Boettner, D. D., and Bailey, M. B. (2010). *Fundamentals of engineering thermodynamics*. John Wiley & Sons.

NFPA (2015). NFPA 704: Standard system for the identification of the hazards of materials for emergency. *National Fire Protection Association*, <http://www.nfpa.org/codes-and-standards/document-information-pages?mode=code&code=704> Retrived 14.02.2015.

Nouman, J. (2012). Comparative studies and analyses of working fluids for organic rankine cycles - orc. Master's thesis, KTH School of Industrial Engineering and Management.

Obernberger, I., Carlsen, H., and Biedermann, F. (2003). State of the art and future developments regarding small scale biomass chp systems with a special focus on orc and stirling engine technologies. *International Nordic Bioenergy. Jyvaskyla*.

Olsen, E. A. (2006). Energibaereren hydrogen. <http://www.forskningsradet.no/prognett-hydrogen/21_Energibreren_hydrogen/1234130628284> Retrived 26.02.2015.

Opcon (2012). Opcon powerbox orc brochure. <http://www.opcon.se/web/Opcon_Powerbox_2.aspx> Retrived 12.01.2015.

Opcon Marine (2015). Commissioning and testing of first reference installation of Opcon technology for ships. <http://www.opcon.se/web/First_installation_1_1.aspx> Retrived 1.02.2015.

Pedersen, M. F. (2015). Sulfur content of fuel. <https://www.dieselnet.com/standards/inter/imo.php#s> Retrived 12.10.2014.

Poullikkas, A. (2005). An overview of current and future sustainable gas turbine technologies. *Renewable and Sustainable Energy Reviews*, 9(5):409 – 443.

Quoilin, S., Broek, M. V. D., Declaye, S., Dewallef, P., and Lemort, V. (2013). Techno-economic survey of organic rankine cycle (orc) systems. *Renewable and Sustainable Energy Reviews*, 22(0):168 – 186.

Quoilin, S., Declaye, S., Tchanche, B. F., and Lemort, V. (2011). Thermo-economic optimization of waste heat recovery organic rankine cycles. *Applied Thermal Engineering*, 31:2885–2893.

Rakesh K. Bumataria, N. K. P. (2013). Stirling engine performance prediction using schmidt analysis by considering different losses. *International Journal of Research in Engineering and Technology (IJRET)*, 02(08).

Rettig, A., Lagler, M., Lamare, T., Li, S., Mahadea, V., McCallion, S., and Chernushevich, J. (2011). Application of organic rankine cycles (orc). In *Proceedings of the World Engineers Convention, Geneva, Switzerland*, pages 4–8.

Roy, J., Mishra, M., and Misra, A. (2011). Performance analysis of an organic rankine cycle with superheating under different heat source temperature conditions. *Applied Energy*, 88(9):2995 – 3004.

Sayin, C., Hosoz, M., Canakci, M., and Kilicaslan, I. (2007). Energy and exergy analyses of a gasoline engine. *International Journal of Energy Research*, 31(3):259–273.

Senft, J. R. (2002). Optimum stirling engine geometry. *International Journal of Energy Research*, 26(12):1087–1101.

Shu, G., Liang, Y., Wei, H., Tian, H., Zhao, J., and Liu, L. (2013). A review of waste heat recovery on two-stroke {IC} engine aboard ships. *Renewable and Sustainable Energy Reviews*, 19(0):385 – 401.

SINTEF (2015). <http://www.sintef.no/home/about-us/> Retrived 9.01.2015.

Sprouse, C. and Depcik, C. (2013). Review of organic rankine cycles for internal combustion engine exhaust waste heat recovery. *Applied Thermal Engineering*, 51(1-2):711–722.

SunPower (2015). Stirling cycle. <http://sunpowerinc.com/engineering-services/technology/stirling-cycle/> Retrived 13.03.2015.

Tchanche, B. F., Lambrinos, G., Frangoudakis, A., and Papadakis, G. (2011). Low-grade heat conversion into power using organic rankine cycles–a review of various applications. *Renewable and Sustainable Energy Reviews*, 15(8):3963–3979.

The Linde Group (2015). Refrigerants. <http://www.linde-gas.com/en/products_and_supply/refrigerants/index.html> Retrived 21.02.2015.

Thombare, D. and Verma, S. (2008). Technological development in the stirling cycle engines. *Renewable and Sustainable Energy Reviews*, 12(1):1 – 38.

UNEP (2012). *Handbook for the The Montreal Protocol on Substances that Deplete the Ozone Layer*. Number ISBN 978-9966-20-009-9. Secretariat for The Vienna Convention for the Protection of the Ozone Layer & The Montreal Protocol on Substances that Deplete the Ozone Layer, United Nations Environment Programme PO Box 30552-00100 Nairobi Kenya, ninth edition.

Walker, G. (1980). *Stirling engines*. Oxford University Press, New York, NY.

Wärtsilä (2013). Product guide wärtsilä 50df. <http://www.wartsila.com/docs/default-source/product-files/engines-generating-sets/dual-fuel-engines/wartsila-o-e-w-50df-pg.pdf?sfvrsn=3> Retrived 21.10.2014.

Wärtsilä (2014). Wärtsilä 50df engine technology. <http://www.wartsila.com/en/engines/df-engines/wartsila50df> Retrived 21.10.2014.

West, C. D. (1986). *Principles and applications of Stirling engines*. Van Nostrand Reinhold Company.

White, M. F. (2008). *Marine Engineering Systems*. Institute of Marine Technology, NTNU.

Woodyard, D. (2009). *Pounder's marine diesel engines and gas turbines*. Butterworth-Heinemann.

Wu, D. and Wang, R. (2006). Combined cooling, heating and power: A review. *Progress in Energy and Combustion Science*, 32(5-6):459–495.

Appendix A

EES Model of Exergy Analysis

```
"EXERGY ANALYSIS FOR EXHAUST STREAM - EES"

"Assumed variables that are investigated"
T_exh=400+273.15          "Temperature of exhaust stream from turbocharger"
lambda=2.2                      "Air/fuel ratio of actual amount of air"
m_dot_fuel = 0.35 [kg/s]       "Mass flow of fuel"
"Molar analysis of gas fuel"
y_N2=0.1285,
y_CH4=0.8658,
y_C2H6=0.005053,
y_C3H8=0.0006632,

y_tot=y_N2+y_CH4+y_C2H6+y_C3H8,    "Total amount of fuel has to be one kmol"

"Fixed variabels"
R=8.314    "Universal gas constant"
P_exh=1.01325 [bar]     "Pressure exhaust"
T_0=25+273.15          "Temperature of reference environment"
T_out=120+273.15 "Temperature of exhaust stream at outlet"
P_0=1.01325 [bar]   "Pressure of reference environment"

"Chemical reference environment"
y|e_N2=0.7567
y|e_O2=0.2035
y|e_H2O=0.0303
y|e_CO2=0.0003

"CALCULATIONS:"

"x=percent load"
"Regression line for T_exh"
T_exh=-0.8039*x+478.14+273.15+5
"Function for mass flow of fuel based on load"
m_dot_fuel=0.004*x + 0.0845

"Temperature of exhaust in Celcius"
T_exh_C=T_exh-273

"Molecular weight of fuel and air"
MW_N2=MolarMass(N2)*y_N2,
MW_CH4=MolarMass(CH4)*y_CH4,
MW_C2H6=MolarMass(C2H6)*y_C2H6,
MW_C3H8=MolarMass(C3H8)*y_C3H8,

MW_fuel=MW_N2+MW_CH4+MW_C2H6+MW_C3H8,

MW_air=MolarMass(air)

"Calculating mass balance for complete combustion with theoretical amount of air"
b=y_CH4+(2*y_C2H6)+(3*y_C3H8)
c=((4*y_CH4)+(6*y_C2H6)+(8*y_C3H8))/2
a=(2*b+c)/2
d=(a*3.76)

"Calculating air/fuel ratio, on a molar and mass basis"
AF_molar_theoretical=(a+(a*3.76))/y_tot
```

AF_mass_theoretical=AF_molar_theoretical*(MW_air/MW_fuel)

"Chemical mass balance with increased air ratio, oxygen and nitrogen values will increase, the rest will stay the same"
e=((lambda*a*2)-(2*b)-c)/2
d_2=((lambda*a*3.76*2)+(2*y_N2))/2

"Molar analysis of combustion products"
y_CO2_p=b/(b+c+d_2+e)
y_H2O_p=c/(b+c+d_2+e)
y_N2_p=d_2/(b+c+d_2+e)
y_O2_p=e/(b+c+d_2+e)

y_tot_products=y_CO2_p+y_H2O_p+y_N2_p+y_O2_p

"Chemical contribution to exergy"
e_bar_ch=R*T_0*((b*LN(y_CO2_p/y|e_CO2))+(c*LN(y_H2O_p/y|e_H2O))+(d_2*LN(y_N2_p/y|e_N2))+(e*LN(y_O2_p/y|e_O2)))

"Thermochemical contribution to exergy"

h_bar_CO2=Enthalpy(CO2,T=T_exh) "Enthalpy of CO2 at exhaust inlet, T_exh"
h_bar_CO2_Tout=Enthalpy(CO2,T=T_out) "Enthalpy of CO2 at exhaust outlet, T_out"
s_bar_CO2=Entropy(CO2,T=T_exh,P=P_exh) "Entropy of CO2 at exhaust outlet, T_exh"
s_bar_CO2_Tout=Entropy(CO2,T=T_out,P=P_exh) "Entropy of CO2 at exhaust outlet, T_out"

h_bar_H2O=Enthalpy(H2O,T=T_exh) "Enthalpy of H2O at exhaust inlet, T_exh"
h_bar_H2O_Tout=Enthalpy(H2O,T=T_out) "Enthalpy of H2O at exhaust outlet, T_out"
s_bar_H2O=Entropy(H2O,T=T_exh,P=P_exh) "Entropy of H2O at exhaust outlet, T_exh"
s_bar_H2O_Tout=Entropy(H2O,T=T_out,P=P_exh) "Entropy of H2O at exhaust outlet, T_out"

h_bar_N2=Enthalpy(N2,T=T_exh) "Enthalpy of N2 at exhaust inlet, T_exh"
h_bar_N2_Tout=Enthalpy(N2,T=T_out) "Enthalpy of N2 at exhaust outlet, T_out"
s_bar_N2=Entropy(N2,T=T_exh,P=P_exh) "Entropy of N2 at exhaust outlet, T_exh"
s_bar_N2_Tout=Entropy(N2,T=T_out,P=P_exh) "Entropy of N2 at exhaust outlet, T_out"

h_bar_O2=Enthalpy(O2,T=T_exh) "Enthalpy of O2 at exhaust inlet, T_exh"
h_bar_O2_Tout=Enthalpy(O2,T=T_out) "Enthalpy of O2 at exhaust outlet, T_out"
s_bar_O2=Entropy(O2,T=T_exh,P=P_exh) "Entropy of O2 at exhaust outlet, T_exh"
s_bar_O2_Tout=Entropy(O2,T=T_out,P=P_exh) "Entropy of O2 at exhaust outlet, T_out"

"Thermomechanical exergi of CO2"
e_bar_mech_CO2=h_bar_CO2-h_bar_CO2_Tout-T_0*(s_bar_CO2-s_bar_CO2_Tout-R*(LN((P_exh)/(P_0))))

"Thermomechanical exergi of H2O"
e_bar_mech_H2O=h_bar_H2O-h_bar_H2O_Tout-T_0*(s_bar_H2O-s_bar_H2O_Tout-R*(LN((P_exh)/(P_0))))

"Thermomechanical exergi of N2"
e_bar_mech_N2=h_bar_N2-h_bar_N2_Tout-T_0*(s_bar_N2-s_bar_N2_Tout-R*(LN((P_exh)/(P_0))))

"Thermomechanical exergi of O2"
e_bar_mech_O2=h_bar_O2-h_bar_O2_Tout-T_0*(s_bar_O2-s_bar_O2_Tout-R*(LN((P_exh)/(P_0))))

"Total thermomechanical exergy "
e_bar_mech=(b*e_bar_mech_CO2)+(c*e_bar_mech_H2O)+(d_2*e_bar_mech_N2)+(e*e_bar_mech_O2)

"TOTAL EXERGY OF COMBUSTION PRODUCTS"
e_bar_mech_kg=e_bar_mech/MW_fuel
e_bar_ch_kg=e_bar_ch/MW_fuel

e_bar_exh=e_bar_ch+e_bar_mech
e_bar_exh_kg=e_bar_exh/MW_fuel

"Percentage of chemical exergy contribution"
Percentage_ch=(e_bar_ch/(e_bar_exh))*100
Percentage_ch2=(e_bar_ch_kg/(e_bar_exh_kg))*100

"Calculation of avalible KW in exhaust"
AvalibleHEAT=e_bar_mech_kg*m_dot_fuel

ENERGY=e_bar_mech2_kg*m_dot_fuel

percent=ENERGY/AvalibleHEAT

load_en=(x/100)*11400

percent_ex=AvalibleHEAT/load_en*100

Appendix B

EES Model of Conventional Subcritical ORC

```
$ARRAYS On

"Setting known variables/information first"
Function CONDPRESSURE(P_cond)
If P_cond<1 [bar] Then P_cond:=1
CONDPRESSURE:=P_cond
End

"Avalible heat from exhaust gas"
{Q_exh=1000}

{x=5}
{b=x+5}
"Put in fluid here"
Fluid$='benzene'
load=1*x
"Efficiency turbine and evaporator"
eta_tur=0.8
eta_pump=0.75

"Assumed input values"
P_evap=41*0.98 [bar]

T_cond=330 [K]
P_cond=pressure(fluid$, T=T_cond, X=0.5)

P_cond_corr=CONDPRESSURE(P_cond)
P_cond2=P_cond_corr*0.98

T_cond_corr=temperature(fluid$, P=P_cond_corr, X=0.5)

"Expansion turbine, process 1-2"
"what about pre heat section"
T_1=temperature(fluid$, X=1, P=P_evap)
h_1=enthalpy(fluid$, T=T_1, X=1);
s_1=entropy(fluid$, h=h_1, P=P_evap);
h_2s=enthalpy(fluid$, s=s_1, P=P_cond_corr)
h_2=h_1 - eta_tur*(h_1-h_2s)
s_2=entropy(fluid$, h=h_2, P=P_cond_corr)
T_2=temperature(fluid$,P=P_cond_corr, s=s_2)

"Process 2-3_ cooling of vapor until condensing part"

"CONDENSING, Process 3-4"
h_3=enthalpy(fluid$, X=1, P=P_cond_corr);
h_4=enthalpy(fluid$, X=0, P=P_cond2)
{T_3=temperature(fluid$, h=h_3, P=P_cond_corr)}
T_3=temperature(fluid$,  X=1, P=P_cond_corr);
T_4=temperature(fluid$,  X=0, P=P_cond2);
s_3=entropy(fluid$, h=h_3, T=T_3);
s_4=entropy(fluid$, h=h_4, T=T_4);

"PUMP WORK, Process 4-5"
v_4=volume(fluid$, X=0, P=P_cond_corr);
W_ps=(v_4*(P_evap-P_cond_corr))*convert(m^3*bar/(kg),kJ/kg);
W_p=W_ps/eta_pump
```

```
h_5=h_4+W_p;
T_5=temperature(fluid$, h=h_5, P=P_evap);
"Thermal efficiency"
n=((h_1-h_2)-(h_5-h_4))/(h_1-h_5);

"Mass flow of working fluid"
m_wf=Q_exh/(h_1-h_5)

"Work turbine"
W_orc_turbine=m_wf*(h_1-h_2)
"Work pump"
W_pn=m_wf*(h_5-h_4)
"Heat in"
Q_in=m_wf*(h_1-h_5)
"Efficiency"
n_test=(W_orc_turbine-W_pn)/Q_in
n_test2=(W_orc_turbine-W_pn)/Q_exh
n_plot=n_test*100

delta=h_5-h_4
bwr=W_pn/W_orc_turbine

load2=(x/100)*11400

percent3=W_orc_turbine/load2*100

"PINCH ANALYSIS - want to find T_exh at pinch point"
h_6=enthalpy(fluid$, P=P_evap, X=0)
{T_exh_pinch=T_exh1-((m_wf*(h_1-h_6))/(m_exh*cp_exh))}

"ARRAY Values"
T[1]=T_1
T[2]=T_2
T[3]=T_3
T[4]=T_4
T[5]=T_5
T[6]=T_1
T[7]=T_1

S[1]=s_1
S[2]=s_2
S[3]=s_3
S[4]=s_4
S[5]=entropy(fluid$, h=h_5, P=P_evap)
S[6]=entropy(fluid$, X=0, h=h_6)
S[7]=s_1

P[1]=P_evap
P[2]=P_cond_corr
P[3]=P_cond_corr
P[4]=P_cond2
P[5]=P_evap
P[6]=P_evap
P[7]=P_evap
```

Appendix C

EES Model of Subcritical ORC with Regeneration and Superheat

```
$ARRAYS On

"Subcritical ORC with regeneration and superheat - EES Model"

"FUNCTION SYSTEM"
Function CONDPRESSURE(P_cond)
If P_cond<1 [bar] Then P_cond:=1
CONDPRESSURE:=P_cond
End

{Function INTERNALPRESSURE(T_int)
If T_int>380 [K] P_int:=P_int-1
CONDPRESSURE:=P_int
End}

"Setting known variables/information first"
"Avalible heat from exhaust gas"
Q_exh=2000

"Put in fluid here"
Fluid$='R245fa'

"Efficiency turbine and evaporator"
eta_tur=0.8
eta_pump=0.75

"Assumed input values, pressure should not exceed condensing pressure"
{P_evap=25*0.98} "-Simulated, keep out of system simulation - install in parametric table"
{T_evap=temperature(fluid$, P=P_evap, X=0.5)}
T_cond=330 [K]
P_cond=pressure(fluid$, T=T_cond, X=0.5)

P_cond_corr=CONDPRESSURE(P_cond)
P_cond_pump=P_cond_corr*0.98

T_int=380 [K]
P_int=pressure(fluid$, T=T_int, x=0.5)
{P_int=9.365 [bar]
{P_int=((P_evap-P_cond_corr)/2)+P_cond_corr } "-optimize intermediate pressure instead of assuming
value"
T_1=563.4 [K]}

{T_1=maxParametric('Table 6', 'T_1', 365, 800)}
T_cond_corr=temperature(fluid$, P=P_cond_corr, X=0.5)

{T_1=temperature(fluid$, P=P_evap, X=0.5)}
T_1=400+263
"Expansion turbine, process 1-2-3"

"Open feed-water heater"
h_1=enthalpy(fluid$, T=T_1, P=P_evap);
s_1=entropy(fluid$, T=T_1, P=P_evap);

h_2s=enthalpy(fluid$, s=s_1, P=P_int)
h_2=h_1-eta_tur*(h_1-h_2s)
s_2=entropy(fluid$, h=h_2, P=P_int)
```

```
T_2=temperature(fluid$,P=P_int, s=s_2)

h_3s=enthalpy(fluid$, s=s_2, P=P_cond_corr)
h_3=h_2 - eta_tur*(h_2-h_3s)
s_3=entropy(fluid$, h=h_3, P=P_cond_corr);
T_3=temperature(fluid$,P=P_cond_corr, S=s_3)

"Process 3-4, cooling of vapor until saturated point"
h_4=enthalpy(fluid$, X=1, P=P_cond_corr);
T_4=temperature(fluid$,  X=1, P=P_cond_corr);
s_4=entropy(fluid$,X=1, P=P_cond_corr)

"Process 4-5, CONDENSING"
h_5=enthalpy(fluid$, X=0, P=P_cond_pump)
T_5=temperature(fluid$,  X=0, P=P_cond_pump);
s_5=entropy(fluid$, X=0, P=P_cond_pump);

"Process 5-6, FIRST PUMP WORK"
v_5=volume(fluid$, X=0, P=P_cond_pump);
W_p_isen5=(v_5*(P_int-P_cond_pump))*convert(m^3*bar/(kg),kJ/kg);
W_p=W_p_isen5/eta_pump
h_6=h_5+W_p;
T_6=temperature(fluid$, h=h_6, P=P_int);
s_6=entropy(fluid$, P=P_int, h=h_6)

"Process 7-8, SECOND PUMP WORK"
h_7=enthalpy(fluid$, X=0, P=P_int)
v_7=volume(fluid$, X=0, P=P_int);
s_7=entropy(fluid$, P=P_int, X=0)
W_p_isen7=(v_7*(P_evap-P_int))*convert(m^3*bar/(kg),kJ/kg);
h_8=h_7+W_p_isen7
T_7=temperature(fluid$, X=0, P=P_int)
T_8=temperature(fluid$, h=h_8, P=P_evap)
s_8=entropy(fluid$, P=P_evap, h=h_8)

T_9=temperature(fluid$, X=0.5, P=P_evap)
s_9=entropy(fluid$,P=P_evap, X=0)
h_9=enthalpy(fluid$, X=0, P=P_evap)


T_10=T_9
s_10=entropy(fluid$,P=P_evap, X=1)
h_10=enthalpy(fluid$, X=1, P=P_int)

"Mass flow of working fluid"
m_wf=Q_exh/(h_1-h_8)
f=(h_7-h_6)/(h_2-h_6)
"Work turbine"
W_orc_turbine=(h_1-h_2)+((1-f)*(h_2-h_3))
W_orc_turbine2=m_wf*((h_1-h_2)+((1-f)*(h_2-h_3)))

"Work pump"
W_pn=(h_8-h_7)+((1-f)*(h_6-h_5))
W_pn2=m_wf*((h_8-h_7)+((1-f)*(h_6-h_5)))

"Heat in and out"
```

```
Q_in_test=(h_1-h_8)
Q_in=(h_1-h_8)*m_wf
Q_out_test=(1-f)*(h_3-h_5)*m_wf

"Thermal efficiency"
n=(((h_1-h_2)+((1-f)*(h_2-h_3)))-((h_8-h_7)+((1-f)*(h_6-h_5))))/(h_1-h_8);

"Efficiency"
n_uten_m=(W_orc_turbine-W_pn)/Q_in_test
n_test=(W_orc_turbine2-W_pn2)/Q_exh

{n_test2=(W_orc_turbine-W_pn)/Q_exh}

bwr=W_pn/W_orc_turbine

"PINCH ANALYSIS - want to find T_exh at pinch point"

{T_exh_pinch=T_exh1-((m_wf*(h_1-h_6))/(m_exh*cp_exh))}



"ARRAY Values"
T[1]=T_1
T[2]=T_2
T[3]=temperature(fluid$, X=1, P=P_int)
T[4]=T_7
T[5]=T_8
T[6]=T_9
T[7]=T_10
T[8]=T_1
T[9]=T_2
T[10]=T_3
T[11]=T_4
T[12]=T_5
T[13]=T_6
T[14]=T_7

{T[8]=T_8
T[9]=T_9
T[10]=T_10
T[11]=T_1}

S[1]=s_1
S[2]=s_2
S[3]=entropy(fluid$,X=1, P=P_int)
S[4]=s_7
S[5]=s_8
S[6]=s_9
S[7]=s_10
S[8]=s_1
S[9]=s_2
S[10]=s_3
S[11]=s_4
S[12]=s_5
S[13]=s_6
```

S[14]=s_7

{S[8]=s_8
S[9]=s_9
S[10]=s_10
S[11]=s_1}

P[1]=P_evap
P[2]=P_int
P[3]=P_cond_corr
P[4]=P_cond_corr
P[5]=P_cond_pump
P[6]=P_int
P[7]=P_int
P[8]=P_evap
P[9]=P_evap
P[10]=P_evap
P[11]=P_evap

{"STATE 1"
h_1=enthalpy(fluid$, T=T_1, P=P_evap);
s_1=entropy(fluid$, h=h_1, P=P_evap);
p_1=P_evap

"STATE 2"
h_2s=(fluid$, s=s_1, P=P_int)
h_2=h_1-eta_tur*(h_1-h_2s)
s_2=(fluid$, h=h_2, P=P_int)
T_2=temperature(fluid$,P=P_int, s=s_2)
p_2=P_int

"STATE 3"
h_3s=enthalpy(fluid$, s=s_2, P=P_cond_corr)
h_3=h_2 - eta_tur*(h_2-h_3s)
s_3=entropy(fluid$, h=h_3, P=P_cond_corr);
T_3=temperature(fluid$,P=P_cond_corr, S=s_3)
p_3=P_cond_corr

"STATE 4"
h_4=enthalpy(fluid$, X=1, P=P_cond_corr);
T_4=temperature(fluid$, X=1, P=P_cond_corr);
p_4=p_cond_corr

"STATE 5"
h_5=enthalpy(fluid$, X=0, P=P_cond_pump)
T_5=temperature(fluid$, X=0, P=P_cond_pump);
s_5=entropy(fluid$, X=0, P=P_cond_pump);
p_5=P_cond_pump

"STATE 6"}

Appendix D

EES Model of Trans-critical ORC

```
$ARRAYS On

"ORC - Trans-critical - EES model"
"Setting known variables/information first"
Function CONDPRESSURE(P_cond)
If P_cond<1 [bar] Then P_cond:=1
CONDPRESSURE:=P_cond
End

"Avalible heat from exhaust gas"
Q_exh=800
"Put in fluid here"
Fluid$='r407c'

"Efficiency turbine and evaporator"
eta_tur=0.8
eta_pump=0.75

"Assumed input values"
P_evap=86 [bar]
T_cond=330 [K]
P_cond=pressure(fluid$, T=T_cond, X=0.5)

P_cond_corr=CONDPRESSURE(P_cond)
P_cond2=P_cond_corr*0.98

T_cond_corr=temperature(fluid$, P=P_cond_corr, X=0.5)

T_1=354 [K]
"Expansion turbine, process 1-2"
"what about pre heat section"
{T_1=temperature(fluid$, X=1, P=P_evap)}
h_1=enthalpy(fluid$, T=T_1, P=P_evap);
s_1=entropy(fluid$, T=T_1, P=P_evap);
h_2s=enthalpy(fluid$, s=s_1, P=P_cond_corr)
h_2=h_1 - eta_tur*(h_1-h_2s)
s_2=entropy(fluid$, h=h_2, P=P_cond_corr)
T_2=temperature(fluid$,P=P_cond_corr, s=s_2)

"Process 2-3_ cooling of vapor until condensing part"
"CONDENSING, Process 3-4"
h_3=enthalpy(fluid$, X=1, P=P_cond_corr);
T_3=temperature(fluid$,  X=1, P=P_cond_corr);
s_3=entropy(fluid$, h=h_3, T=T_3);

h_4=enthalpy(fluid$, X=0, P=P_cond2)
T_4=temperature(fluid$,  X=0, P=P_cond2);
s_4=entropy(fluid$, h=h_4, T=T_4);

{T_3=temperature(fluid$, h=h_3, P=P_cond_corr)}

"PUMP WORK, Process 4-5"
v_4=volume(fluid$, X=0, P=P_cond2);
W_ps=(v_4*(P_evap-P_cond2))*convert(m^3*bar/(kg),kJ/kg);
W_p=W_ps/eta_pump
h_5=h_4+W_p;
```

```
T_5=temperature(fluid$, h=h_5, P=P_evap);
"Thermal efficiency"
n=((h_1-h_2)-(h_5-h_4))/(h_1-h_5);

"Mass flow of working fluid"
m_wf=Q_exh/(h_1-h_5)

"Work turbine"
W_orc_turbine=m_wf*(h_1-h_2)
"Work pump"
W_pn=m_wf*(h_5-h_4)
"Heat in"
Q_in=m_wf*(h_1-h_5)
"Efficiency"
n_test=(W_orc_turbine-W_pn)/Q_in
n_test2=(W_orc_turbine-W_pn)/Q_exh
n_plot=n_test*100

delta=h_5-h_4
bwr=W_pn/W_orc_turbine
{s_crit=4}

T_crit=temperature(fluid$, P=P_evap, s=s_crit)

"PINCH ANALYSIS - want to find T_exh at pinch point"
h_6=enthalpy(fluid$, P=P_evap, T=T_1)
{T_exh_pinch=T_exh1-((m_wf*(h_1-h_6))/(m_exh*cp_exh))}

"ARRAY Values"
T[1]=T_1
T[2]=T_2
T[3]=T_2
T[4]=T_4
T[5]=T_5
{T[6]=T_1}

S[1]=s_1
S[2]=s_2
S[3]=s_2
S[4]=s_4
S[5]=entropy(fluid$, h=h_5, P=P_evap)
{S[6]=s_1}

P[1]=P_evap
P[2]=P_cond_corr
P[3]=P_cond_corr
P[4]=P_cond2
P[5]=P_evap
P[6]=P_evap

H[1]=h_1
H[2]=h_2
H[3]=h_3
H[4]=h_4
H[5]=h_5
H[6]=h_1
```

Appendix E

EES Model of Stirling Engine

"EES - model - STIRLING ENGINE"

"engine under following conditions"

R=8.314

"Input values"
{x=0 [deg]} "plot for entire cycle"
dx=90[deg]

g=0.5

V_SE=0.01 [m^3] "Swept volume of expansion piston"
V_DE=V_SE*g "Dead volume of expansion space"

V_SC=0.01 [m^3] "Swept volume of compression piston"
V_DC=V_SC*g "Dead volume of compression space"

V_reg=0.001 [m^3] "Volume of regenerator"

theta=90 [degrees]
P_mean=100 [bar]
T_H=670
T_C= 360
n= 1700

"temperature ratio"
t=(T_C)/(T_H)

"Swept volume ratio"
v=(V_SC*10^(-6))/(V_SE*10^(-6))

"Dead volume ratio of expansion space"
X_DE=(V_DE*10^(-6))/(V_SE*10^(-6))

"Dead volume ratio of compression space"
X_DC=(V_DC*10^(-6))/(V_SC*10^(-6))

"Dead volume ratio of regenerator space"
X_r=(V_reg*10^(-6))/(V_SE*10^(-6))

"Coeficcients"
a=ARCTAN((v*SIN(theta))/(t+COS(theta)))

S=t+(2*t*X_DE)+((4*t*X_r)/(1+t))+v+(2*X_DC)

B=sqrt(t^2+(2*t*v*COS(theta)+v^2))

c=B/S

"Engine pressure, x= piston position"
P=(P_mean*sqrt(1-c^2))/(1-c*COS(x-a))

"Momental volume, expansion and compression"
V_E=(V_SE/2)*(1-COS(x))+V_DE

V_C=(V_SC/2)*(1-COS(x-dx))+V_DC

Volume= V_E+V_C+V_reg

"Indicated energy, power and efficiency"
W_E=(P_mean*V_SE*pi*c*SIN(a))/(1+sqrt(1-c^2))*convert(bar*m^3, J)

W_C=-(P_mean*V_SE*pi*c*t*SIN(a))/(1+sqrt(1-c^2))*convert(bar*m^3, J)

W_i=W_E+W_C
e=W_i/W_E
e_2=1-t

f=0.3
Power_i=W_i*n*Convert(J/min, kJ/sec)
Power_actual=Power_i*f